a0005

2.13 Microfluidic for Lab-on-a-Chip

Stefan Haeberle[1,2] and Roland Zengerle[1,2], [1] Institute for Micromachining and Information Technology of the Hahn-Schickard-Society (HSG-IMIT), Villingen-Schwenningen, Germany, [2] Laboratory for MEMS Applications, Department of Microsystems Engineering (IMTEK), University of Freiburg, Freiburg, Germany

Glossary

g9000 ***CMOS*** Complementary Metal Oxide Semiconductor
g9005 ***DWP*** Dispensing Well Plate
g9010 ***EDC/NHS*** Carbodiimid/*N*-hydroxysuccinimide
g9015 ***EOF*** Electroosmotic Flow
g9020 ***EP*** Electrophoresis
g9025 ***EWOD*** Electrowetting
g9030 ***FID*** Free Interface Diffusion
g9035 ***GC*** Gas Chromatograph
g9040 ***HPLC*** High Pressure Liquid Chromatograph
g9045 ***HTS*** High Throughput Screening
g9050 ***IDT*** Interdigital Transducer
g9055 ***LSI*** (microfluidic) Large Scale Integration
g9060 ***MSL*** Multilayer Soft Lithography
g9065 ***PCR*** Polymerase Chain Reaction
g9070 ***PDMS*** Polydimethylsiloxane
g9075 ***SAW*** Surface Acoustic Wave
g9080 ***TAS*** Total Chemical-analysis System
g9085 ***TIR*** Total Internal Reflection
g9090 μ***TAS*** micro Total Analysis System

s0005 # 2.13.1 Introduction

s0010 ## 2.13.1.1 Microfluidics

p0005 The history of microfluidics dates back to the early 1950s when efforts to dispense small amounts of liquids in the nano- and subnanoliter range were made for providing the basics of today's ink-jet technology (Le 1998). In terms of fluid propulsion within microchannels of submillimeters cross-section, the year 1979 set a milestone when a miniaturized gas chromatograph (GC) was realized on a silicon wafer (Terry *et al.* 1979). The first high-pressure liquid chromatography (HPLC) column device, fabricated using Si-Pyrex technology, was published by Manz *et al.* (1990b). By the end of the 1980s the first microvalves (Shoji *et al.* 1988) and micropumps (Van Lintel *et al.* 1988) based on silicon micromachining were also presented. All these examples represent microfluidic systems since they enable the precise control of the decreasing fluid volumes on the one hand and the miniaturization of the size of a fluid handling system on the other hand.

p0010 Another important aspect of microfluidics is the exploitation of effects and phenomena that can be utilized only in microdimensions. Smaller channel dimensions drastically increase the surface-to-volume ratio and thus surface-related phenomena like laminar flow, capillarity, fast thermal response, and electrokinetics gain influence. This can be used in microfluidic systems to enhance the performance of analytical procedures. Manz *et al.* (1990a) also proposed the concept of miniaturized total chemical analysis systems (TAS) based on the unique conditions in the microdomain. Today this approach is also known as micro total analysis systems (μTAS) or laboratories on a chip (lab-on-a-chip) as proposed by Harrison *et al.* (1992).

p0015 Following this μTAS or lab-on-a-chip approach, the first applications that emerged in the field of analytical chemistry were based on the electro-osmotic flow (EOF) to pump liquids into small microcapillaries and on electrophoretic separation (EP) to distinguish sample components (Effenhauser *et al.* 1993, Harrison *et al.* 1992, 1993, Manz *et al.* 1992). These developments in the early 1990s drastically increased the academic and commercial interest in microfluidic technologies. This trend continues to the present day, as described in a recent comment on the proliferation of microfluidics in literature and intellectual property, which claims that 581 of 770 microelectromechanical systems (MEMS)-related papers published in 2003 dealt with microfluidics (Kamholz 2004).

p0020 So down to the present day manifold lab-on-a-chip systems have been developed for diverse applications, e.g., for DNA analysis (Burns *et al.* 1998),

DNA amplification (polymerase chain reaction, PCR) (deMello 2003, Kopp *et al.* 1998), proteomics (Lion *et al.* 2003, Marko-Varga *et al.* 2003), sample pretreatment (de Mello and Beard 2003). Recent general reviews on the whole field of lab-on-a-chip systems can be found in Auroux *et al.* (2002), Reyes *et al.* (2002), and Vilkner *et al.* (2004). The enormous impact of microfluidic lab-on-a-chip technologies also becomes obvious by the large number of recently published books. They either cover the whole field of microfluidics (Li 2006, Nguyen and Wereley 2002) or focus on the engineering (Geschke *et al.* 2004) or applications of microfluidic systems (Andersson and van den Berg 2004, Oosterbroek and van den Berg 2003, Tay 2002, Urban 2006). Also journals exclusively dedicated to the field of micro- and nanofluidics (*Microfluidics and Nanofluidics*, Springer) or lab-on-a-chip systems (*Lab on a Chip*, Royal Society of Chemistry) have been published recently.

2.13.1.2 Microfluidics – An Enabling Technology

From a more business-related point of view, it can be stated that nowadays most MEMS-related technology roadmaps and market studies point out the significant technological and scientific impact that microfluidics will have on various industries, especially the life sciences. A dedicated microfluidics roadmap was prepared by Ducrée and Zengerle (2004). In this study the economic development related to microfluidics technologies for the life sciences has been estimated and important market drivers and road blocks have been pinpointed.

Regarding the economic impact of microfluidics, the study anticipates an overall growth rate of more than 30% per annum for microfluidic technologies and products in the life sciences. Drug discovery, medical diagnostics, and therapeutic devices represent the most promising fields. The overall global market of microfluidics in the life sciences has been estimated to be worth approximately 500 million euros in 2002, increasing with an assumed annual growth rate of 19% to 1.4 billion euros in 2008.

Besides the economic impact of microfluidics, technological trends have also been clearly identified in the roadmap. Amongst those the most relevant is the need for microfluidic platforms equipped with a basic set of validated fluidic base operations to arrive rapidly at application-specific microfluidic systems. This system-oriented platform concept contrasts the frequent approaches in which components such as pumps or valves have been optimized at an individual level and assembled afterward.

2.13.1.3 The Need for Microfluidic Platforms

Why are microfluidic platforms needed? As described in Section 2.13.1.1 the impact of microfluidic technologies in the academic world has dramatically increased during the last few years. This is quite amazing since microfluidics is no independent product consumers want to buy. Microfluidics should be merely considered as a toolbox, which is needed to develop innovative new products in such disparate fields as medical, pharmaceutical, and analytical applications. As a consequence, the most important customer for microfluidic know-how and technologies is the research community itself, which develops new products and solutions in the different application areas such as the biotechnology, diagnostics, medical, or pharmaceutical industry.

During the last two decades, thousands of researchers have spent a lot of time developing new microfluidic components or exploring the basic microfluidic operations such as fluid transport, fluid metering, fluid mixing, valving or concentration, and separation of molecules within miniaturized quantities of fluids. Today hundreds of different types of micropumps have been fabricated (Laser and Santiago 2004), hundreds of different types of mixers and hundreds of different types of microvalves are known, and almost no standards are defined in terms of interconnections. It seems to be the right time to raise the question of whether we really need more of those components? On the basis of our experience in the lab-on-a-chip field, a component-based microfluidic approach is much too slow and the R&D effort is much too expensive to explore the huge potential of different applications. In addition, the best performance you can get out of such a component-oriented solution will be far behind what you can get in an integrated system approach, or in other words in a microfluidic platform approach. Therefore we think that the described practice of assembling discrete components such as valves and pumps, at least in the field of lab-on-a-chip applications, belongs to the past and we do not expect it to continue in the future. In our view the research community really needs validated and easy-to-operate microfluidic platforms. They have to offer an adequate number of microfluidic operations that can be easily

combined to build application-specific microfluidic systems. In addition these systems should be fabricated using a standardized cost-efficient technology.

s0025 2.13.1.4 Discrete Solutions for Unique Technical Challenges

p0050 Before pointing out the advantages of the microfluidic platform concept, we describe the opposite: two examples of application-specific integrated systems, which represent unique engineering solutions for unique technical problems. The electronic fountain pen (b0810 Waibel *et al.* 2003) as depicted in **Figure 1** is a good example of such a discrete microfluidic solution. It can be regarded as the first fully functional, highly integrated, miniaturized, and self-sustaining microdosage system of its kind operating under real-world conditions. The main components are a liquid level sensor, a microvalve, and a bubble- and particle-tolerant fluidic system. The pen is optimized with respect to minimum energy consumption. It contains a programmable ASIC and is powered by two standard watch batteries ensuring operation over a period of 2 years under standard conditions.

p0055 The oral drug delivery system (**Figure 2**), currently under development at HSG-IMIT, is a similar example (b0225 Goettsche and Wolff 2006). It has the size of two buccal teeth and will be integrated into the human denture. It consists of a drug reservoir capable of incorporating a solid pill, an osmotic pump, and a flow sensor. The refillable system is loaded by a solid pill and is designed to deliver liquid drug over a period of 2 weeks at rather harsh ambient conditions

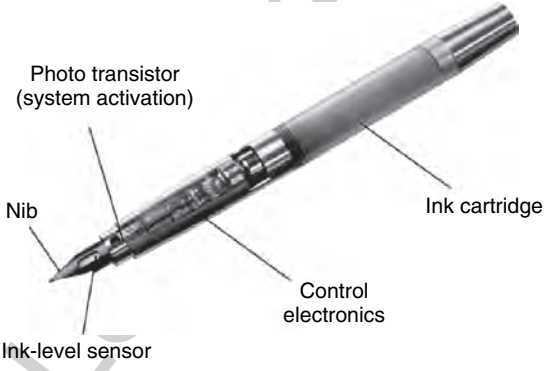

f0005 **Figure 1** Photo of the electronic fountain pen (145 mm × 12 mm). (Reprinted with permission from Waibel G, Kohnle J, Cernosa R, Storz M, Schmitt M, Ernst H, Sandmaier H, Zengerle R, Strobelt T 2003 Highly integrated autonomous microdosage system. *Sens. Actuators A Phys.* **103**, 225–30. Copyright 2003 Elsevier.)

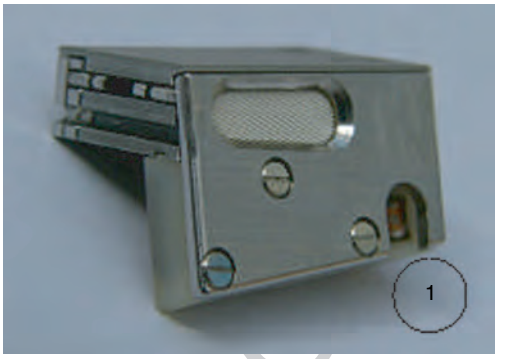

f0010 **Figure 2** Photo of a drug delivery system that can be implanted into a human denture. (Source: Goettsche T, Wolff, A 2006 IntelliDrug – An integrated intelligent oral drug delivery system. *mst-news* **06**, 36–7.)

(mechanical loads, wide temperature range, and contact with any kind of food) inside the human mouth.

p0060 Both microfluidic systems perfectly fulfill the requirements for their specific applications. However, for any other application in the field of microdosage or more general in the field of microfluidics, the specific know-how from developing such a system is only of very limited value and every development of this kind always starts from the scratch again. This causes significant costs and time at a high economic risk. Although we expect this kind of development to make sense for a few selected applications in diverse fields of applications in the future also, it is quite clear that this approach will not succeed for lab-on-a-chip systems or the diagnostic applications that are dealt with in this chapter.

2.13.1.5 What Is a Microfluidic Platform? s0030

p0065 Very similar to the ASIC industry in microelectronics, which provides validated elements and processes to make electronic circuits, a dedicated microfluidic platform comprises a reduced set of validated microfluidic elements. These elements are capable of performing the basic fluidic unit operations required in a given application area. Such basic fluidic unit operations are, for example, fluid transport, fluid metering, fluid mixing, valving, and separation or concentration of molecules or particles. The collection of fluidic unit operations needed for diagnostic applications can have only little overlap with the collection needed for pharmaceutical applications or for applications in microreaction technology. In some cases detection methods also belong to the basic set of microfluidic

t0005 **Table 1** Common features of microfluidic platforms

Microfluidic operations	*Fabrication technology*
Validated elements for basic microfluidic unit operations such as • Fluid transport • Fluid metering • Fluid valving • Fluid mixing • Separation • Concentration • Detection • ...	Validated manufacturing technology for the whole set of fluidic elements (prototyping and mass fabrication) Seamless integration of different elements • Ideally in a monolithic way • Or by a well-defined easy packaging technique

operations, and in other cases this is not the case (**Table 1**). Nevertheless, in all cases the user of a platform should be capable of readily combining the elements within a given platform in order to implement an assay for diagnostic applications or to screen for new compounds in pharmaceutical applications. Often, an efficient development is intimately linked to the availability of (standard) test setups and simulation tools.

p0070 More important than providing a totally complete set of fluidic unit operations in a platform is the fact that all elements have to be amenable to a well-established fabrication technology. Furthermore all elements or modules of a platform have to be connectible, ideally in a monolithically integrated way or at least by a well-defined, ready-to-use interconnection and packaging process. If a platform allows a seamless and simple integration of different fluidic elements in a monolithic way, for example, without sophisticated additional packaging techniques, this provides a significant advantage compared to other platforms. Thus speaking about microfluidic platforms also involves at least one validated fabrication technology to realize complete systems out of the elements. This results in a definition of a platform as follows.

p0075 A microfluidic platform allows to perform a set of fluidic unit operations that are enabled by a set of fluidic elements, which are designed for easy combination with a well-defined (and low-cost) fabrication technology. The platform allows to implement and fabricate different application-specific solutions in an easy and flexible way.

s0035 2.13.1.6 Overview of the Following Chapters

p0080 When comparing microfluidic platforms with the microelectronics industry, the question of whether we really need a diverse set of different microfluidic platforms arises. The coexistence of different platforms and their specific fabrication technologies could be regarded as a drawback since R&D efforts go in many directions and cannot be focused exclusively on one technology (as is complementary metal oxide semiconductor (CMOS) in microelectronics). On the other hand, the diversity of approaches and technologies can be considered as an advantage for their successful adoption in different application fields. Owing to the diversity, specific advantages of certain platforms are likely to succeed in different application areas. It is, however, essential that a specific platform provides all of the characteristic features given in **Table 1**.

p0085 This chapter is intended to give an overview of microfluidic platforms that have been developed until today. We will thereby focus only on platforms for lab-on-a-chip application, being aware that there are also other possible fields of applications for microfluidic platforms such as microprocess engineering or microdosage systems. However, in the field of lab-on-a-chip systems also, we cannot cover all microfluidic platforms, which are known from literature. Prominent examples of platforms that will not be discussed here are certainly the electrokinetic platform (EOF, EP), the microarray platform, and the microwell plate technology platform. These platforms, however, are already well described in many scientific papers and books. It is, furthermore, not intended to assess the different platforms by their value to the industry or to the research community.

p0090 As is evident in the introduction, the scope of this chapter is not to describe single microfluidic components. For detailed reviews on single components such as micropumps (b0230 Gravesen *et al.* 1993, b0430 Laser and Santiago 2004, b0660 Shoji and Esashi 1994, b0835 Woias 2005), valves (b0565 Oh and Ahn 2006), mixers (b0340 Hessel *et al.* 2005, b0555 Nguyen and Wu 2005), microfluidic technologies in general (b0700 Squires and Quake 2005, b0735 Stone *et al.* 2004), or

simulation techniques for the design of lab-on-a-chip systems (Erickson 2005[b0180]) we also refer to the published work.

p0095 In the following, each microfluidic platform is described in the same way. First, we motivate the platform approach and give a short introduction on the basic setup and functional principle. Then, the main unit operations realized on the platform and an application example based on their selection are presented. Finally, each section closes with a discussion on the strength and the challenges of the platform as we can see them today.

s0040 2.13.2 Capillary-driven Test Strips (Lateral Flow Assays)

s0045 2.13.2.1 Introduction

p0100 The capillary-driven test strip platform is the state of the art in point-of-care diagnostics, with billions of units that are produced in an extremely cheap manner. It is amazing that within the lab-on-a-chip or microfluidics community, not very much is known about this easiest way to perform assays on such an easy to handle widely used platform (e.g., diabetes testing, pregnancy testing).

p0105 The first test strip is certainly the indicator paper for pH measurement, which is also a representative for the most simple assay on the capillary-driven test strip platform. It consists only of one single fleece with an integrated colorimetric reagent (**Table 2**). The sample liquid is transported into the fleece of the test strip by capillary forces and a color change, depending on the pH value of the sample liquid, occurs. This color change is initiated by a reaction between the sample and the reactant. Starting from that most simple point of assay format, more complex configurations with multiple reagents or even several fleeces enable the implementation of more complex assays like immunoassays.

p0110 The so-called lateral flow assays are well known in the diagnostic field since the 1960s. Although this can be regarded as the most successful microfluidic platform for lab-on-a-chip applications in terms of applications and commercialized products, hardly any publication from a microfluidic point of view exists.

p0115 The possibility of performing an automated on-site measurement, using a cheap and small disposable test strip, combined with the simple actuation principle that does not need any energy supply, gives the platform a huge potential for point-of-care and patient self-testing applications. Today, millions of diabetics all over the world use these diagnostic devices to measure their glucose concentration several times per day and therewith adjust their medication.

p0120 The basic principle of the platform is the passive liquid transport via capillary forces within the capillaries of a fleece or microstructure layer. The physical background of these actuation principle is described in Section 2.13.2.1.1.

t0010 **Table 2** Degrees of complexity and application examples on the capillary-driven test strip platform

Capillary configuration		*Application examples*
Single fleece with colorimetric reactant		Indicator paper (pH measurement)
Single fleece with multiple reactants and colorization		BSE test, TNT test
Multiple fleeces with different zones of reactants, often cased		Pregnancy test, cardiac markers, drug test
MEMS-based capillary channels, multiple complex reactions		Detection of up to 100 different proteins (immunoassays)

Complexity

s0050 #### 2.13.2.1.1 About capillary forces

p0125 One effect that becomes more and more important when scaling down fluidic channels is the capillary force. A capillary pressure difference

$$\Delta p_\theta = \frac{2\sigma}{r}\cos\theta \qquad [1]$$

appears across the liquid–gas interface with surface tension σ in a capillary of radius r and contact angle θ. For hydrophilic contact angles <90° (partially wetting) the pressure in the liquid phase exceeds the pressure in the gas phase, leading to a further wetting of the capillary. For hydrophobic contact angles >90° (partially nonwetting) the meniscus withdraws respectively.

p0130 An important effect when dealing with capillary-driven liquid flows is contact line pinning. It causes the sudden stop of the proceeding meniscus at edges that represent a geometrical singularity. This has to be taken into account when designing microfluidic structures on the capillary test strip platform since no additional pressure is available to overcome this stop. On the other hand, however, this mechanism can be used to control the course of capillary priming on the platform.

s0055 ### 2.13.2.2 Unit Operations Controlled by Capillary Forces

s0060 #### 2.13.2.2.1 Sample loading

p0135 Several methods for sample loading exist. For bigger volumes, the sample is filled into a start reservoir from where it penetrates the underlying capillaries. If the sample volumes are not sufficient, the addition of a dilution buffer is sometimes required to enhance or allow the capillary transport in the first place. The second method, especially used in patient self-testing applications, is the direct capillary filling of the strip from the sampling point. For blood diagnostic assays, for example, the test strip is directly contacted with the blood spilled out of the finger tip that has been locally pricked with a lancet before.

2.13.2.2.2 Separation

s0065

p0140 Separation steps are required for analyzing human whole blood, for example, since the red blood cells with a volume fraction >40% would interfere with the assay. As the blood passes through a separation fleece, cells are filtered from the blood (Clark *et al.* 2002). Also microfilters or membranes with a more defined pore size can be used. An exemplary immunoassay test strip is depicted in **Figure 3**. The separation fleece is placed directly underneath the start reservoir into which the blood sample is added.

b0110

2.13.2.2.3 Transport

s0070

p0145 Depending on the complexity of the test strip, liquid propulsion is accomplished via capillary forces in fleeces and/or highly precise micromachined structures (**Table 2**). Though the system gains control when using microstructures, its fabrication becomes more expensive on the other hand. Some of the essential features of both types of capillary pumping structures are given in **Table 3**. Due to these considerations, the requirements of the assay decide which propulsion method should be used and certainly the combination of these two can increase the controllability of the assay protocol while still keeping the costs low.

p0150 An important issue for liquid transport with merely capillary-driven systems is the transport balance. Since the maximum volume of labeled sample should pass the detection zone in order to have an optimum sensitivity, certain arrangements have to be made. The volume of the transport zones, for example, should be kept small, so that only a small fraction

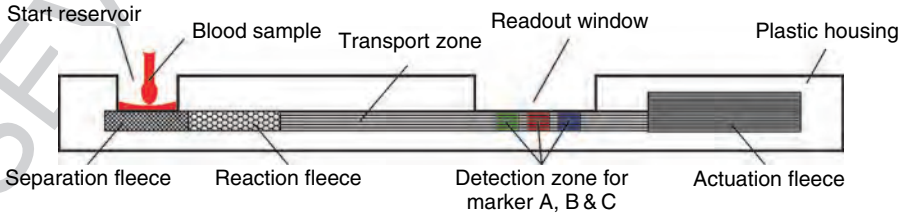

f0015 **Figure 3** Simplified cross-section of a typical capillary-driven test strip set-up for an immunoassay. The blood sample is applied at the start reservoir and passes through the separation fleece where the red cells are separated from the plasma. The plasma enters a reaction fleece containing labeling reagents comprising fluorescent antibodies that bind to the proteins in the blood plasma. The sample is then transported through the detection zone with immobilized complementary antibodies to the markers under investigation (A, B, and C). The actuation fleece at the end of the strip ensures that the whole liquid volume is sucked through by the capillary liquid propulsion through all fleeces. All fleeces are typically packed into a low-cost plastic housing.

t0015 **Table 3** Comparison of fleeces and microstructures for capillary propulsion in test strips

Properties	*Fleeces*	*Microstructures*
Cost	Cheap	Expensive
Availability	Good (various types)	Bad (must be created)
Realization of filtering	Easy	Elaborate
Flow guiding	3D structures	2D structures
Control of flow direction	Bad (isotropic, toward unsaturated fleece)	Good (follows structure)
Flow prediction	Not exact	Good

of the initial sample volume remains within that dead volume. Another measure for a good volume balance is to ensure that the capillarity of the input zone (separation and labeling fleece) is lower than the capillarity of the actuation fleece, leading to a complete drainage of the sample into the actuation fleece before the liquid propulsion terminates.

p0155 A very fundamental requirement for a successful assay is that the initially added sample volume exceeds a critical minimum. Otherwise, the complete wetting of all the essential test strip zones cannot be assured and the assay fails.

s0075 ***2.13.2.2.4 Incubation***

p0160 During an assay protocol on the capillary-driven test strip platform, the sample has to get in contact and react with several predeposited reagents. They are integrated into the fleece or microstructure of the strip during fabrication. This is mostly done by fleeces that are saturated with the reagent and dried afterward. If needed, the reactant molecules can also be covalently bound to the surface using standard immobilizing techniques like the carbodiimid (EDC)/*N*-hydroxysuccinimide (NHS) chemistry.

p0165 The setting of an appropriate incubation time for reagent dissolution is managed by different zones within the test strip, exhibiting different wetting properties. The basic principle behind this approach is depicted in **Figure 4**. First, the liquid primes the reaction chamber, where a dry reagent is predeposited in a pillar microstructure. This is achieved very fast due to a low contact angle of 10° only. The propagation of the liquid meniscus is then slowed down within a so-called time gate with an increased contact angle of $\theta = 80°$ and consequently a reduced capillary force. The time for the dissolution of the dry reagent is set by the length of the time gate and ends as soon as the liquid reaches the detection zone with an increased capillary pumping force ($\theta = 10°$) speeding up the flow again.

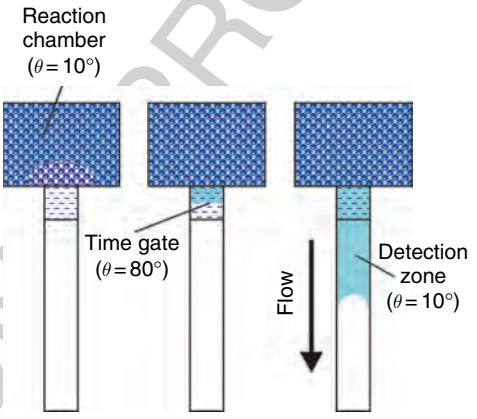

Figure 4 Schematic realization of a certain incubation time in the capillary-driven test strip platform. The liquid flow is throttled in the time gate of reduced wettability ($\theta = 80°$) thus leading to an extended period of time for reaction within the reaction chamber. Consequently, the dried reagents can be dissolved completely before the liquid proceeds along the detection zone. f0020

s0080 ***2.13.2.2.5 Mixing***

p0170 The dissolution of the preloaded dried reagent situated in the reaction fleece, described as an incubation step before, can also be regarded as a kind of mixing operation. A characteristic feature of the capillary test strip platform is the fact that mixing generally is purely passive and is based only on diffusion. It cannot be accelerated externally and is also one of the major drawbacks of this kind of platform. In order to keep the mixing time short, a high surface-to-volume ratio within the reaction chamber is preferred. However, the dissolution time typically still lies in the range of several minutes and thus the capillary flow through the reaction chamber has to be throttled as described before.

s0085 ***2.13.2.2.6 Metering***

p0175 The metering of liquids is an important unit operation for quantitative assays. Within a test strip, metering is done by the defined volumes of the fleeces and

microstructures. The liquid flow stops automatically as soon as the actuation fleece (**Figure 3**) is fully wetted with liquid. This way the amount of liquid that has passed the detection zone is well defined. The only thing that has to be ensured is that the start reservoir is filled with enough liquid at the beginning of the assay, i.e., with the volume of the complete test strip (all fleeces and microstructures) and a certain reliability excess to ensure proper functioning.

s0090 ***2.13.2.2.7 Amplification***

p0180 The results from a test strip assay are mostly read out by optical markers such as fluorescent molecules. Since the concentration of these molecules within the sample liquid is potentially small, they have to be accumulated within the detection zone. The sample volume passes through the detection zone with an adequate flow rate, ensuring the non-diffusion-limited binding of the marked sample molecules to the immobilized capture molecules in the detection zone. A remarkable fluorescent signal is obtained after a multiple of the detection zone volume has passed the immobilized molecules. This can be regarded as a microfluidic amplification unit operation.

s0095 ***2.13.2.2.8 Readout***

p0185 The fluorescent emission of the detection zone is excited using a laser diode of corresponding wavelength. The phase-shifted (longer wavelength) fluorescent response is detected using a photodiode and an appropriate optical filter within common test strip readers. If regions of different capture molecules are immobilized within the detection zone, the test strip is moved with a stepper motor underneath the detection unit (laser diode and photodiode).

p0190 Some assays are also read out using electrochemical mechanisms. The glucose concentration of a blood sample is determined by measuring the electrical charge generated during the enzymatic oxidation of glucose to gluconic acid, for example. The test strip reader applies an external electric potential and measures the current, which is a function of the number of electrons generated.

p0195 Besides the above-described device-based readout methods, the reading of assay results with the naked eye is also possible. This is of interest for those applications where a cheap and fast readout is required. A manual readable signal is produced by binding small gold or latex particles to the detection molecule, which accumulate at the detection zone and color it. However, only clear and binary signal-generating assays such as pregnancy tests are capable of manual readout.

2.13.2.3 Application Example: The Cardiac® Reader

s0100

Cardiac markers are very important in emergency medicine. They allow a fast decision if a patient with chest pain is suffering from an acute cardiac infarction and has to be treated accordingly. Only the combination of several markers enables a clear diagnostic conclusion on whether the patient had a heart attack or not. Since this diagnostic information and the need for adequate medication should be gained as fast as possible, a lab-on-a-chip system for the point-of-care measurement is demanded.

p0200

The Cardiac Reader® from Roche[b0625] (2006) is a commercial point-of-care system for the detection of four different cardiac markers (myoglobin, troponin T, D-dimer, and NT-probBNP). The test strip reader and the corresponding test strips are depicted in **Figure 5** and allow the determination of these four markers within minutes from a single blood sample. The system is used in doctor's offices or emergency rooms.

p0205

The complete test strip consists of different fleeces for liquid transport, blood separation, and readout. First, 150 µl of heparinized venous whole blood is added onto the inlet region above two

p0210

Figure 5 The Cardiac® Reader and the four different test strips (Source: Roche 2006 Basel, CH, www.roche.com, accessed 2006.)

f0025

reagents containing fleeces. Within these fleeces, two antibodies specifically bind to the antigen (e.g., troponin T protein) of the blood sample. One antibody is labeled with biotin, the other with a gold nanoparticle. After the binding step, the blood sample is transported through a separation fleece, where the cellular constituents are removed.

p0215 In the last assay step, the antigen–antibody complex is transported along a detection zone, featuring immobilized strepdavidin proteins, which bind to the biotin of the complex. Thus the protein complex is captured in the detection region, and the assay result is read out optically via a dark line generated by the accumulating gold nanoparticles. To control the assay performance, antigens are immobilized in a control region subsequently passed by the sample liquid. A successful assay run with a negative result, that is, no Troponin T within the blood sample, can be determined by a dark line arising at this control position only (Raschke 2005). The complete assay, starting from the application of the blood sample until the readout of the result, takes 8–12 min.

s0105 2.13.2.4 Strengths and Challenges of the Platform

p0220 The major strength of the capillary-driven test strip platform is certainly the robust microfluidic flow propulsion principle, relying on capillary forces only. No external energy is required, which opens up a wide field of applications especially for simple color-changing assays such as pH measurement or pregnancy tests. However, complex immunoassay protocols have also been implemented during the last few years. Therefore this special microfluidic platform is setting a benchmark in terms of costs and integrated, automated assay implementation for all microfluidic platforms discussed in this chapter.

p0225 Drawbacks of the platform certainly arise from its simplicity. Assay protocols in the capillary-driven systems follow a fixed process scheme, imprinted in the microfluidic channel design. Passive liquid propulsion by capillary forces only cannot be influenced actively once the process is started. As a consequence the exact timing of assay steps depends on variations of viscosity and surface tension of the sample. Therefore the precision of the assay result, for example, is on the order of 10%, which is not always sufficient for several future challenges in the implementation of diagnostic assays. More complex diagnostic assays also cause a larger number of process steps such as reactant dissolution. As previously described, this mixing operation cannot be accelerated in the capillary test strip platform, which leads to long assay times.

p0230 Crucial unit operations for the assay precision are metering and incubation steps whose accuracy is limited to the merely capillary-driven system. A further critical point is the long-term stability of the wetting properties inside the fleeces or the microstructures. Usually, the materials are plasma treated or coated by an additional layer to ensure the desired contact angle and thus wetting behaviors. These surface activations or coatings have to be stable at different temperatures and over a long period of time as they define the test strip lifetime.

2.13.3 Pressure-driven Systems s0110

2.13.3.1 One Step Forward in Controllability and Complexity s0115

p0235 Assay protocols in capillary-driven systems follow a fixed process scheme, imprinted in the microfluidic channel design. Passive liquid propulsion by capillary forces only cannot be influenced actively once the process is started. In addition the exact timing depends on variations of viscosity and surface tension of the sample, and mixing is rather slow. This certainly offers other platform technologies the chance to show up and get into the market. As an example, pressure-driven platforms enable the control of the running processes. Liquid flows can be stopped, reversed, and their flow rates and ratios can be adjusted online in order to change the course of the assay. A platform-integrated pressure source is required to make this step forward in controllability possible. So the gain of control is accompanied by an increased complexity of the system.

2.13.3.2 Unit Operations in Pressure-driven Microfluidics s0120

2.13.3.2.1 Fluid transport (Laminar flow) s0125

p0240 Independent from the liquid propulsion method, the pressure-driven liquid flow within microchannels has some common properties. Strictly laminar flow due to the small Reynolds numbers within the channels of small cross section in combination with the no-slip boundary condition at the channel walls lead to a parabolic velocity profile. Thus, the flow velocity depends on the position within the cross section of

the channel, i.e., long residence time near the walls and short residence time in the center of the channel.

p0245 The laminar volumetric flow rate I_v through microchannels

$$I_v = \frac{\pi}{8\eta}\frac{r^4}{l}\Delta p \qquad [2]$$

depends on the applied pressure difference Δp, length l, and radius r of the channel as well as the liquid viscosity η (law of Hagen–Poiseuille).

p0250 Different possibilities for pressure generation are described below and are also categorized as shown in **Figure 6**. A constant pressure source can be activated only once and operates autonomously afterward. This is similar to capillary systems, whereas the potential pressures and thus flow rates can be considerably higher compared with merely capillary-driven flows. In addition, liquid propulsion sustains after the whole structure is filled with liquid since no capillary pressure-generating air–liquid interface is required.

p0255 The easiest way to accomplish a pressure-driven flow by a constant pressure source is certainly using an external pressure cartridge, connected to the microfluidic chip. However, the macro- to microfluidic interfacing problem has to be solved for these off-chip solutions, which is a common problem when dealing with microfluidics (b0190 Fredrickson and Fan 2004). This fluidic interface has to be pressure tight and should not lead to a lot of additional dead volume.

p0260 Constant pressure can also be generated on the chip by integrating, e.g., a spring-loaded liquid reservoir. Again, the interfacing problem remains if the reservoir is loaded while already integrated in the chip. More simple techniques for pressure generation on the chip use, for example, thermal phase transition effects and can be switched on via a heater.

p0265 If the pressure can be switched on and off, respectively, and if its amplitude can be adjusted within a certain working range, the system gains in controllability. The actuation mechanisms used for pressure generation can be basically divided into hydraulic (liquid) and pneumatic (gas) principles. Liquid propulsion is accomplished by either applying an overpressure at the inlet (pushing of fluid) or applying an underpressure at the outlet (sucking of fluid) of a microchannel structure. Depending on the microfluidic structures as well as the application, both methods can be advantageous in terms of bubble-free priming and leak tightness.

p0270 All off-chip macropump solutions require a macro-to-micro interfacing technology, as described in the previous section, leading to a certain dead volume required for interconnection tubing. Although, the dead volume can be decreased by placing a micropump onto the microfluidic chip, a micro-to-micro interface is still needed for interconnection. This is not consistent with the ideal microfluidic platform that allows to realize all fluid unit operations in a monolithically integrated manner using the same fabrication technology. Only this way expensive and error-prone liquid interfaces can be avoided. A large number of micropumps have been presented during the last two decades (b0430 Laser and Santiago 2004, b0660 Shoji and Esashi 1994, b0835 Woias 2005). Many of these pumps are based on the combination of a displacement chamber with two active or passive microvalves. These devices are discussed in more detail in Chapter 2.06 and are not considered here.

p0275 More simple and robust pressure-generating principles, like the displacement of a membrane via a finger push or a manually operated syringe, have also been demonstrated as interesting alternatives.

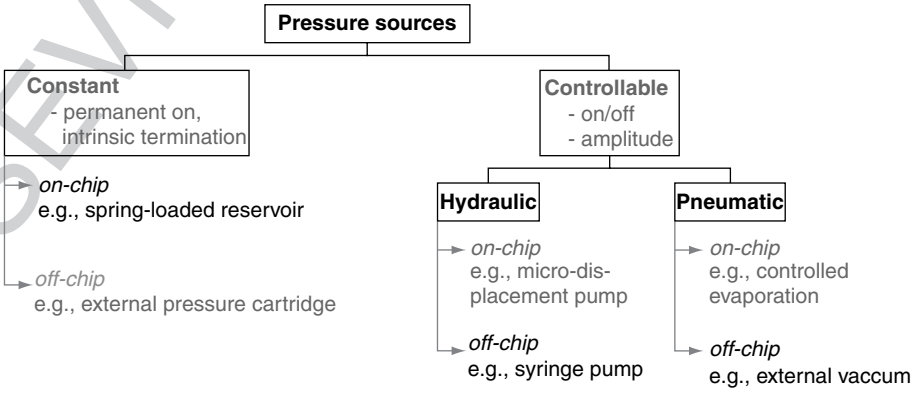

f0030 **Figure 6** Different pressure sources for microfluidic platforms.

These methods are used in point-of-care testing applications, where a simple and low-energy consuming pumping principle is required. In the following, three examples of novel on-chip pumping mechanisms based on thermal effects are described.

p0280 Two nonmechanical implementations of micropumps that allow monolithic integration and that are based on the phase change of a working fluid are depicted in **Figure 7**. Heating elements, integrated into the microfluidic channels, increase the temperature of the fluid locally when actuated. This leads to a phase change of the liquid volume at the position of the heater (evaporation) if the temperature exceeds the boiling point. A virtual movement of the bubble by actuating several discrete and serial aligned heaters subsequently has been proposed by b0690 Song and Zhao (2001) (see **Figure 7**, *left*). Using this actuation principle, deionized water has been pumped through a 37.2 cm-long Pyrex glass tube (1.0 mm inner diameter) using 12 serial-aligned heating elements (heating power, 8–12 W). A maximum pressure head of 57 mm H_2O and a maximum volumetric flow rate of 300 µl min^{-1} are reported. Another pumping principle, also based on the thermal phase change is depicted in **Figure 7** (*right*). This device consists of two triangular-shaped heat sources only b0880 (Yokoyama *et al.* 2004). The heat flux inside the heater has its maximum at the apex of the triangle, defining the seed position of the bubble during evaporation. A flow rate of 12.5 mm s^{-1} at a driving frequency of 1 Hz has been achieved within a microchannel of 220 mm length and 600 µm × 120 µm cross section using two of the depicted micropumps (overall: four heaters).

Another pumping method that is also based on p0285 thermal actuation is depicted in **Figure 8** b0915 (Zimmermann *et al.* 2005). The device consists of three independent microchannels, arranged perpendicular to three linear Peltier elements. The channels have an open filling zone, a sealed microchannel in which the assay can be performed, and a likewise open pumping zone. The device is initially primed with liquids by capillary forces via the filling zone. Afterward, the Peltier-1 cools the filling zone to prevent evaporation, i.e., loss of sample or reagent. The ability to keep 90% of 0.6 µL solution in an open filling zone for 60 min is reported.

For liquid propulsion, the Peltier-3 additionally p0290 heats the pumping zone leading to a controlled evaporation of liquid at the open interface. The evaporation of liquid sets the flow rate in the microchannel. The functional principle can be considered as a capillary pump maintaining the capillary pressure on both sides of the channel. Flow rates ranging from $\sim 1.2\,nl\,s^{-1}$ to $\sim 30\,pl\,s^{-1}$ have been demonstrated using this principle. The flow rate perfectly matches with the binding kinetics of the molecules inside the liquid to the channel surface, which is diffusion limited, and does exclude faster flow rates.

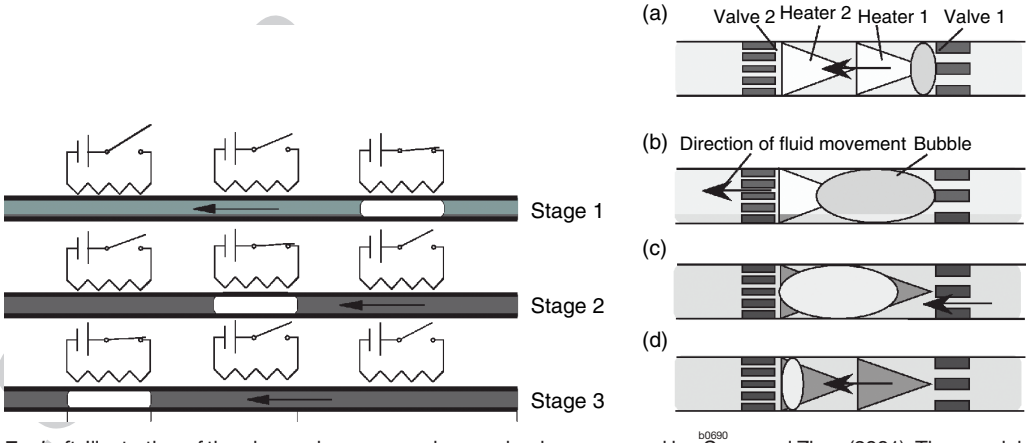

f0035 **Figure 7** *Left*: Illustration of the phase-change pumping mechanism proposed by b0690 Song and Zhao (2001). Three serial-aligned and sequentially actuated heating elements initiate a moving vapor bubble and thus a directed liquid propulsion (stages 1–3). (Source: Song Y J, Zhao T S 2001 Modelling and test of a thermally-driven phase-change nonmechanical micropump. *J. Micromech. Microeng.* **11**, 713–19, IOP Publishing Limited.) *Right*: Basic principle of the thermal micropump described in (a) start of heating (heater 1 on, heater 2 off); (b) bubble growing (heaters 1 and 2 on); (c) start of condensing (heater 1 off, heater 2 on); (d) bubble collapsing (heaters 1 and 2 off). (Reprinted with permission from Yokoyama Y, Takeda M, Umemoto T, Ogushi T 2004 Thermal micro pumps for a loop-type micro channel. *Sens. Actuators A Phys.* **111**, 123–8. Copyright 2004 Elsevier.)

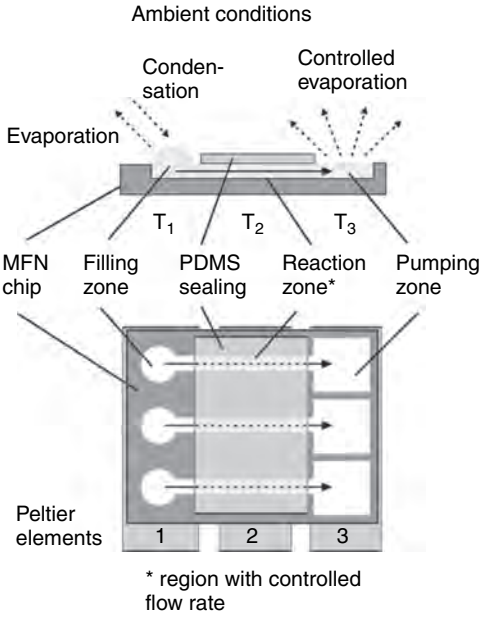

f0040 **Figure 8** Controlled evaporation method for liquid propulsion. Three microchannels are aligned perpendicular to a set of three Peltier elements allowing the temperature control at the filling, reaction, and pumping zone. Cooling of the filling zone and heating of the pumping zone initiate a controlled evaporation of liquid at the pumping zone. Thus, a liquid flow through the channel is initiated, while preventing evaporation at the inlet zone. (Source: Zimmermann M, Bentley S, Schmid H, Hunziker P, Delamarche E 2005 Continuous flow in open microfluidics using controlled evaporation. *Lab Chip* **5**, 1355–9, Reproduced by permission of The Royal Society of Chemistry.)

s0130 ***2.13.3.2.2 Valving***

p0295 A large variety of different active microvalves has been reported during the last two decades (b0565 Oh and Ahn 2006) associated to the development of displacement micropumps. However, especially in the field of lab-on-a-chip applications, the required power supply and the high costs of these active valves seem to limit their practical use in pressure-driven systems (**Table 4**).

Therefore, passive microvalves based on capillary stops, which are defined by a change in the channel cross section or the wetting properties of the channel, are more suitable for disposable systems. These valves work similar to passive valving structures in merely capillary-driven systems with the only difference being that the valve can be actively opened at any time by applying an additional pressure load onto the valve. p0300

s0135 ***2.13.3.2.3 Mixing***

Since no turbulences can be generated within the laminar flow regime, mixing is related to diffusion processes only in microfluidic channels. Hundreds of micromixing principles and structures have been presented during the last few years to overcome this limitation, see b0540 Hessel *et al.* (2005) and b0555 Nguyen and Wu (2005) for a detailed and up to date overview. p0305

The basic idea of all micromixers is to increase the interfacial area between the fluids that should be mixed. Well-established methods for continuous mixing are multilamination (b0165 Ehrfeld *et al.* 1999, b0335 Hessel *et al.* 2003) and split-and-recombine (b0090 Chen and Meiners 2004, b0095 Cheng *et al.* 2001, b0645 Schonfeld *et al.* 2004) flow schemes. A large number of alternating thin lamellae of the liquids A and B are generated within these mixers (A−B−A−B−A···). This increases the interfacial area between the two liquids, which fastens up the homogenization of the two liquid phases via diffusion. p0310

In a multilamination mixer, the initial liquid flows (phases A and B) are split into several substreams, guided to a junction area and then merged into an alternating phase pattern (A−B−A−B−A−B···). The split-and-recombine principle depends on the repetitive splitting of a phase pattern and combining the substreams again. This way the number of phase interfaces is doubled by each split-and-recombine stage (e.g., A−B leads to A−B+A−B). p0315

Another method to increase the interface between two liquid flows is transversal advection. Centrifugal p0320

t0020 **Table 4** Comparison of active and passive microvalves

Properties	*Active valves*	*Passive valves*
Power supply	Required	Not required
Moving parts	Yes	No
Capable of complex fluid processing	Yes	Limited
Cost-efficient	No	Yes
Works well with fluids containing higher solvent or surfactant concentration	Yes	No
Design	Multilayer structures	Simple
Structure size	Large	Small

forces within bended channels, for example, are utilized to generate an additional flow component perpendicular to the initial direction of flow (Jiang *et al.* 2004, Sudarsan and Ugaz 2006). Due to this transversal advection, the contact interface increases along the channel and thus mixing is supported. Advection can also be induced in simple straight channels at low Reynolds numbers (<100) by manufacturing a (staggered herring bone-shaped) surface texture on one channel wall (Johnson *et al.* 2002, Stroock *et al.* 2002).

p0325 All the principles described so far are intended to mix different liquid flows and therefore called continuous micromixers. However, the mixing of liquids, located within a microchamber, can also be of interest. Active micromixers are mainly used for this purpose, e.g., by moving magnetic particles through the chamber.

2.13.3.2.4 Metering

s0140 p0330 Metering on pressure-driven platforms is typically realized by controlling liquid flows into or through reaction chambers possibly supported by flow rate sensors. With these methods, however, metering, isolation, and further processing of a discrete liquid volume are not possible. Therefore additional active or passive valving structures are required that can release the liquid out of a metering chamber after it has been metered to a defined volume via an overflow channel. Such a structure utilizing a passive, hydrophobic valve for stopping the liquid and metering it to a defined volume has been presented by Yamada and Seki (2004). Metered liquid volumes of 3.5 and 20 nl have been demonstrated in these structures.

2.13.3.2.5 Switching

s0145 p0335 Flow switching can be realized in a straightforward approach by integrating several (at least two) active microvalves, e.g., on the two continuative channels of a T-shaped structure. Depending on the desired flow path, one of both valves is opened while the other remains closed. However, for complex liquid processing, which is required for the implementation of assay protocols on the platform, a large number of active valves have to be integrated.

p0340 Another possibility to switch continuous liquid flows between several outlet channels is based on hydrodynamic focusing (Lee *et al.* 2001a, b). Generally, a sample flow that is symmetrically enframed by two sheath flows at the junction of a Y-shaped channel is focused to a thin stream line under laminar conditions (**Figure 9**) due to the so-called hydrodynamic focusing effect (Knight *et al.* 1998). Depending on the ratio of the flow velocities $\overline{v}_1$, $\overline{v}_2$, and $\overline{v}_3$, the sample liquid stream ($\overline{v}_2$) is directed toward one of the seven outlet ports (A–G). This switching method, however, is based on continuous flows and consequently a certain sample volume is required for liquid routing. This limits the applicability of the method to applications with large sample volumes only.

2.13.3.2.6 Separation

s0150 p0345 Separation processes are basic techniques to decrease the complexity of material mixtures and are often required in analytical chemistry. Many different physical and chemical separation methods are used in classic analytical assays, e.g., sieving, centrifugation, chromatography, crystallization, adsorption, distillation. Several of these methods have been used in microfluidic systems during the past few

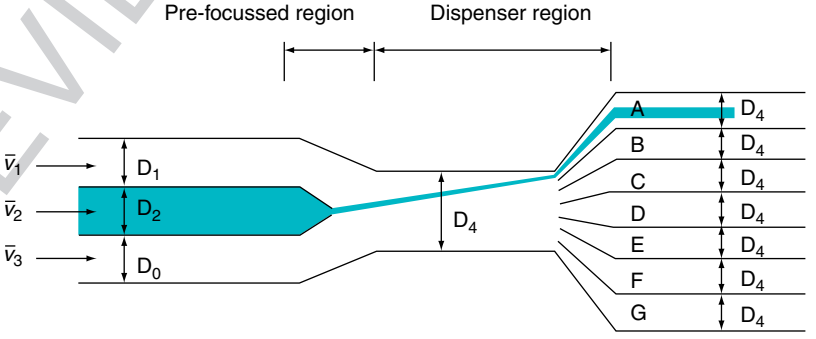

f0045 **Figure 9** Principle of the continuous flow switch based on hydrodynamic focusing. The liquid stream $\overline{v}_2$ is focused by two lateral flows $\overline{v}_1$ and $\overline{v}_3$ within the prefocused region and then deflected into one of seven outlets (A–G) within the dispenser region. (Source: Lee G B, Hung C I, Ke B J, Huang G R, Hwei B H 2001a Micromachined pre-focused 1×*N* flow switches for continuous sample injection. *J. Micromech. Microeng.* **11**, 567–73, IOP Publishing Limited.)

years, and novel separation principles utilizing the fundamental different hydrodynamics in microchannels have also been proposed.

p0350 A separation method that depends on the different diffusion constants of particles of different sizes is the so-called H-Filter, developed and distributed by the company Micronics Inc. (2006). The functional principle of the structure is depicted in **Figure 10**. A sample liquid containing particles of different sizes (Inlet 2) and an extraction liquid without particles (Inlet 1) are combined at one side of a H-shaped channel network. Subsequently, they are guided through the horizontal connecting channel and are completely split into two fractions of equal flow rate at the outlet of the channel.

p0355 The flow within the connecting channels stays undisturbed due to the laminar flow conditions. Therefore, the particles present in the sample liquid leave the structure via outlet 2 as far as they do not enter the upper flow portion in the horizontal channel by diffusion. By setting the flow rate, the residence time within the connecting channel and thus the timeframe for the diffusion of the particles can be adjusted. Smaller particles can diffuse a larger distance within a certain timeframe compared with bigger ones. Thus, a fraction of small particles are found within the extraction liquid at outlet 1 and the bigger particles stay within the sample liquid at outlet 2 (Weigl *et al.* 2003). Using this method, the extraction of the antibiotic cephradine from human blood with a recovery of ~32% has been demonstrated (Jandik *et al.* 2002).

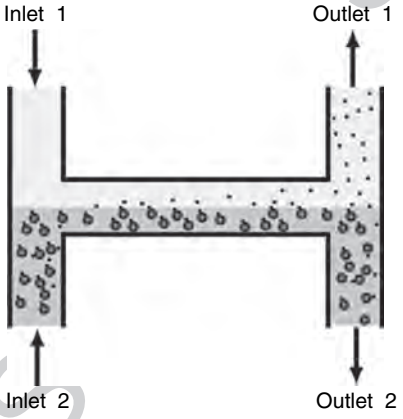

f0050 **Figure 10** Functional principle of the H-filter. Depending on their diffusion coefficient, the particles start to diffuse across the fluid interface within the horizontal channel. Under optimized conditions, 50% of the population of small particles can be removed from a sample containing large particles also. (Reprinted with permission from Weigl B H, Bardell R L, Cabrera C R 2003 Lab-on-a-chip for drug development. *Adv. Drug Deliv. Rev.* **55**, 349–77. Copyright 2003 Elsevier.)

p0360 Another method that is based on particle diffusion utilizes the asymmetric bifurcation of laminar flow around obstacles. The particles follow different migration paths, depending on their size. Microspheres of 0.8, 0.9, and 1.0 μm size were successfully sorted within 40 s in such a device (Huang *et al.* 2004).

p0365 A hydrodynamic particle separation method, the so-called pinched flow fractionation (Yamada *et al.* 2004), is based on the parabolic flow profile and on the fact that the center of the particle cannot get close to the channel wall than the radius. The particles of different sizes within the sample flow are aligned to the channel wall by a second pinching liquid flow after a Y-shaped junction. The channel then expands and the flow spreads while retaining laminar conditions. Thus, each particle follows the streamline of its center. This leads to a separation of the particles perpendicularly to the flow direction according to their size. Using the pinched flow fractionation principle, the successful separation of 15- and 30-μm-diameter particles has been demonstrated. Even a mixture of 1- to 5-μm particles can be separated using an improved structure based on this principle (Takagi *et al.* 2005).

p0370 Another hydrodynamic method, called hydrodynamic filtration (Yamada and Seki 2005), is based on the topology of the particles and the laminar flow profile (**Figure 11**). Here, no additional liquid flow is needed for the alignment of the particles along the channel wall as is the case for the pinched flow fractionation. In the first part of the structure (concentration and alignment), only a small fraction of the liquid is withdrawn through the side channels (**Figure 11(a)**). Thus, neither of the particles enter the side channel since their center still lies beyond the flow fraction directed to the side channel (dashed line). Due to the permanent volume extraction on both sides of the channel, however, the particles are aligned onto both channel walls after some concentration steps.

p0375 In a subsequent side channel (first selection), the relative flow rates are adjusted to extract small particles from the suspension within the main channel (**Figure 11(b)**). At the second selection branch, the flow rate into the side channel is increased once again to extract the bigger particles. The concentration of polymer microspheres with diameters of 1–3 μm was increased 20- to 50-fold, and they were collected independently according to the size using such a

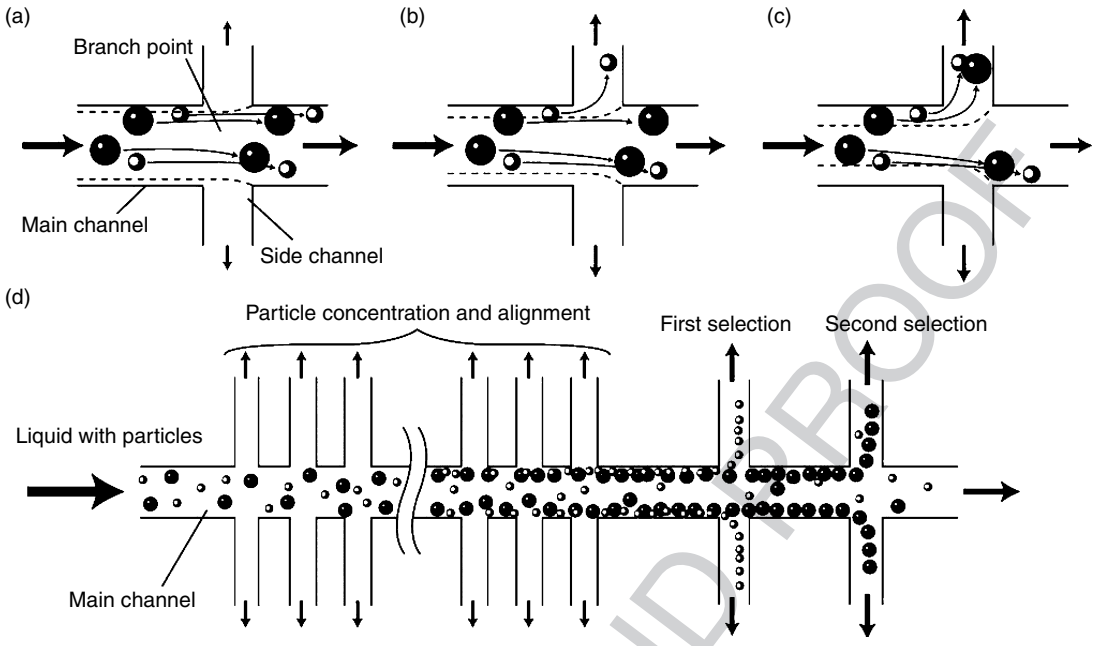

f0055 **Figure 11** The hydrodynamic filtration method. The situation at a branch point for different flow ratios is depicted in (a)–(c). The relative flow rate into the side channel is (a) low, (b) medium, or (c) high; (d) The complete structure consists of a concentration and alignment as well as a selection part. (Source: Yamada M, Seki M 2005 Hydrodynamic filtration for on-chip particle concentration and classification utilizing microfluidics. *Lab Chip* **5**, 1233–9, Reproduced by permission of The Royal Society of Chemistry.)

structure. In addition, selective enrichment of leukocytes from blood was successfully demonstrated (b0865 Yamada and Seki 2005). Using an improved device for continuous particle concentration and size-dependent separation based on the same principle but featuring an additional splitting and recombining of the fluid flow, the concentration of 2.1- to 3.0-µm particles can be increased 60- to 80-fold (b0870 Yamada and Seki 2006).

s0155 ## 2.13.3.3 Application Examples

s0160 ### *2.13.3.3.1 Portable handheld analyzer: i-STAT®*

p0380 The i-STAT® analyzer from Abbott Point of Care (2006) is a portable diagnostic platform. Several disposable cartridges for the determination of a multitude of blood parameters (blood gases, electrolytes, coagulation, cardiac markers, and hematology) can be read out using the same handheld analyzer (**Figure 12**, *left*). Only the low-cost polymer cartridge is contaminated with the blood sample and can be disposed after the diagnostic assays while the readout and assay processing analyzer is reused. The system

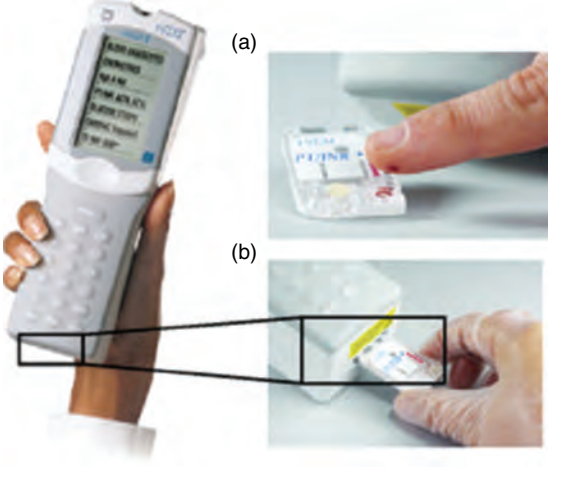

f0060 **Figure 12** *Left*: The portable i-STAT® analyzer for clinical blood tests. *Right*: Depending on the blood parameters to be measured, (a) a certain disposable cartridge is filled with blood by capillary forces from the fingertip and (b) later loaded into the analyzer for assay processing and readout. (Source: Abbott P-C 2006 East Windsor, NJ, USA, www.abbottpointofcare.com, accessed 2006.)

reduces the time-to-result for the determination of important blood parameters down to several minutes, enabling faster diagnostic decisions.

p0385 The reagent solution for sensor calibration is contained in the cartridge within a foil pouch. As depicted in **Figure 12**, the blood sample is filled into the cartridge by capillary forces (**Figure 12(a)**) and placed into the analyzer (**Figure 12(b)**). During the subsequent assay cycle, the analyzer presses the front of the cartridge, causing a barb to puncture the pouch. This releases the calibrant solution and additionally generates a pressure-driven flow over the silicon sensor array for measurement. Subsequently, the analyzer presses an air bladder on the cartridge, which pushes the calibrant into the waste reservoir and the blood sample over the sensor array. Thereby, the blood parameters are determined depending on the type of cartridge and presented at the display of the handheld analyzer.

s0165 ***2.13.3.3.2 Diffusion-based assays: T-Sensor®***

p0390 Micronics Inc. (2006) has developed the microFlow™ platform for the implementation of automated diffusion-based assays. The system consists of a disposable plastic card containing the microfluidic structures and a microfluidic work station for external pressure generation (syringe pumps) and detection. Microfluidic unit operations such as separation in the ActiveH™ card with an integrated H-filter or controlled mixing via diffusion through the ActiveT™ card, can be combined to conduct diffusion-based assays.

p0395 The microFlow platform as well as the ActiveT card containing the microfluidic T-Sensor® is depicted in **Figure 13**. A stable sheath flow is generated under laminar conditions at the junction of three inlet channels. No chaotic mixing occurs in the subsequent detection stream due to the strictly laminar flow conditions in the microchannel. The only transport of material from one stream to another is by diffusion. Consequently two diffusion zones on both sides of the central stream evolve. The left zone between the reference solution and the detection liquid represents a system-integrated real-time calibration. The other zone evolves at the right side of the detection stream being in contact with the sample liquid. The faster diffusion of smaller molecules also enables the detection of smaller components of interest present in a complex sample without previous separation. The reaction between the reference and the detection as well as between the sample and the detection stream is measured via a single fluorescent readout across the complete channel.

2.13.3.4 Strength and Challenges of the Platform

s0170

p0400 Pressure-driven platforms are certainly the most investigated ones in terms of the number of developed microfluidic components like micropumps, micromixers, microvalves, etc. However, only a small number of platform applications have been commercialized so far. The main reason for this is that many of the proposed components are based on different fabrication technologies. Thus, their combination on a pressure-driven platform causes liquid interfacing problems. However, the advantages of the pressure-driven approach are obvious: an increased level of controllability as compared with pure capillary-based test strips, easy integration of almost all

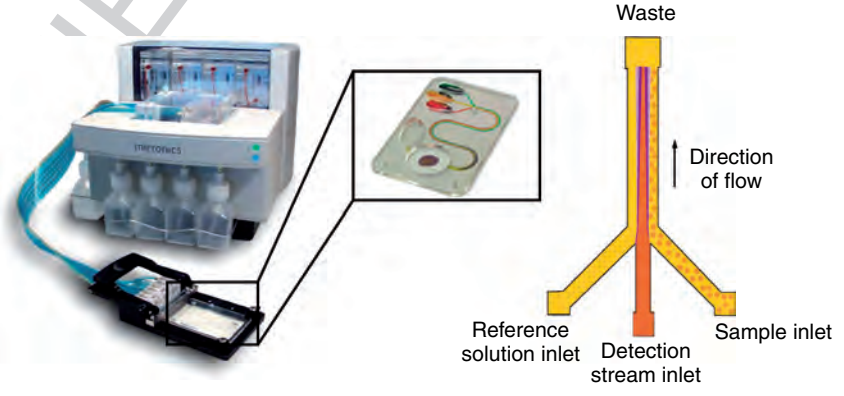

f0065 **Figure 13** *Left*: The microFlow™ platform with an ActiveT™ card in the insert. *Right*: The functional principle of the T-Sensor® structure. The detection stream meets at the junction part with a reference liquid on the left and the sample liquid on the right side, respectively. (Source: Micronics Inc. 2006 Redmond, WA, USA, www.micronics.net, accessed 2006.)

biochemical sensor principles, and the compatibility to standard lab equipment.

p0405 The real potential of a pressure-driven platform becomes evident in Section 2.13.4, where the microfluidic large-scale integration (LSI) platform – a special type of pressure-driven platform – is described, which is probably the most sophisticated platform concept presented in the field so far.

s0175 2.13.4 Microfluidic Large-scale Integration

s0180 2.13.4.1 Introduction

p0410 Before the beginning of the 1990s, the screening for novel active agents in the pharmaceutical industry was done by laboratory staff in manually pipetted assays. A biological target molecule is exposed to many compounds in order to find a positive, i.e., matching compound (hit). The assay result is mainly read out optically (change in color or fluorescent signal) after the reaction. Since the texture of the biological target molecule is unknown, all possible combinations out of a compound library are tested. This merely statistical approach is called combinatorial chemistry.

p0415 Over the years, the number of screening experiments rapidly grew just as the compound libraries increased, making manual processing impossible. With the advent of highly automated liquid handling instrumentations such as pipetting robots, the number of experiments per day can be increased enormously. Over 100 000 experiments can be performed within a single day using these so-called high throughput screening (HTS) technologies. A current trend is the further reduction of the liquid volumes per screening experiment, e.g., by novel dispensing systems for liquid volumes in the nanoliter and picoliter range (see Section 2.13.7). Besides cost issues the finite amount of (biological) target molecules is the main driving force for this progression.

p0420 However, when shrinking reaction volumes why not also miniaturize the liquid handling devices to do thousands of chemical experiments on the footprint of a stamp? In the early 1990s, the realization of such an integrated microfluidic platform seemed unrealistic in terms of simply shrinking microvalves, micropumps, and mixers developed so far. Comparable to the invention of the transistor in 1947, a pivotal innovation in microfluidics was needed to overcome the existing barrier. This innovation arose with a novel fabrication technology for microfluidic channels, called soft lithography. Using this technology, the monolithic fabrication of all necessary fluidic components from one single elastomer material (polydimethylsiloxane, PDMS) became possible, similar to the silicon-based technology in microelectronics.

2.13.4.1.1 PDMS – Soft lithography s0185

PDMS is an inexpensive but still powerful material p0425 offering several advantages compared to silicon or glass. It is a cheap, rubber-like elastomer with good optical transparency and biocompatibility. It can be structured using the soft lithography technique based on the replication molding on micromachined molds. It has first been used by George Whitesides's group for the fabrication of optical devices (Xia *et al.* 1996) and stamps for chemical patterning (Xia and Whitesides 1998a, b). A general and detailed up-to-date view of the use of PDMS in different fields of applications can be found in Sia and Whitesides (2003).

Thereafter, microfluidic devices have also p0430 been manufactured using PDMS technology (Delamarche *et al.* 1997, Duffy *et al.* 1998, Effenhauser *et al.* 1997, Fu *et al.* 1999, Hosokawa *et al.* 1999). So far, however, PDMS has been used merely as a passive material for the realization of microfluidic channels. The strength of the technology, however, really became obvious, when Stephen Quake's group expended the technology toward the multilayer soft lithography (MSL) process (Quake and Scherer 2000, Unger *et al.* 2000). With this technology, several layers of PDMS can be hermetically bonded on top of each other resulting in a monolithic, multilayer PDMS structure. The single layers are formed from a master structure either by casting or by using spin coating (**Figure 14**). One of the two layers contains a sparse cross-linking agent, while the other has an excess concentration. Both layers are separately prehardened, removed from the masters, and aligned to each other. Afterward, the PDMS stack is again baked, initiating the reaction of the cross-linking agent on the layer interface. A monolithic, multilayer elastomer structure results, which is finally bonded to a glass substrate for easier handling. Today, this technology is pushed forward by the company Fluidigm Corporation in the United States (Fluidigm Corporation 2006).

2.13.4.2 Microfluidic Large-scale Integration: Unit Operations s0190

2.13.4.2.1 Valving s0195

The resulting microfluidic platform mainly depends p0435 on the elastomer properties of PDMS with a low Young's modulus value of ~750 kPa (Lotters *et al.*

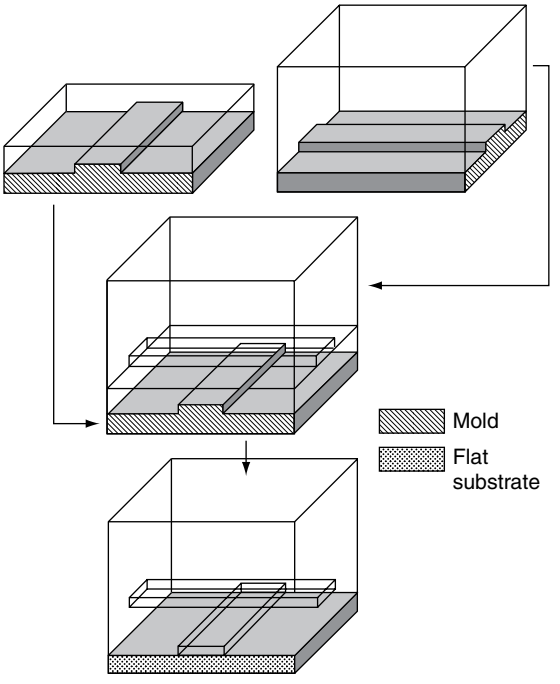

f0070 **Figure 14** The multilayer soft lithography (MSL) fabrication principle. Two fluidic channel layers are casted from microfabricated molds. In a second step both layers are combined and compounded chemically. At last the compound is placed on a glass substrate for robust handling. (Reprinted with permission from Unger M A, Chou H P, Thorsen T, Scherer A, Quake S R 2000 Monolithic microfabricated valves and pumps by multilayer soft lithography. *Science* **288**, 113–16. Copyright 2000 AAAS.)

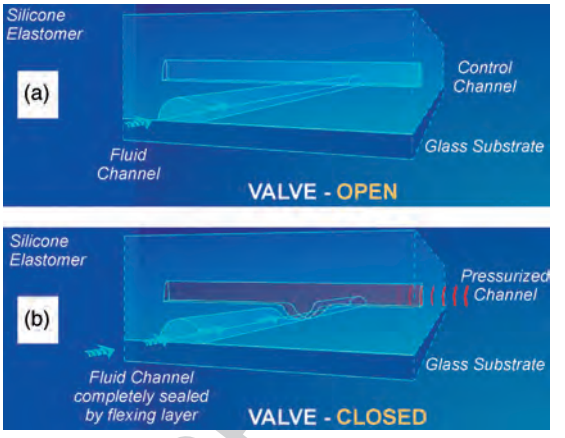

Figure 15 Schematic sketch of the microfluidic NanoFlex™ valve realized in the multilayer soft lithography (MSL) technology. (a) Liquid can pass through the fluid channel as long as no pressure is applied to the control channel. (b) An increased pressure within the control channel causes the thin elastic polydimethylsiloxane (PDMS) membrane between the two channel layers to deflect into the fluid channel and blocks the liquid flow therein, i.e., the valve is closed. (Source: Fluidigm Corporation 2006 San Francisco, USA, www.fluidigm.com, accessed 2006.) f0075 b0185

1997). Based on this elasticity, the basic microfluidic unit operation is a valve, which is made of a planar glass substrate and two layers of PDMS on top of each other. The lower elastomer layer contains the fluidic ducts and the upper elastomer layer features pneumatic control channels. To realize a microfluidic valve, a pneumatic control channel crosses a fluidic duct as depicted in **Figure 15**. A pressure applied to the control channel squeezes the elastomer into the lower layer, where it blocks the liquid flow. Because of the small size of this valve on the order of $100 \times 100\,\mu m$, a single integrated fluidic circuit can accommodate thousands of valves. Compared to the development in microelectronics, this approach is called microfluidic large-scale integration (LSI) (Thorsen *et al.* 2002). b0770

p0440 The valve technology called NanoFlex™ is the core technology of the complete platform. Placing two of such valves at the two arms of a T-shaped channel, for example, realizes a fluidic switch for the routing of liquid flows between several adjacent channels. Other unit operations based on the MSL technology are described in the following sections.

2.13.4.2.2 Pumps and mixers s0200

The platform offers two possibilities to transport liquids. On the one hand, external pumps can be used to generate liquid flows within the fluid channel layer. With that approach, the PDMS multilayer device works merely passively, controlling the externally driven liquid flows with the integrated valves. On the other hand, an integrated pumping mechanism can be achieved by combining several microvalves and actuating them in a peristaltic sequence (**Figure 16(b)**). p0445

Also a micromixer for the accelerated homogenization of liquids can be realized using the above-described pumping mechanism (**Figure 16(c)**). The liquids to be mixed are segmentally introduced into the fluidic loop through the left inlet, while the right outlet valve is still closed. Afterward, the inlet and the outlet valve are closed and the three control channels on the orbit of the mixing loop are displaced with a peristaltic actuation scheme leading to the circulation of the mixture within the loop (Quake and Scherer 2000). Thereby the liquids are mixed and afterward flushed out of the mixer by a washing p0450 b0600

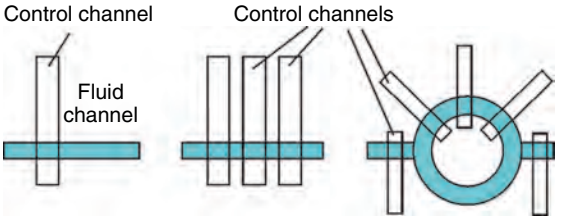

f0080 **Figure 16** Realization of the main unit operations on the multilayer polydimethylsiloxane (PDMS)-based platform. Based on the NanoFlex™ (a) a valve, (b) an integrated peristaltic micropump, (c) and a micromixer can be designed.

liquid (inlet and outlet valves are opened again). Using this mixing scheme, an increase in the reaction kinetics of surface binding assays by nearly two orders of magnitude has been demonstrated (Chou b0105 *et al.* 2001).

p0455 Another mixing concept in the microfluidic LSI platform involves simply opening the valve between two different chambers containing different liquids. In this mixing scheme, the liquids mix only by diffusion. Although a merely diffusional mixing is very slow, it is also very controllable in return. A controllable and slow mixing process in particular is required for protein crystallization, which is described in more detail in Section 2.13.3.3.1.

2.13.4.2.3 Multiplexing

s0205 p0460 The key principle to tap the full potential of the LSI approach is the multiplexing technology, which allows the control of N fluid channels with $2 \log_2 N$ b0770 control channels as depicted in **Figure 17** (Thorsen *et al.* 2002). This, for instance, means that 256 fluid channels can be controlled individually by 33 pneumatic control channels.

p0465 Thorsen *et al.* demonstrated a microfluidic storage device with 1000 independent compartments of approximately 250 pl volume and 3574 microvalves. Therefore, two multiplexers, one for the row decoding and the other for the column decoding, have been used. The complete microfluidic chip has a surface area of 25 mm × 25 mm.

2.13.4.2.4 Metering

s0210 p0470 Liquid volumes can also be metered using crossed fluid channels and a set of microvalves. Addressed by a multiplexer, the liquid is loaded into a certain fluid channel in the first step of the metering protocol (**Figure 18**). Afterward the valves between the different chambers are closed and thus the continuous

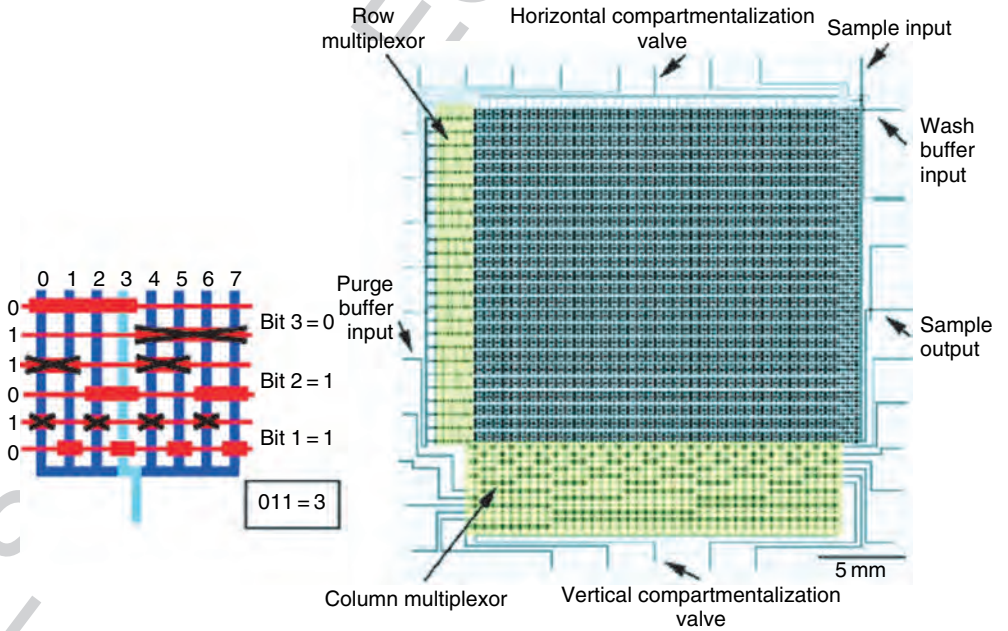

f0085 **Figure 17** *Left*: Operational diagram of the microfluidic multiplexer: eight vertical fluid channels can be individually controlled by six horizontal control channels. The pressurized control channels block the fluid channels only at positions where the width of the control channel is widened. *Right*: Mask design for the microfluidic memory storage device. (Reprinted with permission from Thorsen T, Maerkl S J, Quake S R 2002 Microfluidic large-scale integration. *Science* **298**, 580–4. Copyright 2002 AAAS.)

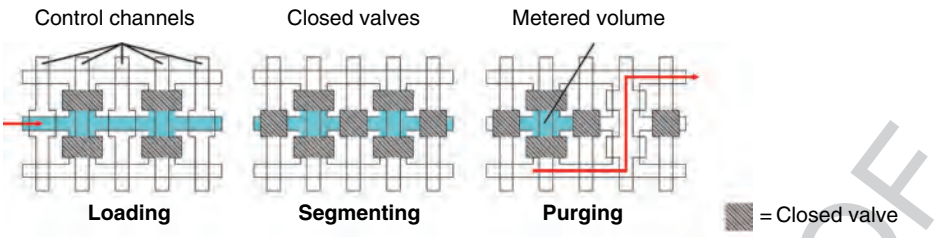

f0090 **Figure 18** Using crossed fluid channels, liquid metering is also possible on the microfluidic large-scale integration (LSI) platform. In the first loading step, a certain fluid channel is addressed using the multiplexer structure and filled with liquid. In the second step, the liquid within that channel is segmented by closing the valves between the chambers. In the last step, fluid that should not be kept is purged via two additional fluid channels on both sides of the metering channel.

liquid plug within the fluid channel is segmented into several equal-sized (if the chambers all have the same dimensions) liquid compartments. During the last step, a washing liquid is pumped through the system, addressed to the fluid channel right next to the metering fluid line. All chambers that should not contain a metered volume of the initial liquid after the metering process are now purged vertically since the vertical valves to the two neighboring channels are now open. As a result a metered liquid volume is retained in designated metering chambers only.

p0475 The described unit operations should demonstrate the enormous possibilities of the platform. Depending on the design of the fluid channel and the control channel layer, many different processes for the conduction of certain assay protocols can be realized. To give an impression on these possibilities, two application examples, protein crystallization and nucleic acid processing, are described in Section 2.13.4.3, both realized on the microfluidic LSI platform.

s0215 ## 2.13.4.3 Application Examples

s0220 ### *2.13.4.3.1 Protein crystallization*

p0480 How does this protein that causes a certain disease look like? Answering this question in an acceptable period of time would cause a revolution in the merely statistically driven pharmaceutical research based on the HTS of large compound libraries. The trail-and-error approach would be replaced with a more rational procedure; the systematic tailoring of a complementary active compound to the known structure of the target protein would then be feasible (structural biology).

p0485 In order to investigate the structure of a protein, first of all it has to be transferred into a crystalline state suitable for X-ray crystallography. As there is currently no way to predict crystallization conditions *a priori*, a large number of experiments are required to uncover successful crystallization conditions. It is obvious that a microfluidic-based solution would have many advantages, since it requires only a small amount of protein, and precise volume definition as well as controllable mixing processes by diffusion can be implemented.

p0490 The crystallization method that is used in the microfluidic LSI platform is called free interface diffusion (FID) (b0650 Salemme 1972). It is based on the counterdiffusion of the protein and the precipitant solution through the liquid–liquid interface between these two phases. During the diffusion process, the concentration profile changes and crystal growth is initiated as soon as the appropriate conditions are met. In conventional FID setups a stable and undisturbed liquid–liquid interface between the protein and the precipitant solution has to be assured by proper liquid handling to avoid unwanted mixing. Because of buoyancy-driven convection caused by density differences this can hardly be achieved in macroscopic capillaries.

p0495 Within a microfluidic crystallization structure, however, a stable interface with diffusion-based mixing only can be implemented very easily (negligible gravitational effects due to high surface-to-volume ratio). The successful growth of protein crystal has been demonstrated in a microfluidic chip based on the LSI technology (b0300 Hansen and Quake 2003, b0305 Hansen *et al.* 2002). Overall, 144 crystallization experiments can be performed in parallel on the presented microfluidic chip. One such microfluidic unit cell is depicted in **Figure 19(a)** and comprises microchambers of 5, 12.5, and 20 nl. They are arranged and coupled to define mixing ratios of 1:4, 1:1, and 4:1 with a fixed total volume of 25 nl.

p0500 The crystallization assay starts with the filling of the chambers while the valve between the chambers (horizontal yellow bar in the middle) is still closed (**Figure 19(b)**). The air is vented via diffusion

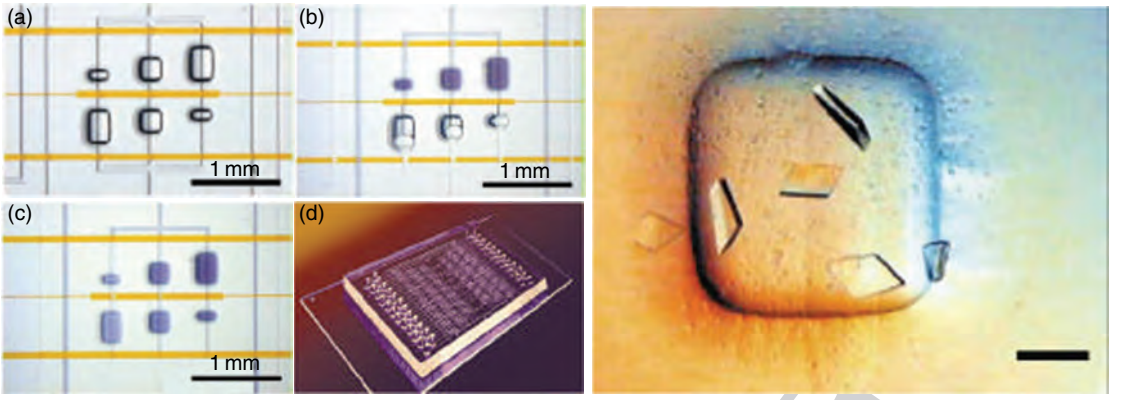

f0095 **Figure 19** *Left*: Microfluidic crystallization structures. (a) Three crystallization assays with different mixing ratios (1:4, 1:1, 4:1) and a fixed total volume of 25 nl. (b) The central interface valve is closed and the chamber is filled with solution while the air diffuses through the bulk elastomer. (c) The intermediate valve is opened, initiating the diffusional mixing process. (d) The complete chip features 48 unit cells performing 144 simultaneous crystallization experiments while using 3 μl of protein sample only. *Right*: Example of protein crystals grown in the described microfluidic structure (scale bar, 100 μm). They have been grown within 12 h only, while the conventional process takes over a week. (Reprinted with permission from Hansen C, Quake S R 2003 Microfluidics in structural biology: Smaller, faster··· better. *Curr. Opin. Struct. Biol.* **13**, 538–44. Copyright 2003 Eksevier.)

through the gas-permeable bulk elastomer during the filling of the dead-end chambers. The filling valves are closed in the next step and the counterdiffusion is initiated as soon as the middle valve is opened (**Figure 19(c)**). The concentration within both chambers now changes with time due to the diffusion of species through the connecting channel. A crystal growth initiates in chambers with proper transient concentrations distributions only.

p0505 The channel between the two chambers has a small cross-section (10 μm × 100 μm) compared to that of the two chambers (300 μm × 100 μm). Thus, it acts like a diffusion impedance, slowing down the diffusion process and implying almost homogeneous concentrations within the chambers. As a concentration gradient is apparent only along the length of the channel, the rate of equilibrium can be influenced by the geometry of the structure (namely the length of the channel and the ratio of the chamber volume to the channel cross-sectional area). The end point itself, however, is predefined by the volume of the two precisely fabricated chambers. The accurate control over the kinetics of equilibration without changing the chemical evolution has important implications for crystal optimization where it is often desirable to approach crystallization conditions slowly while conserving the successful thermodynamic variables (b0300 Hansen and Quake 2003).

p0510 The parallel implementation of 48 unit cells in a single crystallization chip facilitates 144 different simultaneous protein crystallization reactions while consuming only 3.0 μl of protein solution – only 20 nl per assay (**Figure 19(d)**). **Figure 19** (*right*) shows a crystal that has been grown within 12 h using the microfluidic LSI chip. In a conventional system, this process lasts over 1 week. The protein crystallization technology on the LSI platform has been commercialized by the company Fluidigm (Topaz® technology).

2.13.4.3.2 Nucleic acid isolation

s0225 p0515 A second application example of the microfluidic LSI platform is the purification of nucleic acids from a small amount of cells. The isolation of DNA or mRNA from microbial or mammalian cells, including their lysis on-chip, has been showed by Stephen Quake's group at Stanford (b0350 Hong and Quake 2003, b0355 Hong *et al.* 2004). For the extraction of DNA from a cell suspension, the cell membrane has to be destroyed first (lysis of the cell). Then, the DNA has to be specifically separated from the residual cell constituents within the solution. This extraction protocol is completely implemented on the microfluidic platform using the basic unit operation structures for valving, metering, mixing, and switching of fluids.

p0520 The channel network for performing the DNA isolation assay is depicted in **Figure 20(f)**. Three extractions can be performed in parallel with three rotary reactors aligned vertically (the different fluid channel lines are colored with food dye for visualization). The chip is operated in two different modes, loading and processing. In the loading mode, the

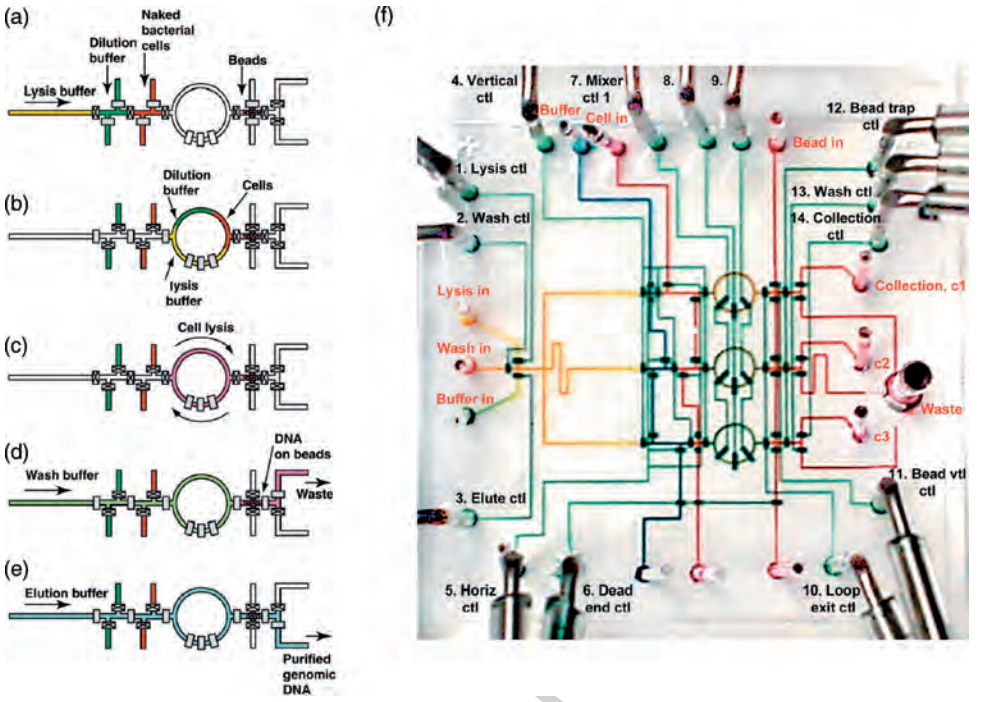

f0100 **Figure 20** Microfluidic large-scale integration (LSI) DNA purification chip (f) and the course of an isolation protocol. (a) The bacterial cell culture, the dilution, and the lysis buffer are introduced into the chip via fluid channels (open valve, rectangle; closed valve, x in rectangle). (b) The vertical valves are opened, and the three liquids are externally pumped into the circular mixing channel. (c) Mixing is initiated by circular peristaltic pumping. (d) The mixture containing the lysed cells is flushed by a washing buffer over a column of microbeads. The DNA molecules bind to the bead surface and the buffers and the residual cell constituents are directed toward the waste outlet. (e) The elution buffer is flushed over beads, the DNA molecules are transferred into the liquid phase again and leave the structure through the lower outlet. (Reprinted with permission from Macmillan Publisher Ltd: Hong J W, Studer V, Hang G, Anderson W F, Quake S R 2004 A nanoliter-scale nucleic acid processor with parallel architecture. *Nat. Biotechnol.* **22**, 435–9. Copyright 2004.)

valves of the control layer are activated, so that the liquids flow in the north/south direction. During this step, the horizontal metering chambers are loaded with the diluent buffer (green), the bacterial cell solution (red), and the bead suspension (white) as depicted in **Figure 20(a)**. Then, the control valves on the north/south channels are closed leading to segments of the respective liquids. Also a certain volume of bead suspension is metered within the microchannel to define the number of beads that lead to a defined binding capacity for the later solid-phase extraction (100 pg of DNA on the beads of diameter 2.8 µm).

p0525 To exploit the high integration possibilities of the platform, the three isolation structures differ with regard to the volume of the bacterial cell solution. The volumes used in the top, middle, and bottom structure are 1.6, 1.0, and 0.4 nl, respectively. Since the total volume of each rotary reactor is the same (5 nl), 0.4-, 1.0-, and 1.6-nl dilution buffer are metered on the platform and added to the cell solution. Subsequently, the chip is switched to the processing mode: valves are actuated such that flow is allowed only in an east/west direction and all the three batch reactors are operated in parallel. Lysis buffer (3.0 nl) is injected from the left to flush the cell solution and the dilution buffer into the rotary reactor (**Figure 20(b)**).

p0530 Within the rotary reactor, the three different valves are actuated sequentially to generate a circulating flow. This reduces the mixing time from several hours for merely diffusional mixing to several minutes in the micromixing scheme (**Figure 20(c)**). As a result, the bacterial cells within the reactor are completely lysed after some minutes and can be forwarded to the next process step.

p0535 Now, the valve at the outlet of the rotary reactor is opened, and the solution containing the lysed cells is flushed out of the ring over the aggregated beads and leaves the structure via the upper waste outlet (**Figure 20(d)**). The beads are retained within the channel by a partially closed valve, where the beads larger than the valve opening cannot pass through. The DNA molecules within the lysed solution bind

to the bead surface. In a subsequent washing step, all unbound components are washed away from the bead column and likewise drained through the waste outlet.

p0540 Purified DNA is recovered from the chip in the last process step, by introducing elution buffer from the left side of the chip, which passes over the aggregated beads. The DNA is transferred back into the liquid phase and leaves the system through the lower DNA outlet. Two valves at the end of the structure act as a fluidic switch, guiding the liquid flow either toward the waste or toward the purified DNA outlet. The DNA gained from the on-chip isolation is now readily available for further analysis or manipulation. **Figure 20(f)** shows the complete microfluidic chip for four parallel DNA isolation assays; it has 26 access holes, 1 waste hole, and 54 integrated valves within the overall 20 mm× 20mm chip.

p0545 Purified genomic DNA from less than 28 bacterial cells (*Escherichia coli* culture) could be successfully isolated on the platform. Additionally, seven chips were used as negative controls in which pure water was introduced instead of bacteria, and no signal was detected within the off-chip detection (PCR amplification). Thus, it could be shown that it is possible to reduce the required amount of bacterial cells for the isolation of the needed DNA using the microfluidic LSI platform. This corresponds to an increase in the sensitivity of this process by three to four orders of magnitude compared with that of conventional methods (Hong[b0355] *et al.* 2004).

p0550 Based on this technology, a complete nucleic acid processor is currently being developed in Stephen Quake's group at Stanford University. Starting from single cells, the isolation of nucleic acid, with a subsequent synthesis of cDNA (Marcus[b0510] *et al.* 2006a), PCR (Liu[b0474] *et al.* 2003), or real-time polymerase chain reaction (RT-PCR) (Marcus[b0515] *et al.* 2006b) completes the platform for complete single-cell gene expression analysis.

s0230 2.13.4.4 Strength and Challenges of the Platform

p0555 The microfluidic LSI platform has certainly the potential to become one of the foremost microfluidic platforms for highly integrated applications. It is a flexible and configurable technology, which stands out owing to its suitability for LSI. The PDMS fabrication technology is comparably cheap and robust, and it can be used to fabricate disposables. Reconfigured layouts can be assembled from a small set of validated elements, and design iteration periods for new chips are on the order of days. Some of the system functions are hardware defined by the fluidic circuitry but others, such as process sequences, can be programmed from outside easily. The approach of building up an entire processor from a very limited set of elementary units resembles the microelectronics industry in which functional steps are configured by a circuit of transistors and capacitors.

p0560 Limitations of the platform are related to the material properties of PDMS: for example, chemicals that are not inert to the elastomer cannot be processed, or elevated temperatures, such as in microreaction technology, are not feasible. Also the implementation of applications in the field of point-of-care diagnostics, where often a handheld device is required, does not seem to be beneficial using the LSI platform. The external pressure sources and valves have to be shrunk to a smaller footprint, which is technically feasible of course, but the costs would be higher in comparison to other platform concepts.

2.13.5 Centrifugal Microfluidics s0235

p0565 The approach of using centrifugal forces to process samples and reagents dates back to the end of the 1960s (Anderson[b0020] 1969, Burtis[b0070] *et al.* 1972). At that time, centrifugal analyzers were used to transfer and mix a series of samples and reagents in the volume range from 1 up to 110 µl into several cuvettes followed by spectrometric monitoring of reactions and real-time data processing. In the beginning of the 1990s, the company Abaxis Inc. (2006) developed the portable clinical chemistry analyzer (Schembri[b0635] *et al.* 1992, 1995[b0640]). The system consists of a plastic disposable rotor for processing the specimen, dried reagents preloaded to the cartridge, and an analyzer instrument for actuation and readout (**Figure 21**).

p0570 The next generation of centrifugal devices emerged from the technical capabilities offered by microfabrication and microfluidic technologies (Duffy[b0150] *et al.* 1999, Ekstrand[b0175] *et al.* 2000, Madou[b0485] and Kellogg 1998, Madou[b0490] *et al.* 2001). Length scales of the fluidic structures in the range of a few hundred micrometers allow parallel processing of up to a hundred units assembled on the disk. This enables a high throughput of many tests by highly parallel and automated liquid handling. In addition, the new opportunities arising from the miniaturization of the centrifugal fluidics cut down the assay volumes to <1 µl. In particular, fields such as drug screening, where precious samples are analyzed, benefit from the low assay volumes.

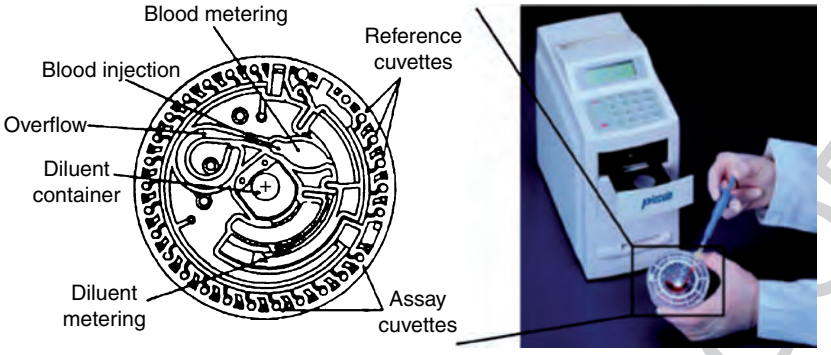

f0105 **Figure 21** *Left*: Schematic of the rotor comprising the fluidic channels, reservoirs, and the cuvettes for optical detection. (Source: Schembri C T, Ostoich V, Lingane P J, Burd T L, Buhl S N 1992 Portable simultaneous multiple analyte whole-blood analyzer for point-of-care testing. *Clin. Chem*. **38**, 1665–70. Reproduced by permission of American Association for Clinical chemistry.) *Right*: Image of the portable analyzer. (Source: Abaxis Inc. 2006 Union City, CA, USA, www.abaxis.com, accessed 2006.)

Furthermore, the miniaturized assays can also offer shorter time-to-result and thus either higher throughput or shorter therapeutic turnaround times for critical care applications. The centritugal microfluidic approach is also referred to as 'lab-on-a-disk'.

s0240 ### 2.13.5.1 Introduction to the Lab-on-a-Disk Approach

p0575 The basic concept of centrifugal microfludics is the transport of fluids within a rotating channel by means of the centrifugal force. For a module rotating with an angular frequency $\omega = 2\pi v$, the centrifugal force density

$$f_\omega = \rho\omega(\omega \times \mathrm{r}) \qquad [3]$$

acts on a fluid of mass density ρ at a radial position r. This pumping force is directed in a radial outward direction, thus driving liquid plugs toward outer diameters as long as they possess a net radial plug length. Besides the liquid properties, only the radial position and the rotational speed define the pumping force and thus the liquid handling actuation. This eases the parallelization of several identical microfluidic structures being placed on one rotating substrate at different angular, but the same radial position. Although these structures experience the same centrifugal force, they still operate independently of each other, thus making this scheme of parallelization very robust.

p0580 The substitution of pressure-generating pumping devices by the pulse-free centrifugally initiated fluid flow enables complex liquid handling processes within a completely passive microstructure. Without any moving part, the rotating modules called disks or CDs can be fabricated using cost-efficient microfabrication technologies for plastics like injection molding. The processes are readily available from the audio compact disk industry, where microstructure polymer discs have been injection molded for several decades. Low-cost disposable disks combined with a nondisposable rotary drive and detecting unit build the modular centrifugal microfluidic platform.

p0585 Besides the centrifugal force, the Coriolis force can also be used to manipulate liquid flows on the centrifugal platform as depicted in **Figure 22**. It acts on every moving liquid portion within the rotating frame of reference and scales with the flow velocity as well as the frequency of rotation. The Coriolis pseudo force is always directed perpendicular to the direction of flow and even prevails over the centrifugal force over a critical frequency of rotation (b0135 Ducrée *et al.* 2005).

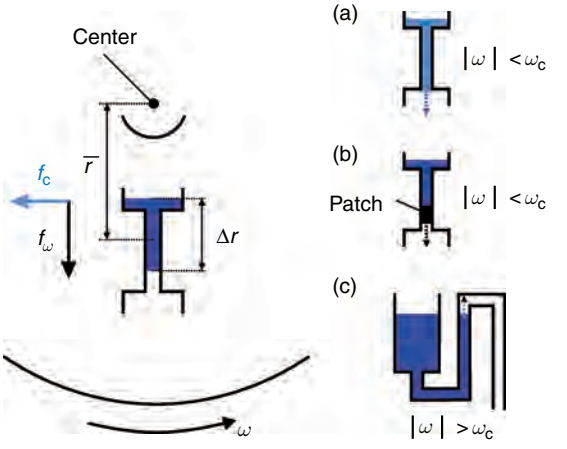

f0110 **Figure 22** Principal centrifugal approach and schematic sketch of the three valving techniques on the centrifugal platform. (a) Geometric capillary valve, (b) hydrophobic valve, and (c) hydrophilic siphon valve.

s0245 ## 2.13.5.2 Microfluidic Unit Operations on the Centrifugal Platform

s0250 ### 2.13.5.2.1 *Fluid transport*

p0590 On the centrifugal platform, two pressure-generating mechanisms are employed to accomplish complex liquid processing protocols. The centrifugal force f_ω (see eqn [3]) enables the liquid transport in radial outward direction. This actuation principle can be scaled over a wide range by the frequency of rotation. Small flow rates in the order of nanoliter per second can be accomplished to extract molecules from a continuous flow while passing immobilized capture molecules. For this purpose the residence time for the streaming molecules have to be larger than the time for diffusion of the immobilized molecules. In return also high throughput up to $1\,\mathrm{ml\,s^{-1}}$ has been reported in a 3 cm-long microchannel of $260\,\mu\mathrm{m} \times 195\,\mu\mathrm{m}$ cross section for microprocess engineering applications (Haeberle *et al.* 2005). So scaling of flow rates over six orders of magnitude has been demonstrated. Many different (bio-) fluids can be processed on the platform, independent of their chemical composition, ionic strength, conductivity, or pH value opening a wide field of possible applications.

p0595 The second microfluidic effect that plays an important role for liquid propulsion is capillarity. As soon as the disk is at rest or rotates with a small frequency of rotation, the always coexistent capillary pressure gains impact. If there is at least one liquid–gas transition, a pressure drop appears at the interface. Liquid plugs can be transported in any direction, especially toward the center of the disk also in a hydrophilic channel using the capillary pumping mechanism. This is due to the fact that the capillary pressure is independent of the angular and radial position of the channel. It, for example, allows the complete initial priming of microchannels if the proceeding meniscus experiences a higher capillarity than the capillary pressure at the other end of the liquid plug. Most of the microfluidic structures for the different unit operations described in this section are based upon the interplay of centrifugal and capillary transport mechanisms.

s0255 ### 2.13.5.2.2 *Valving*

p0600 Stopping of liquid flows, that is, the realization of a liquid valve, can be realized with different microfluidic structures on the centrifugal platform. A very simple valve arises at the sudden expansion of a microfluidic channel, e.g., into a bigger reservoir. The valving mechanism of this capillary valve is based on the surface tension that develops at this expansion and prevents further proceeding to the liquid–gas interface (**Figure 22(a)**). Under rotation, however, a certain pressure load

$$p_\omega = \rho\omega^2\overline{r}\Delta r \qquad [4]$$

due to the artificial gravity is applied on the liquid–gas interface. It depends on the liquid density ρ, the frequency of rotation ω, the mean radius $\overline{r}$, and the radial length Δr of the liquid plug (Duffy *et al.* 1999). As soon as this pressure exceeds the surface tensional counter pressure, the valve breaks. For a given liquid plug position and length, i.e., for a given set of geometric parameters, the valve can be influenced by the frequency of rotation only and a critical burst frequency ω_c can be attributed to every valve structure.

p0605 Another possibility to stop the liquid flow within a channel is the local hydrophobic coating of the channel walls. The hydrophobic patch defines the stop position for the liquid–gas interface within a hydrophilic channel of constant channel cross section (**Figure 22(b)**). Also this valve is opened as soon as the rotational frequency exceeds the critical burst frequency ω_c and the pressure load due to the liquid plug above the hydrophobic valve overcomes capillarity. The net capillary pressure

$$\Delta p_\theta \propto 2\sigma\left(\frac{\cos(\theta_1)}{r_1} - \frac{\cos(\theta_2)}{r_2}\right) \qquad [5]$$

of a liquid plug with surface tension σ, located in a channel of radius r_1 at the first and r_2 at the second liquid–gas interface can be used besides the radial plug length and position of the plug to engineer the critical burst frequency ω_c.

p0610 A third method utilizes the interplay of inertial and capillary forces in a different way. At high frequencies of rotation, the centrifugal force tends to leverage of the two liquid–gas interfaces within a U-shaped hydrophilic siphon channel of different cross sections (**Figure 22(c)**). Only a small difference in the radial position caused by the unequal channel cross sections and thus capillary pressures can be observed, which is negligible for high frequencies of rotation. Below a critical frequency ω_c, however, the meniscus proceeds toward the smaller duct due to the higher capillary force therein. As soon as the meniscus has passed the bend and proceeds in a radial outward direction again there comes a moment when a net radial length $\Delta r > 0$ exists. From that moment on, the centrifugal force supports the moving meniscus and the whole liquid plug escapes the siphon.

p0615 All the valves described are passive structures that do not need any movable parts within the chip. They are opened or closed by the frequency of rotation only. Therefore they can be considered as preprogrammed microfluidic networks with imprinted geometric parameters once fabricated. An alternative approach for the control of liquid flows on the centrifugal platform is followed by the company Spin-X Technologies (2006), Switzerland. A laser beam individually opens fluidic interconnects between different channel layers on a plastic substrate (virtual laser valve, VLV). This enables an online control of the liquid handling process on the rotating module almost independently of the geometry of the structures. Consequently, metered volumes and incubation times can be manipulated within a wide range. Hence, the Spin-X platform works with a standardized fluidic cartridge that is not custom-made for each specific application, but can be programmed right before the measurement or even online during a running process.

s0260 ***2.13.5.2.3 Metering and aliquotting***

p0620 The valving principles, described in Section 2.13.5.2.2, present the basic fluidic function for many unit operations on the centrifugal platform. Using hydrophobic valves, for example, the exact metering of liquid volumes can be accomplished, which is one of the most important unit operations needed for all quantitative assay protocols. Especially in point-of-care applications, only an undefined sample volume, for example, a droplet of blood derived from the fingertip, is available. However, for quantitative analysis a defined sample volume is required, which has to be defined within a designated metering structure. The high precision of microfabrication technologies facilitates small coefficients of variations (CVs = standard deviation/mean value) down to metered volumes in the lower nanoliter range (Steinert *et al.* 2007).

b0730

p0625 Typical metering structures exhibit a hydrophobic valve at the outlet and an overflow channel connected to a metering chamber of designated volume (Steigert *et al.* 2005). During the metering process, the liquid initially fills the metering chamber at a frequency below the burst frequency ω_c. The liquid stops at the hydrophobic valve (**Figure 23**). Venting of the chamber is done via the outlet or a separate venting channel. After the metering chamber is completely filled with liquid, the excessive fluid volume is removed via an overflow channel and is cut off at a defined position at the inlet of the structure. Thereby, the volume is defined to the geometrically imprinted volume of the metering chamber while the valve still holds back the liquid since the centrifugal pressure falls short of the critical pressure of the valve.

b0715

p0630 In the last step, the frequency is increased and the hydrophobic valve breaks to release the metered liquid portion through an outlet channel toward further downstream processes. Using this technology, metered liquid volumes from the microliter to the nanoliter range with an extremely high reproducibility, e.g., a CV < 5% for a volume of 300 nl, have been demonstrated (Steigert *et al.* 2006).

b0720

p0635 By arranging several metering structures of, for example, different volumes interconnected via an appropriate distribution channel, simple aliquotting structures can be realized (Zoval and Madou 2004).

b0920

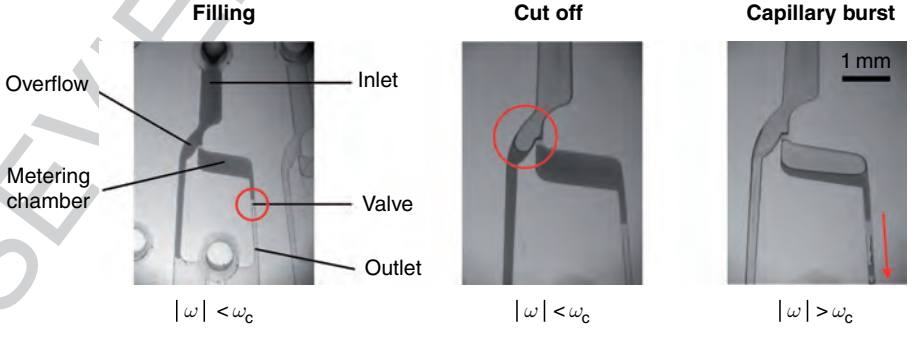

f0115 **Figure 23** Metering structure based on a hydrophobic valve. In the initial filling stage, the fluid network is primed with an undefined sample volume. After the metering chamber is filled, the residual fluid is cut off at a frequency still beyond the critical burst frequency of the valve ω_c. In the last step the frequency is increased over the burst frequency of the valve leading to a radial drainage of the metered volume through the structures outlet. (Source: Steigert J, Grumann M, Brenner T, Riegger L, Harter J, Zengerle R, Ducrée J 2006 Fully integrated whole blood testing by real-time absorption measurement on a centrifugal platform. *Lab Chip* **6**, 1040–4. Reproduced by permission of The Royal Society of Chemistry.)

These structures split a sample into several defined volumes enabling the parallel conduction of several assays from the same sample. Multiparameter diagnostics and pharmaceutical screening are possible applications where such an aliquotting structure is required.

s0265 ### 2.13.5.2.4 Mixing

p0640 Mixing of miscible fluids within the laminar regime on the centrifugal platform can be in the simplest case accomplished by joining two microfluidic channels to a single meander-shaped channel. By maintaining the feeding flows, a stoichiometric correct mixing ratio can be achieved. The required length of the mixing channel depends on the flow rate, i.e., the retention time within the channel, as well as the diffusional velocity in the transversal direction. In general, mixing processes can be speeded up by increasing the interfacial area between the phases to be mixed. However, if two liquid streams are simply contacted within the laminar regime, the contact interface equals the channel height and does not increase in the downstream direction. An increasing interfacial area along the direction of flow is possible if the liquid moves not only along the channel but also perpendicular to it (transversal advection).

p0645 Considering mixing of continuous liquid flows within a radial-directed rotating channel, the transversal-directed Coriolis force f_C automatically generates a transversal liquid flow $u(f_C)$ as depicted in **Figure 24** (Ducrée *et al.* 2005, 2006, Haeberle *et al.* 2005). The Coriolis force scales with the radial flow velocity $u(f_\omega)$, which has its maximum in the center of the channel due to the parabolic radial velocity profile (no slip boundary condition at the channel walls). Therefore, at the center of the channel, the flow experiences the highest Coriolis force f_C directed laterally. This leads to a transversal liquid movement $u(f_C)$ from the center to the left and backward on the upper and lower channel parts where the smallest Coriolis counter force is present. This transversal advection, also called Coriolis stirring, constantly increases the interfacial area between the two concurrent liquid flows and thus accelerates mixing.

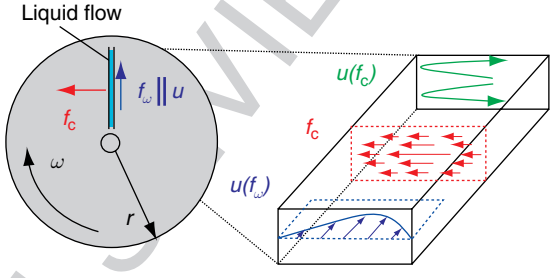

f0120 **Figure 24** The Coriolis stirring effect within a radial, rotating microchannel. The inhomogeneous transversal Coriolis force field f_C initiates a transversal advection $u(f_C)$ thus increasing the interface between two liquid streams. (Source: Haeberle S, Brenner T, Schlosser H P, Zengerle R, Ducrée J 2005 Centrifugal micromixer. *Chem. Eng. Tech.* **28**, 613–16. Reproduced by permission of Wiley VCH.)

p0650 A continuous centrifugal micromixer, utilizing the Coriolis stirring effect, showed an increasing mixing quality toward very high volume throughputs of up to 1 ml s^{-1} per channel. This is enabled by the increasing impact of the transversal Coriolis force toward higher flow rates (Haeberle *et al.* 2005). It opens an interesting and so far barely explored microprocess engineering field for centrifugal microfluidic technologies, which however is not discussed in detail here.

p0655 Besides the mixing of continuous liquid flows, the homogenization of discrete and small liquid volumes inside small chambers is also of importance especially when analyzing small sample volumes (batch-mode mixing). One possibility to enhance the mixing of two small liquid portions is to guide them into a common chamber. The streams violently splash against a common chamber wall causing their efficient mixing (Zoval and Madou 2004).

p0660 Another possibility is the active agitation of the liquid within a mixing chamber either by using periodically actuated magnetic microparticles under rotation (Grumann *et al.* 2005) or by means of an inertial effect induced by a fast change of the sense of rotation (shake-mode mixing). The course of mixing within a microchamber under the impact of the shake mode is depicted in **Figure 25** (*left*). The course of mixing strongly depends on the applied mixing scheme as depicted in **Figure 25** (*right*). The shake-mode mixing under an alternate spinning protocol drastically enhances the mixing efficiency. Characteristic mixing times on the order of several seconds compared to several minutes for pure diffusion-based mixing can be achieved. The shake-mode mixing has been integrated into a complete colorimetric assay protocol as described in Section 2.13.5.3.4.

s0270 ### 2.13.5.2.5 Switching

p0665 Switching liquid flow from one common channel to one of at least two continuative channels is very important, e.g., for extraction protocols. A promising switching method on the centrifugal platform should

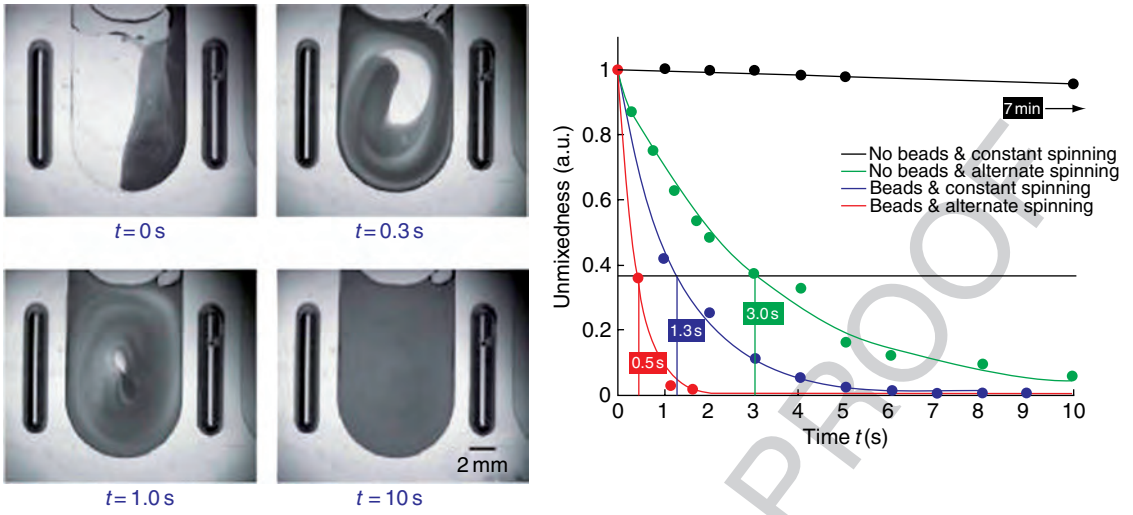

f0125 **Figure 25** *Left*: Two initially separated liquids (pure water on the left and ink on the right) are mixed under the impact of the shake-mode mixing within 10 s. *Right*: Typical mixing times for different mixing schemes: no beads and constant spinning represent mixing via diffusion only. Alternate spinning describes the shake-mode mixing scheme. Additional magnetic beads within the chamber can be used to further decrease mixing times. (Reprinted with permission from Steigert J, Grumann M, Brenner T, Mittenbühler K, Nann T, Rühe J, Moser I, Haeberle S, Riegger L, Riegler J, Bessler W, Zengerle R, Ducrée J 2005 Integrated sample preparation, reaction, and detection on a high-frequency centrifugal microfluidic platform. *J. Assoc. Lab. Autom.* **10**, 331–41. Copyright 2005 Elsevier.)

be possible without the integration of any active or moving part. Following this philosophy, a liquid switch availing the transversal Coriolis force to guide liquid flows between two outlets at the branching of an inverse Y-shaped channel has been presented (b0055 Brenner *et al.* 2005).

p0670 The functional principle is depicted in **Figure 26**. Depending on the sense of rotation, the Coriolis force is either directed to the left (counterclockwise rotation) or to the right (clockwise rotation). One common radial channel is split toward a left and a right reservoir at the branching. The liquid stream is directed into one of these reservoirs depending on the direction of the Coriolis force, i.e., the sense of rotation. A fully reliable switching behavior has been reported for frequencies above ~55 Hz for a continuous flow. An improved version of Coriolis-based switching operates on individual droplets and enables switching of small flow rates of 160 nl s^{-1} only at low frequencies down to a few Hz (b0290 Haeberle *et al.* 2006b).

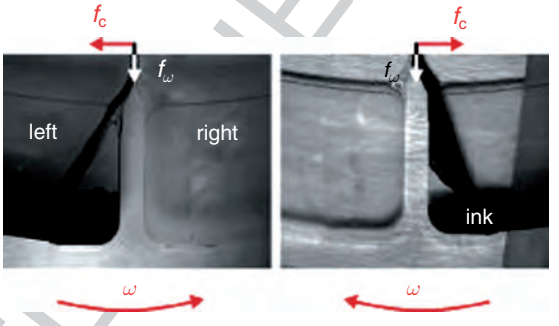

f0130 **Figure 26** Liquid streams are switched between two possible outlet channels at the Coriolis flow switch, an inverse Y-shaped channel. (Source: Brenner T, Glatzel T, Zengerle R, Ducrée J 2005 Frequency-dependent transversal flow control in centrifugal microfluidics. *Lab Chip* **5**, 146–50. Reproduced by permission of The Royal Society of Chemistry.)

p0675 Another method for liquid routing based on different wetting properties of the continuative channels has been reported by b0275 Gyros AB (2006), Sweden. The liquid stream is initially guided toward a radial channel, exhibiting a hydrophobic patch at the beginning. Therefore, the liquid is deflected into another channel, not the hydrophobic channel next to the radial one. For high frequencies of rotation, the approaching liquid possesses sufficient energy to overcome the hydrophobic patch and is therefore routed into the radial channel. This enables the frequency-dependent routing of liquid flows between two consecutive channels (b0170 Ekstrand and Thorsen 2005).

2.13.5.2.6 Droplet formation

s0275

p0680 Monodisperse droplet emulsions can be generated in an adopted flow focusing structure under the centrifugal gravity field. Trains of water droplets dispersed into a continuous oil stream with droplet volumes

between 5 and 22 nl with a CV of the droplet diameter below 2% are reported (Haeberle *et al.* 2006c). The flow focusing structure contacts a central water-guiding channel to two symmetric oil flows at a junction. During the droplet formation process, a water plug is expelled out of the central channel into the junction area and is subsequently forced through a geometrical constriction. This leads to the controlled break-off of small water droplets into the continuous oil flow and thus a monodisperse droplet emulsion. Additional droplet-based unit operations like splitting of droplets or droplet sedimentation have also been realized on the centrifugal multiphase platform.

s0280 ***2.13.5.2.7 Separation***

p0685 Within the artificial gravity field under rotation, different phases can be separated if they possess different mass densities. This process is called sedimentation and is used as a standard routine in laboratory centrifuges. Since lab-on-a-chip systems, especially within the field of point-of-care testing, deal with raw biological samples, which have to be pretreated before the analytical assay can be conducted, a system-immanent separation method is of great importance.

p0690 The extraction of plasma from a blood sample is the prevalent first step in a complete analytical protocol starting from an untreated whole blood sample. Since blood plasma is less dense than the white and red blood cells it is found in the upper phase, the so-called supernatant after sedimentation. The separation of the cellular and plasma phase in a sedimentation chamber, however, is just one part of a complete plasma extraction process. The second step is the spatial extraction of the gained plasma from the cellular pellet, located at the bottom of the chamber. This extraction is done by manual or automated pipetting in classic macroscopic plasma extraction protocols. However, to arrive at an extraction method capable of the seamless integration into automated centrifugal platform protocols, the plasma phase has to be extracted automatically within the microfluidic channel network.

p0695 Two methods have been proposed to achieve an integrated plasma extraction on the centrifugal platform. In the first method, plasma and cells are separated in a sedimentation chamber. A capillary extraction channel branches from the sedimentation chamber at radial position where only plasma is expected. It is used to extract the supernatant plasma phase at lower frequencies via capillary action (b0640 Schembri *et al.* 1995). The whole blood sample has to be metered prior the sedimentation process in order to guarantee proper function and also to result in a metered extracted plasma volume. A complete analyzing system using this extraction method is described in more detail in Section 2.13.4.3.

p0700 Another method uses a preseparation of the cellular and plasma phase during the sample flow through an azimuthal-aligned channel of just 300 µm radial width (b0285 Haeberle *et al.* 2006a). The obtained plasma fraction is thereafter split from the cellular components by a decanting process (**Figure 27**, *left*).

p0705 The whole extraction proceeds as follows: Initially, a raw blood sample is metered to a fixed volume defined by an overflow channel next to the outlet of the metering chamber. Subsequently, the metered sample is forwarded via the drain channel to the decanting structure. Within the drain channel the blood is preseparated with the plasma phase flowing on top of the cellular phase. The two joint streams separate when they enter the decant chamber. The more dense cellular phase sinks outward while the less dense plasma phase stays on top. When the decant chamber is entirely filled, pure plasma in the supernatant overflows into a plasma chamber (**Figure 27**, *right*). The course of separation concludes when the entire blood sample has been transported from the metering chamber into the

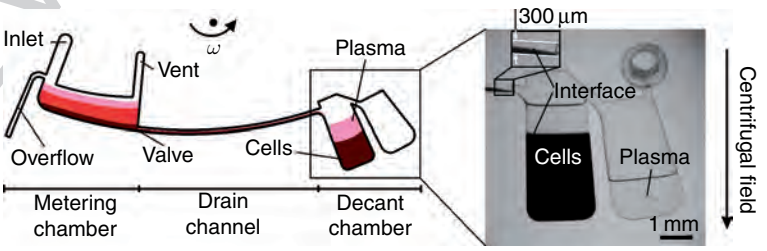

f0135 **Figure 27** *Left*: Flow scheme of the decanting structure for plasma extraction from a raw blood sample. *Right*: Purified plasma is decanted into a separate reservoir while the cellular pellet is retained at the bottom of the decant chamber. (Source: Haeberle S, Brenner T, Zengerle R, Ducree J 2006a Centrifugal extraction of plasma from whole blood on a rotating disk. *Lab Chip* **6**, 776–81. Reproduced by permission of The Royal Society of Chemistry.)

decant and the plasma chamber. The extracted plasma volume is defined by the chamber geometries and can therefore be directly forwarded to further downstream processes, e.g., by a capillary duct.

p0710 This centrifugal flow separation technique extracts 2 µl of plasma from a raw blood sample that is initially metered to 5 µl. Typical separation times of 20 s can be achieved for moderate spinning frequencies of 40 Hz. The residual cell concentration in the bulk plasma is <1‰.

s0285 ## 2.13.5.3 Application Examples

s0290 ### *2.13.5.3.1 Blood test (Abaxis Picolo®)*

p0715 The Abaxis Picolo® system (Abaxis Inc., 2006) is a centrifugal analyzer for near-patient testing (Schembri *et al.* 1992, 1995). The rotor, with a diameter of approximately 8 cm, is made of molded 2 cm-thick polymethylmethacrylate (PMMA) plastic (see **Figure 21**). It consists of a series of many interlinked chambers and passages. The movement of fluid is controlled by a series of stop junctions, capillaries, and siphons managed by the use of centrifugal force. The center of the rotor hosts a diluent container while dried reagent beads are placed in cuvettes in the periphery of the rotor. Fifteen cuvettes are reserved to analyze the patients' sample and further ten are used as internal quality control. The loading port for blood injection is coated with heparin to prevent blood coagulation.

p0720 The operator adds an unmetered blood sample between 90 and 120 µl. The sample preparation steps such as metering, blood separation, and mixing are performed in the rotor in an automatic fashion. Once the rotation starts, the centrifugal force propels the diluent outward into a chamber that contains a ball coated with dye. Simultaneously, the blood sample is metered to 75 µl and moves into the separation chamber, where 20 µl of plasma is obtained within 30 s. The blood plasma is afterwards diluted and distributed to the cuvettes for detection. The chemical reactions in the cuvettes are optically monitored and checked with an enzymatic control in the reference cuvettes before the results from the analysis are reported. The centrifugal platform enables point-of-care measurements of multiple analytes, e.g., glucose of whole blood samples in about 10 min. At present, Abaxis supplies the Piccolo platform for medical and veterinary diagnostics.

s0295 ### *2.13.5.3.2 Enzyme-linked immunosorbent assay (LabCD)*

p0725 Madou *et al.* from University of California, Irvine, CA, showed a series of capillary valves to perform enzyme-linked immunosorbent assays (ELISAs) on the centrifugal platform (Lai *et al.* 2004). An antibody is immobilized in the detection reservoir 2 in an off-chip protocol (**Figure 28**). Different reagents are then loaded into their corresponding reservoirs, numbered 3–7 on the CD, which is then mounted on a motor plate.

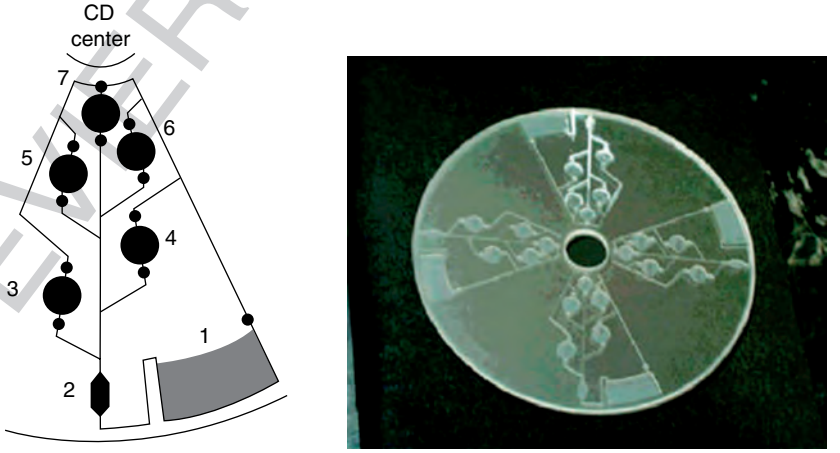

f0140 **Figure 28** *Left*: Channel design for the enzyme-linked immunosorbent assay (ELISA) assay. Several reservoirs containing different sample and washing solutions can be opened serially depending on the frequency of rotation. *Right*: Picture of the compact disk fabricated by computer numerical control (CNC) milling with four identical assay structures. (Reprinted with permission from Lai S, Wang S, Luo J, Lee L J, Yang S T, Madou M J 2004 Design of a compact disk-like microfluidic platform for enzyme-linked immunosorbent assay. *Anal. Chem.* **76**, 1832–7. Copyright 2004 American Chemical Society.)

p0730 Under rotation (360 rpm), first the sample solution is released from reservoir 3 into reservoir 2 for the antigen–antibody binding process. The capillary valve at the outer radius of reservoir 3 is designed with the lowest burst frequency to accomplish an automated assay procedure. After an incubation step, reservoir 2 is washed with washing solution from reservoir 4 at a higher frequency of rotation (560 rpm, greater than burst frequency of reservoir 4). Following this serial flow-through assay scheme, the conjugate solution (reservoir 5) is released at 790 rpm, the detection chamber is washed (reservoir 6) at 1190 rpm, and finally the substrate solution (reservoir 7) is flushed through reservoir 2 at 1280 rpm. Immediately after the release of the substrate, the disk is stopped and the assay result is detected using an inverted fluorescent microscope.

p0735 It can be shown that the centrifugally conducted assay has the same performance in terms of detection range as the conventional method on the 96-well microtiter plate, while having advantages over the conventional method such as less reagent consumption and shorter assay time.

s0300 ***2.13.5.3.3 Protein quantification (Gyrolab Bioaffy®)***

p0740 Gyros AB (2006), Sweden uses a flow-through sandwich immunoassay at the nanoliter scale to quantify proteins within the Gyrolab™ Workstation. Therefore, a column of prepacked and streptavidin-coated microparticles is integrated in each of the total 112 identical assay units on the microfluidic CD. Each unit has an individual sample inlet and a volume definition chamber that leads to an overflow channel. Defined volumes (200 nl) of samples and reagents can be added to the prepacked particle column (**Figure 29**). Samples and reagents can be added to a specific unit via an individual inlet port or via a common inlet feeding defined clusters. Capillary action draws samples and reagents into the microstructures where volumes are precisely defined. This enhances reproducibility and reliability as well as eliminates concerns about pipetting precision. After the sandwich assay protocol is completed, the assay result is read out using a detection reagent bound to the target protein and laser-induced fluorescence. The laser-induced fluorescent (LIF) detector is incorporated into the Gyrolab Workstation.

p0745 Using this technology, multiple immunoassays with 200 nl of sample have been carried out to determine the imprecision of the assay result. The day-to-day (total) imprecision (CV) of the immunoassays on the microfluidic CD is <20% (Honda *et al.* 2005). The assays were carried out within 50 min, while in comparison the traditional ELISA in a 96-well plate typically takes a few hours, with sample volumes of a few hundred microliters.

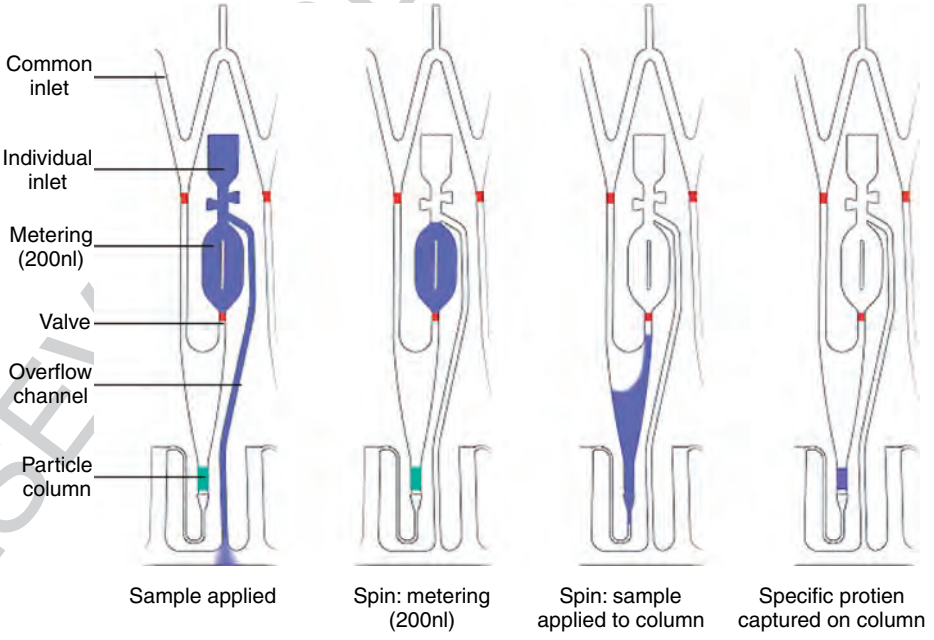

f0145 **Figure 29** Metering step of the sandwich immunoassay protocol shown for one microstructure unit in Gyrolab Bioaffy® system. The sample is applied to the individual inlet port and metered to a volume of 200 nl. Subsequently, it flows through a column of functionalized particles. A certain protein specifically binds to a surface-immobilized capture protein and is read out in a subsequent assay step. (Source: GYROS AB 2006 Uppsala, Sweden, www.gyros.com, accessed 2006.)

s0305 ***2.13.5.3.4 Alcohol test (Bio-Disk)***

p0750 A fully integrated colorimetric assay for the determination of the alcohol concentration in human whole blood has been shown on the centrifugal Bio-Disk platform (b0720 Steigert *et al.* 2006). After loading the reagents into the reagents reservoir, a droplet of untreated human blood derived from fingertip is loaded into the inlet port of the microstructure. All process steps of the assay are implemented by a fully automated frequency protocol.

p0755 First, a small 500 nl blood volume is metered from the sample and purged into the detection chamber at a frequency exceeding the burst frequency of the hydrophobic valves. At this frequency, the assay reagents also enter the reaction chamber. To enforce rapid mixing the sense of rotation is frequently reversed for 10 s, leading to a homogeneous mixture (shake-mode mixing). Thereby an enzymatic reaction is initiated by changing the color of the mixture depending on the alcohol concentration. During the subsequent sedimentation step, the disk is spun at a frequency of 30 Hz for 30 s so that all the cells contained within the blood sample settle at the radial outer end of the detection chamber. After sedimentation, the absorbance is monitored in real time during constant spinning for about 100 s to obtain the optical density of the mixture.

p0760 According to the Beer–Lambert law, the absorbance (or optical density) linearly depends on the molar extinction coefficient of the solution, which is governed by the products of the colorimetric reaction and thus the alcohol concentration. Since the absorbance scales with the optical path length l_{abs}, the sensitivity of this readout method can be enhanced by elongating the path of the laser beam through the analyte solution. A flat polymer substrate, however, enables only small optical lengths in readout schemes perpendicular to the disk surface. Therefore micromachined V-grooves placed on both sides of the detection chamber to deflect the laser beam by total internal reflection into the disk plane have been applied on one side of the disk (total internal reflection (TIR) set-up, **Figure 30**).

p0765 Using this automated assay and readout protocol the concentration of alcohol in human whole blood can be determined within 150 s only. The results are comparable to common point-of-care tests and require a minute blood volume of just 500 nl.

2.13.5.4 Strengths and Challenges of the Platform

s0310

p0770 The modular set-up of the system with cheap, disposable, and easy exchangeable plastic cartridges is certainly one major advantage of the centrifugal microfluidic platform, especially in the field of diagnostics. The cost-efficient fabrication predominantly originates in the simple and passive microfluidic elements that can be easily combined in a monolithic way within the same fabrication process. Those elements allow to implement all unit operations needed to perform complex assay protocols in an automated way. Due to the rotational symmetry of the disks optionally a high degree of parallelization can be achieved. All processes are controlled by the frequency of rotation

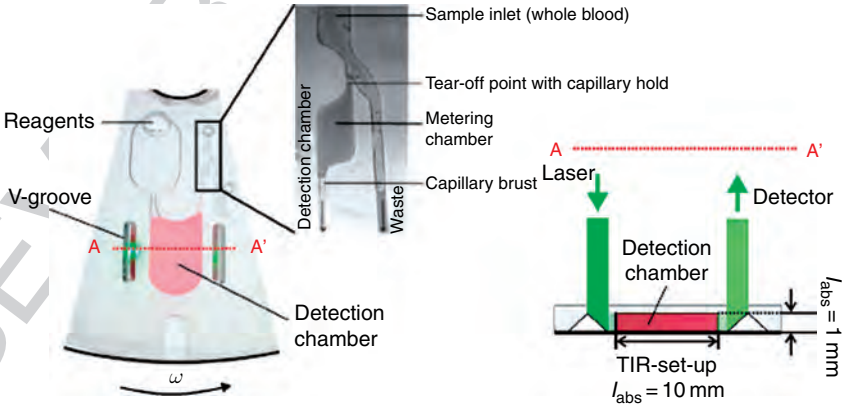

f0150 **Figure 30** *Left*: Microfluidic structure for the fully integrated alcohol determination starting from a raw sample of human blood. First, the sample is metered and then mixed with the reagent within the detection chamber. *Right*: Readout is accomplished by the total inner reflection of a laser beam into the disk plane to elongate the optical path length l_{abs} from approximately 1 to 10 mm (TIR set-up). (Source: Steigert J, Grumann M, Brenner T, Riegger L, Harter J, Zengerle R, Ducrée J 2006 Fully integrated whole blood testing by real-time absorption measurement on a centrifugal platform. *Lab Chip* **6**, 1040–4. Reproduced by permission of The Royal Society of Chemistry.)

of one single macroscopic rotary engine only. In addition the centrifugal microfluidic platform can be easily applied to a wide range of different applications due to the fact that it allows scaling of the pulse-free flow rates by six orders of magnitude.

p0775 As soon as any additional actuation or sensing function is required on the module while rotating, things however become tricky from a technical point of view if a contact-free interfacing is not applicable. The platform also lacks flexibility compared to other that allow online programming of fluidic networks within one piece of hardware that fits all needs (see Sections 2.13.6.3 and 2.13.6.4). Most of the logic functions as well as their critical frequencies are imprinted into the channel network.

s0315 2.13.6 Droplet-based Microfluidic Platforms

s0320 2.13.6.1 Introduction

p0780 The principal idea behind droplet-based microfluidic systems is the use of single droplets as reaction confinements for biological assays or chemical reactions. Dominant interfacial and surface tensional forces in the microdimension enable the precise generation and spatial stabilization of these droplets. Since the droplets are kept isolated within an immiscible surrounding fluid like air or oil, lateral dispersion (Taylor dispersion) can be avoided while moving the droplets to different locations.

p0785 Droplets as reaction confinements can be regarded as nanoliter-sized batch reactors for mixing and reacting in contrast to the merely flow-through concept of the other platforms described so far. Many parallel screening reactions, each consuming only a minute amount of reagents, are enabled inside the small-sized droplets. The reproducibility of the reaction conditions is very high, since the droplet volume as well as the reaction conditions within the droplet, i.e., temperature and mixing conditions, can be controlled precisely. This is of paramount interest, especially for HTS applications in the pharmaceutical industry.

p0790 The droplet-based microfluidic systems can be fundamentally divided into two basic setups, the channel-based and the planar surface-based approach described in **Table 5**. The channel-based systems are mostly pressure-driven with the droplet generation and manipulation depending on the actuation via liquid flows within closed microchannels. On the planar surface-based platforms, droplets can be arbitrarily moved in two dimensions representing planar programmable laboratories on-chip. They are actuated by electrowetting-on-dielectric (EWOD) or surface acoustic waves (SAW).

p0795 The different mechanisms to transport and manipulate droplets on the three different droplet-based microfluidic platforms, namely the pressure-driven, electrowetting-driven, and SAW-driven platform, are discussed in the following sections.

2.13.6.2 Pressure-driven Unit Operations s0325

2.13.6.2.1 Basic set-up s0330

p0800 The pressure-driven, droplet-based platform depends on the two-phase liquid flow through microchannels. The two immiscible phases are dispersed into each other so that a sample liquid (e.g., aqueous

t0025 **Table 5** Description of the two basic set-ups for droplet-based microfluidic platforms

Approach	*Schematic sketch*	*Description*
Channel-based	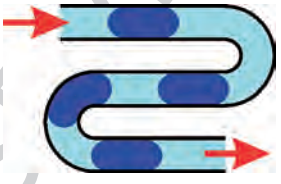	Liquid flow-driven actuation (pressure-driven) Simultaneous motion in one dimension, droplet movement defined by geometry, closed microchannels, fixed droplet arrangement in channel under stable conditions possible, e.g., for droplet storage
Surface-based	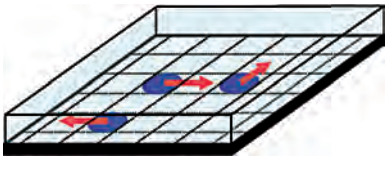	Actuation by SAW or EWOD, individual motion in two dimensions, arbitrary droplet movement on surface, planar (open) surface, online control of assay protocol

solution) forms plugs of a certain length, separated by the carrier liquid (e.g., oil) along the channel. The flow scheme is called segmented flow, since the size of the inner phase droplet exceeds the cross-sectional dimensions of the channel leading to squeezed liquid plugs. The two-phase flow is pumped throughout the channels by an externally applied pressure.

s0335 ***2.13.6.2.2 Droplet generation and metering***

p0805 The most elementary unit operation on the pressure-driven, droplet-based platform is the initial generation of the droplets. This step can also be considered as metering, since the liquid volumes involved in the latter reaction within the droplet are defined during the droplet formation process. Generally, two different microfluidic structures have been reported for a controlled droplet generation, the flow focusing structure (Anna *et al.* 2003, b0030 Joanicot and Ajdari 2005, b0380 and the T-junction (Nisisako *et al.* 2002, b0560) (**Figure 31**).

p0810 Besides these two most prominent methods, other microfluidic structures for droplet formation, mainly for emulsification in the field of microprocess engineering, have also been proposed. Vertical microchannels leading into a steady continuous phase (Kobayashi *et al.* 2005, b0405) or liquid plugs sliding down from a microterrace (Sugiura *et al.* 2001, b0750), for example, are used to generate droplets with a higher throughput. Also the production of double emulsions, e.g., water-in-oil-in-water (W/O/W), has been shown in a serial arrangement of T-junctions (Okushima *et al.* 2004, b0570) or within more complex

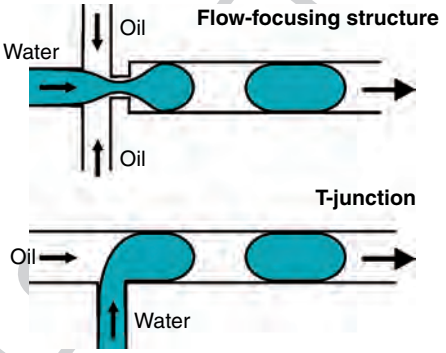

f0155 **Figure 31** Both microfluidic channel arrangements, the flow-focusing structure depicted on the top and the T-junction depicted on the bottom, can be used to reproducibly initiate a droplet break-off. The sketches describe the arrangement of water as the sample and oil as the carrier phase.

interleaved microcapillaries arrangements (Utada *et al.* 2005, b0795).

The flow-focusing device and the T-junction, p0815 however, are more adequate for the injection of droplets into small microchannels inducing a segmented flow scheme. For both structures, the size of the droplet is influenced by the strength of the shear forces at the channel junction (higher shear forces lead to smaller droplets). Thus, the droplet diameter can be controlled via the flow rates and flow rate ratios of the two phases. In order to ensure a complete isolation of the single droplets, the wetting properties of the channel walls have to be assumed to be non-wetting for the sample phase. Thus, the sample phase droplets are not in contact with the walls and no leakage out of them can cause changing concentrations during a reaction.

Also the injection of gaseous bubbles into a con- p0820 tinuous liquid stream at a flow focusing structure has been demonstrated (Garstecki *et al.* 2004, b0200 2005b). b0210 Using these mechanisms, gas–liquid segmented flows can be generated within microchannels, which are, for example, used for the enhanced mixing of two liquid phases as described in Section 2.13.6.2.6.

2.13.6.2.3 Sample load s0340

In order to use the droplets inside a channel as reac- p0825 tion confinements, the different liquid educts have to be loaded into the droplets first. A method to combine three different sample liquid streams by a sheath flow arrangement with subsequent injection as a common droplet into the carrier fluid has been shown by the group of Rustem F. Ismagilov at the University of Chicago, USA (Song *et al.* 2003b, b0685) (**Figure 32**). Different concentrations and ratios of two reagent substreams and a dilution buffer merge into one droplet and perform a so-called on-chip dilution (Song and Ismagilov 2003, b0675). The mixing ratios can be adjusted by the volume flow ratio of the three streams as depicted in the two exemplary photographs in **Figure 32**. Food dye has been used to color the reagents green and red and to visualize their portion within the generated droplet depending on the corresponding flow rates.

Using a combination of two opposing T-junctions p0830 connected to the same channel, the formation of droplets of alternating composition has been demonstrated (Zheng *et al.* 2004b, b0900). This method can be used for protein crystallization (see Section 2.13.6.2.9) or indexing within continuous flow screening experiments on the droplet-based platform. There, the first droplet of each droplet pair is used to conduct

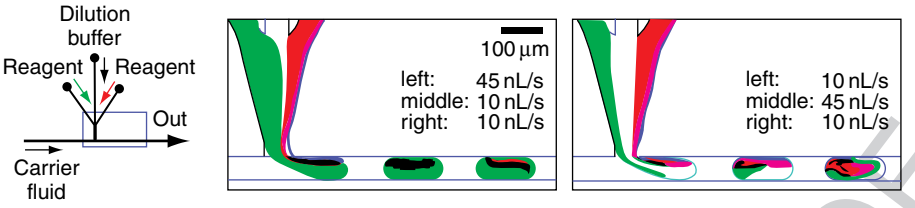

f0160 **Figure 32** On-chip dilution depicted with two exemplary situations at the droplet formation T-junction. Different flow rates of the reagent streams (food dye colored green and red), separated by the transparent dilution buffer stream in the middle, are injected into the droplet. Different concentrations of the two reagents are then loaded into the droplet for reaction. (Reprinted with permission from Song H, Ismagilov R F 2003 Millisecond kinetics on a microfluidic chip using nanoliters of reagents. *J. Am. Chem. Soc.* **125**, 14613–19. Copyright 2003 American Chemical Society.)

the reaction, and the second droplet is used to index the composition of the first droplet. Using a similar technique, the injection of an additional reactant into a liquid plug moving through the channel at an additional downstream T-junction has also been demonstrated (b0655 Shestopalov *et al.* 2004).

p0835 However, not only liquid chemical reagents but also other components like cells have been loaded into droplets as reported in b0320 He *et al.* (2005). Therefore, a flow focusing device has been used with an aqueous cell suspension as the sample phase flowing through the central channel. The selective encapsulation of single cells into droplets of femtoliter volume has been demonstrated.

s0345 ### 2.13.6.2.4 Merging and splitting of droplets

p0840 Merging of the droplets of different sizes and possessing different velocities to form single droplets has been demonstrated by Ismagilov *et al.* (b0685 Song *et al.* 2003b). In the same work, they also show the controlled splitting of droplets at a channel branching point. A constriction of the channels at the branching leads to longer and narrower droplets that could be split into two subdroplets. The size of the two split droplets was proportional to the relative flow rates in the two outlet channels. Using a similar method, the formation of droplet emulsions with controlled volume fractions and drop sizes has been demonstrated (b0465 Link *et al.* 2004).

s0350 ### 2.13.6.2.5 Transport

p0845 The droplets are transported via a pressure-driven flow through the microchannels. Since the droplets typically are bigger in size than the channel cross section, they form a plug within the channel, segmenting the continuous phase (segmented flow). This keeps the phase configuration along the channel stable since no liquid is exchanged between the plug interspaces. This way, plugs can be moved spatially separated through a channel network.

p0850 This has been used, e.g., for a polymerization process. Liquid monomer droplets have been hardened by exposing UV light to the droplets- carrying microchannel. Using this method, nonspherical particles can also be generated by polymerizing within a microchannel of small cross section wherein the droplets are squeezed and thus become disk shaped (b0125 Dendukuri *et al.* 2005).

s0355 ### 2.13.6.2.6 Mixing

p0855 The starting point of the mixing process is set to the time when the droplet is generated and released into the pressure-driven segmented flow (**Figure 32**) or when two droplets are merged. In the first case a buffer liquid separates the two reagent flows prior to the injection into a droplet. The two reagents are then mixed by a recirculating flow inside the droplets due to shear forces induced by the motion along the stationary channel wall (b0775 Tice *et al.* 2003). This effect is even more pronounced if two liquids of differing viscosities (2.0 and 18 mPa s) are mixed within the droplet as reported in b0780 Tice *et al.* (2004).

p0860 Based on the recirculation flow, a mixing scheme for the pressure-driven, droplet-based platform has been proposed using winding microchannels as depicted in **Figure 33** (b0680 Song *et al.* 2003a). Within each 90° channel curvature the orientation between the phase pattern in the droplet and the direction of motion is changed so that the inner recirculation leads to stretching and folding of the phases. Therewith, the number of phase lamellae within the droplet continuously increases by every bend along the channel. Under favorable conditions, submillisecond mixing can be achieved and has been employed for the multistep synthesis of

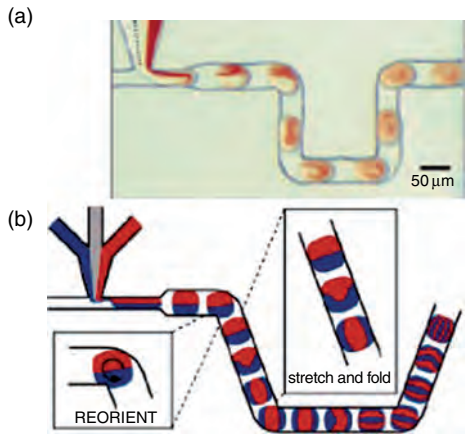

f0165 **Figure 33** Mixing within liquid droplets moving through bending microfluidic channels shown (a) experimentally and (b) schematically. (Source: Song H, Bringer M R, Tice J D, Gerdts C J, Ismagilov R F 2003a Experimental test of scaling of mixing by chaotic advection in droplets moving through microfluidic channels. *Appl. Phys. Lett.* **83**, 4664–6. Reproduced by permission of American Institute of Physics.)

nanoparticles, for example (b0655 Shestopalov *et al.* 2004). A detailed and theoretical description of this mixing effect is given in b0060 Bringer *et al.* (2004).

p0865 Besides the mixing within liquid droplets, dispersed into another liquid carrier phase, mixing within the carrier phase can also be accelerated by a segmented flow. The injection of gas bubbles into a continuous liquid stream forming a segmented gas–liquid flow has been described by Klavs Jensen and his group at the MIT (b0240 Gunther *et al.* 2004, b0245 2005). The gas bubbles are introduced into the liquid flow and initiate recirculation flows within the liquid segments in between due to the motion along the channel wall. The gas bubbles can be completely separated from the liquid stream using a planar capillary separator after the reaction is completed. Using this technology, the synthesis of colloidal silica particles has been demonstrated (b0395 Khan *et al.* 2004). Compared to a pressure-driven flow without segmentation, the axial dispersion is eliminated in the proposed gas–liquid flow scheme. Therefore, the residence time distribution of the reactants is also narrowed leading to less polydisperse particles.

p0870 Another microfluidic mixing scheme based on a gas–liquid segmented flow uses an additional repeated separation and recombining of the channel (b0205 Garstecki *et al.* 2005a). Homogenization of two aqueous streams has been demonstrated after 10 branching units for various flow rates (Reynolds numbers between 0.01 and 100) using this mixing scheme.

2.13.6.2.7 Incubation

s0360

p0875 The incubation time of the reagents combined inside a droplet at the injection position can easily be calculated at a certain point of observation from the traveling distance of the droplet divided by the droplet velocity. A unique feature of the platform is that a time-resolved monitoring of the incubation can easily be done by scanning along the channel from the injection point to more downstream positions. Thereby the kinetics of chemical reactions in the order of some milliseconds can easily be investigated and have been reported. On the other hand, incubation times on the order of a week for storing applications have been demonstrated. This is enabled by the droplet compartments that are separated by the carrier fluid, which prevents evaporation and diffusion. Using this approach, several 60 nl liquid droplets containing one or a few cells were generated within a microfluidic chip and were then flushed into a Teflon® capillary tube for cultivation. The cell densities were still as high as in conventional systems after 144 h of growth within the droplets (b0525 Martin *et al.* 2003).

2.13.6.2.8 Switching

s0365

p0880 Switching on the droplet-based and pressure-driven platform means the controlled routing of single droplets. All liquid routing technologies, available on the pressure-driven platform described in Section 2.13.3.2.5, can be used to switch droplets in the channel-type droplet-based microfluidic platform. If certain droplets out of a train of droplets should be separated, for example, an X-shaped channel crossing can be used. As soon as the droplet of interest passes the junction within the main flow, a short pressure pulse is applied at a side channel to direct the droplet into one of the two remaining outflow channels.

2.13.6.2.9 Application example: protein crystallization

s0370

p0885 Protein crystallization (see Section 2.13.4.3.1 for description) has been implemented on the pressure-driven, droplet-based platform by Ismagilov and coworkers (b0890 Zheng *et al.* 2003, b0905 2004c). The basic principle is depicted in **Figure 34(a)**: droplets of three liquids namely the protein solution, the buffer, and the precipitant are dispersed into the oil carrier phase. The precipitant concentration inside the

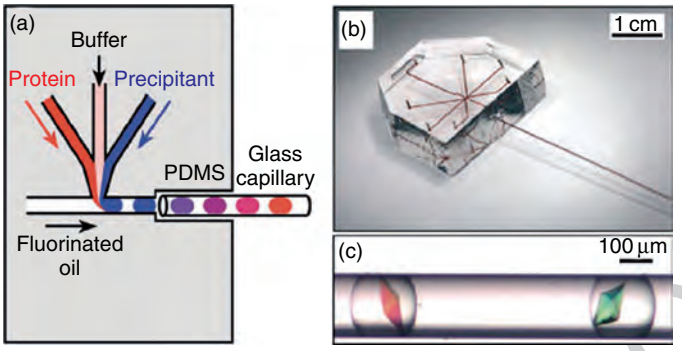

f0170 **Figure 34** (a) Schematic illustration of the protein crystallization device and (b) the complete set-up consisting of a polydimethylsiloxane (PDMS) chip and a glass capillary. (c) Examples of thaumatin crystals that were grown inside droplets in a capillary. (Source: Zheng B, Tice J D, Roach L S, Ismagilov R F 2004c A droplet-based, composite PDMS/glass capillary microfluidic system for evaluating protein crystallization conditions by microbatch and vapor-diffusion methods with on-chip X-ray diffraction. *Angew. Chem. Int. Ed.* **43**, 2508–11. Reproduced by permission of Wiley VCH.)

droplet is adjusted via the buffer and precipitant flow rate. Therewith, different concentrations are generated and transferred into a glass capillary for later detection. Nonspecific protein adsorption onto the liquid–liquid interface can be suppressed by adding certain surfactants to the carrier phase (b0620 Roach *et al.* 2005). As depicted in **Figure 34(b)**, the droplets containing the protein crystals can be directly forwarded into a glass capillary ready for the X-ray analysis (b0855 Yadav *et al.* 2005).

p0890 As described earlier in this chapter, successful protein crystallization is initiated for a certain precipitation concentration only. Therefore, the conduction of many crystallization experiments within a short time and with a reduced amount of protein sample is favorable and is enabled by the described sample loading technique. Examples of crystallized thaumatin proteins are depicted in **Figure 34(c)**. The effect of mixing on the nucleation of protein crystallization has been investigated by combining the described crystallization structure with a winding mixing channel as described in Section 2.13.6.2.6 (b0080 Chen *et al.* 2005). Fast chaotic mixing has been found to be favorable for the formation of well-formed proteins within the droplets (b0910 Zheng *et al.* 2005).

p0895 Besides the described method for crystallization, an alternative process in which the concentration within one droplet is changed over time has also been developed by the group of Ismagilov, based on water diffusion between droplets (b0895 b0905 Zheng *et al.* 2004a, c). In this case, a carrier liquid that enables diffusion between the droplets, that is, a water-permeable liquid, is selected. Alternating droplets of protein and precipitant on the one hand and a high-concentration salt solution on the other hand are generated using two opposing droplet generation structures (b0900 Zheng *et al.* 2004b). Water diffuses through the oil carrier phase from the low salt concentration, i.e., from the protein-containing droplet to the high-concentration droplet. This steadily increases the concentration within the protein-containing droplet until the suitable crystallization condition is achieved.

p0900 Recent developments on the pressure-driven, droplet-based platform aim at HTS applications. Therefore a large number of droplets, each containing a different reagent, are separated and surrounded by a fluorinated carrier fluid within a microcapillary. In order to prevent coalescence during possibly long storage times, a gas bubble is injected between the droplets as an additional separation phase (b0885 Zheng and Ismagilov 2005). Based on this three-phase liquid–liquid–gas system, reliable and HTS assays can be performed, which could be an alternative for well plates in the future (b0085 Chen and Ismagilov 2006).

2.13.6.3 Electrowetting-driven Unit Operations

s0375

2.13.6.3.1 Basic set-up

s0380

p0905 The electrowetting effect was first described by Gabriel Lippmann in 1875 while the recent developments were initiated in the early 1990s by introducing the idea of using thin insulating layers to separate the conductive liquids from the metallic electrodes in order to eliminate the problem of electrolysis (taken from b0540 Mugele and Baret (2005) on electrowetting). This paved the way for the

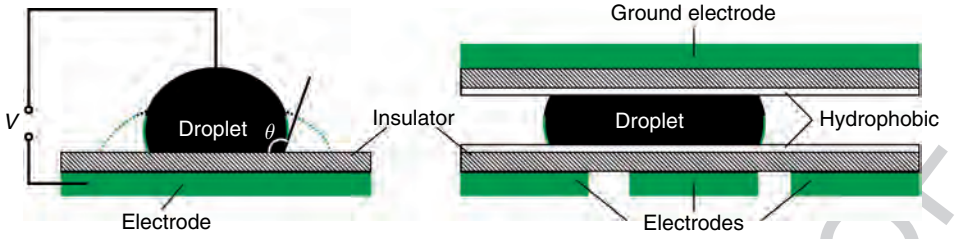

f0175 **Figure 35** *Left*: The electrowetting principle. If a voltage V is applied between a conductive liquid and an electrode separated by an insulating layer, the contact angle θ of the liquid–solid interface can be decreased. *Right*: Schematic diagram of the electrowetting actuation of liquid droplets. Several individual addressable control electrodes (bottom) are used to locally change the contact angle and thereby initiate a droplet movement.

application of the electrowetting effect as a liquid propulsion principle for lab-on-a-chip systems.

p0910 The principal setup of an EWOD (Lee *et al.* 2002) setup is depicted in **Figure 35** (*left*) with a liquid droplet on top of an insulating dielectric layer. A voltage V can be applied between the conductive liquid droplet and the electrode leading to a change in the contact angle, θ

$$\gamma_{lg}\cos\theta = \gamma_{sg} - \gamma_{sl} + \frac{1}{2}\frac{\varepsilon_0\varepsilon_r}{d}V^2 \qquad [6]$$

depending on the interfacial tension at the liquid–gas interface γ_{lg}, solid–gas interface γ_{sg}, and solid–liquid interface γ_{sl}. The thickness of the insulator d and the dielectric parameters ε_0 and ε_r define the impact of a voltage change on the contact angle. So EWOD can be simply described as a tool to control the contact angle of conductive liquids (Mugele *et al.* 2005).

p0915 Using the EWOD set-up, a microfluidic actuation method for moving droplets between two parallel electrodes has been published by Pollack *et al.* (2000) from the Duke University in Durham and by Chang-Jin (CJ) Kim from the University of California, Los Angeles, CA (UCLA) (Lee and Kim 2000). A schematic cross-section of an EWOD actuator is depicted in **Figure 35** (*right*). Several individual addressable control electrodes are located on the bottom of the device to control the droplet path. They are typically arranged in 2D arrays. An additional hydrophobic layer (mostly Teflon) is added to the insulator surface to enhance the droplet movement. A common ground electrode in contact with the liquid droplet replaces the extended electrode.

p0920 The droplet, which is enclosed between the two electrode plates, features a certain volume so that it covers parts of two addressable electrodes at all times. If a voltage is applied on one of the control electrodes covered by the droplet, the contact angle is reduced at this part of the droplet. This initiates droplet movement along the paths given by the activated pads. Because the path of the droplets is determined by the pattern of electric potentials, the EWOD-driven, droplet-based platform is easily programmable. This allows different assays to be run by different programs on the same piece of hardware.

p0925 Besides the transport of aqueous solutions, several other liquids like organic solvents, ionic liquids, aqueous surfactants solutions (Chatterjee *et al.* 2006), and also biological fluids like whole blood, serum, plasma, urine, saliva, sweat, and tears (Srinivasan *et al.* 2004) have also been successfully transported on the EWOD droplet-based platform.

p0930 An alternative actuation principle for surface-based droplet manipulation that does not require a second electrode in contact with the droplet is dielectrophoresis. The basic unit operations, like droplet generation, movement, metering, and merging, using this alternative actuation have been demonstrated recently (Gascoyne *et al.* 2004, Schwartz *et al.* 2004). However, they are not discussed in detail in the following sections that focus on EWOD-based unit operations only.

2.13.6.3.2 Metering

s0385 p0935 The dispensing, i.e., initial metering unit operation, is probably the most critical step on the EWOD-driven, droplet-based platform. Although droplets may be formed by simply pulling liquid out of a reservoir, the location of the tear-off can hardly be predicted. In the method depicted in **Figure 36**, metered droplets are formed from an on-chip reservoir in three steps (Srinivasan *et al.* 2004). First, a liquid column is extruded from the reservoir by activating a series of electrodes adjacent to it. Second, once the column overlaps the electrode on which the droplet is to be formed, all the remaining electrodes are turned off to

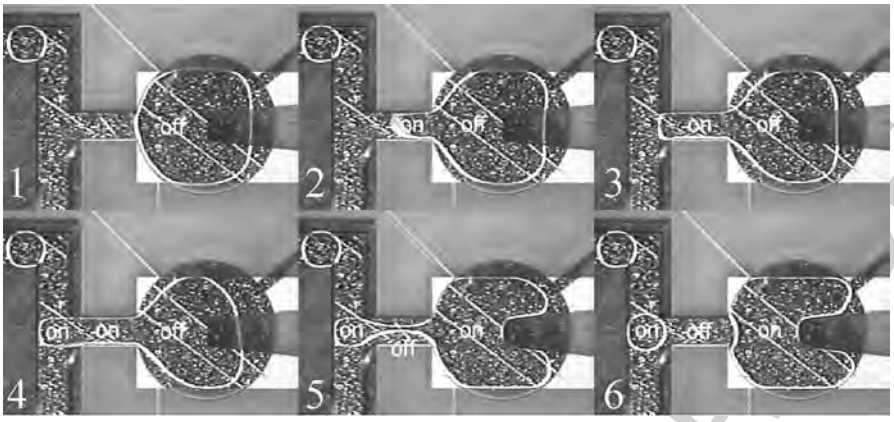

f0180 **Figure 36** Droplet formation from an on-chip reservoir using electrowetting forces only. First, a liquid column is extruded from the reservoir and tears off after the connecting electrode is turned off. (Source: Srinivasan V, Pamula V K, Fair R B 2004 An integrated digital microfluidic lab-on-a-chip for clinical diagnostics on human physiological fluids. *Lab Chip* **4**, 310–15. Reproduced by permission of The Royal society of Chemistry.)

form a neck in the column. The reservoir electrode is then activated in the third and last step to pull back the liquid and break the neck completely to form a droplet. Using this droplet metering structure, droplets of 20 nl volume can be generated with a standard variation below 2% (b0705 Srinivasan *et al.* 2004).

p0940 Since the droplet dispensing is a crucial step for the performance and the accuracy of all assays on the EWOD platform, additional measures for a controlled liquid metering such as on-chip capacitance metering for volume control (b0610 Ren *et al.* 2004) or the use of numerical methods for the design of EWOD structures (b0040 Berthier *et al.* 2006) have been proposed.

s0390 ***2.13.6.3.3 Mixing***

p0945 The most basic of miscible liquids within droplets on the EWOD platform is by oscillating the droplet between two electrodes. Before this active mixing scheme is used, the two droplets containing the liquids to be mixed have to be merged into a single droplet. This coalesced droplet is then moved along the electrodes in an oscillating fashion to induce advectional effects inside the droplet. An increasing frequency of droplet movement leads to reduced mixing times. The mixing process can be further accelerated by oscillating over a longer linear electrode array. The shortest mixing time for two 1.3-µl droplets in linear oscillation on four electrodes was about 4.6 s (b0585 Paik *et al.* 2003b). In another work, the mixing time was further reduced to less than 3 s using 2D arrays (b0580 Paik *et al.* 2003a).

s0395 ***2.13.6.3.4 Merging and splitting of droplets***

p0950 Together with droplet generation from a reservoir and the droplet transport along electrode arrays, the controlled merging and splitting of droplets complete the four fundamental fluidic operations considered essential to build digital microfluidic circuits for lab-on-a-chip applications (b0100 Cho *et al.* 2003).

p0955 The realization of droplet splitting and merging on three linearly aligned EWOD electrodes is depicted in **Figure 37** (b0595 Pollack *et al.* 2002). The initial droplet volume is first elongated toward the middle electrode by applying a voltage on it (**Figure 37(b)**). After a certain time delay, required for the stabilization of the droplet, the voltage is switched from the middle to the right electrode, initiating a division of the droplet into two subdroplets placed on the left and the right electrode, as depicted in **Figure 37(c)** and **37(d)**. For a subsequent merging of the droplets, the voltage is again switched from the right to the middle electrode, moving the right subdroplet back again to the middle position and bringing it in contact with the left subdroplet (**Figure 37(e)–(f)**).

s0400 ***2.13.6.3.5 Readout***

p0960 Different readout schemes for biochemical assays have been applied to the EWOD-driven, droplet-based platform. Colorimetric, enzymatic assays that are important for diagnostic applications have been successfully implemented and glucose concentration measurements on several biological fluids (serum, plasma, urine, and saliva) with good comparable results have been demonstrated (b0705 Srinivasan *et al.* 2004).

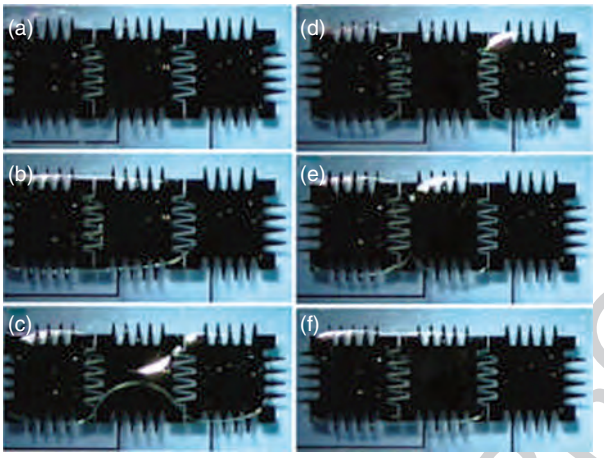

f0185 **Figure 37** A sequence of photographs showing the droplet splitting and merging. (a) Initially, only the left electrode is activated. (b) The middle electrode is then activated and, (c) and (d) after a delay, the voltage is switched from the middle to the right electrode resulting in division of the droplet. (e) and (f) The original droplet is reassembled by switching the voltage on the right electrode back to the middle electrode. (Source: Pollack M G, Shenderov A D, Fair R B 2002 Electrowetting-based actuation of droplets for integrated microfluidics. *Lab Chip* **2**, 96–101. Reproduced by permission of The Royal Society of Chemistry.)

p0965 Another example with regard to the use of an EOWD system for the automated sample preparation of peptides and proteins for matrix-assisted laser desorption/ionization mass spectrometry (MALDI-MS) is reported (b0820 Wheeler *et al.* 2004). In this work, standard MALDI-MS reagents, analytes, concentrations, and recipes have been demonstrated to be compatible with this technique, and mass spectra comparable to those collected by conventional methods were obtained.

s0405 2.13.6.4 SAW-driven Unit Operations

s0410 *2.13.6.4.1 Basic set-up*

p0970 An alternative to the electrowetting-based actuation of droplets on a plane surface has been proposed by Achim Wixforth and his group at the University of Augsburg, Germany (b0825 Wixforth 2003). The approach is based on SAW, which are mechanical waves with amplitudes of typically only a few nanometers. In contrast to ordinary sound waves, which are of longitudinal type, SAW are transversal waves. Their amplitude can be either parallel to the surface (Love waves) or perpendicular to the surface (Rayleigh waves) or of mixed type. For the manipulation of droplets on the SAW-based platform, typically Rayleigh waves are used.

p0975 The SAW are generated by a piezoelectric transducer chip (e.g., quartz), which can be fabricated by placing interdigital electrodes (interdigital transducer, IDT) on top of a piezoelectric layer, for example. Liquid droplets are placed on the hydrophobic surface of the chip and can be moved by the SAW on the surface. Appropriate AC signals are applied to the electrodes only at a certain region of the piezoelectric layer. Thus the SAW are exclusively generated at the desired location and can be focused on the droplet. If the acoustic pressure exerted on the liquid droplet is high enough, the droplet can be deformed or even be moved as depicted in **Figure 38** (b0830 Wixforth *et al.* 2004).

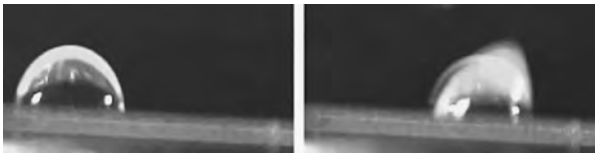

f0190 **Figure 38** Side view of an approximately 50-nl droplet on the hydrophobic surface (contact angle of about 90°) of a piezoelectric substrate. *Left*: Resting droplet. *Right*: The droplet is hit by SAW impinging from the left resulting in a momentary asymmetry of the wetting angles of the droplet. (Source: Wixforth A, Strobl C, Gauer C, Toegl A, Scriba J, von Guttenberg Z 2004 Acoustic manipulation of small droplets. *Anal. Bioanal. Chem.* **379**, 982–91. With kind permission of Springer Science and Business Media.)

p0980 This approach is also sometimes referred to as flat fluidics, because no cover or slit is required as in the EOWD approach but only a flat surface where the SAW are generated is needed. Today, this technology is being pushed forward by the company Advalytix AG (2006), Germany.

s0415 ***2.13.6.4.2 Metering***

p0985 Metering is accomplished by a combination of locally changed wetting properties of the surface and the actuation via SAW. One possible metering process is depicted in **Figure 39**. An initial water plug of approximately 100 nl is placed on an oval hydrophilic zone on the chip surface (**Figure 39(a)**). After the first actuator (IDT) is activated, SAW propagate horizontally toward the liquid plug, pushing it to the right across another small hydrophilic metering spot (**Figure 39(b)**). After the actuation, the liquid volume withdraws to the hydrophilic regions on the chip, leaving behind a small metered liquid portion (**Figure 39(c)**). This droplet is subsequently moved upward by another IDT for

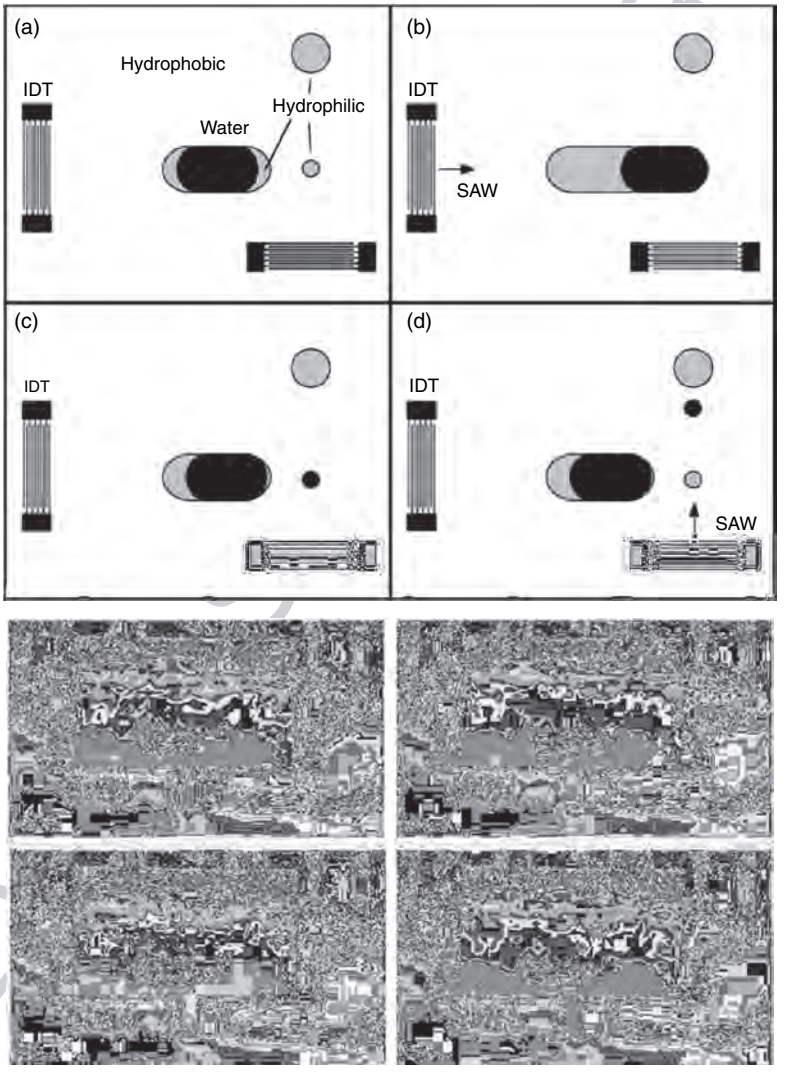

f0195 **Figure 39** Acoustically driven metering process on the SAW platform. (a)–(d) Hydrophobic and hydrophilic areas are indicated in the schematic sketch on the top. First, the horizontally acting interdigital transducer (IDT) pushes the water droplet to the right across the hydrophobic substrate. After the actuation, the droplet withdraws meanwhile separating a small liquid volume, which remains at the small hydrophilic spot, as depicted in (c). In the last step, this metered liquid portion is pushed upward toward another hydrophilic zone. Corresponding photographs of the actual experiment are also depicted. (Source: Wixforth A, Strobl C, Gauer C, Toegl A, Scriba J, von Guttenberg Z 2004 Acoustic manipulation of small droplets. *Anal. Bioanal. Chem.* **379**, 982–91. With kind permission of Springer Science and Business Media.)

further processing (**Figure 39(d)**). At the bottom of **Figure 39**, a sequence of experimental photographs shows the metering process on the open chip surface.

s0420 ***2.13.6.4.3 Mixing***

p0990 Mixing presents a system-immanent unit operation on the SAW-driven, droplet-based platform. A droplet, which is placed on the substrate and is hit by SAW, experiences an internal streaming due to the vibrating forces of the wave. If the amplitude is not large enough for a droplet movement, the liquid inside the droplet is efficiently stirred while its position on the substrate is retained. The internal streaming is depicted in **Figure 40** where a fluorescent dye is dissolved into a 50-nl droplet under SAW agitation.

s0425 ***2.13.6.4.4 Merging and splitting of droplets***

p0995 Using the SAW-based mechanism for droplet movement in combination with a certain pattern of different wetting areas on the chip surface, droplet splitting as described in Section 2.13.6.4.2 as well as droplet merging can be accomplished.

p1000 The splitting of one droplet into several smaller volumes of the same size, i.e., aliquotting, is realized by moving the initial droplet over a hydrophobic/hydrophilic chessboard zone. Since the transport of a droplet depends nonlinearly on the droplet size, the initial droplet of bigger volume is constantly moved forward, while small, picoliter-sized droplets remain on the hydrophilic parts of the wetting pattern (Wixforth 2003). b0825

s0430 ***2.13.6.4.5 Incubation and entrapment***

p1005 For some assay protocols, longer incubation steps at elevated temperatures are also required, e.g., for a PCR amplification. The liquid plug is placed above a microheating element on the substrate surface for these incubation steps. However, since the nanoliter-sized droplet possesses a high surface-to-volume ratio, the liquid volume decreases rapidly due to evaporation. Hence to avoid evaporation, the aqueous liquid plug is covered with an oil plug having a smaller contact angle. This droplet in droplet configuration still can be moved via SAW on the substrate surface. Using this technology, a PCR assay within a 200-nl droplet enclosed in mineral oil was performed with an online monitoring of the DNA concentrations and provided a sensitivity of 0.1 ng (Guttenberg *et al.* 2005). b0270

s0435 ***2.13.6.4.6 Readout***

p1010 The fabrication of the electrodes for the actuators (IDT) as well as the fabrication of the wetting patterns on the substrate is done by high-precision lithographic processes. Therefore, heaters, electrodes, or different types of sensors based on surface micromachining can easily be integrated in a straightforward way. Also, optical readout schemes have been realized for the online fluorescent monitoring of the RT-PCR progress, for example (Guttenberg *et al.* 2005). b0270

s0440 **2.13.6.5 Strengths and Challenges of the Platform**

p1015 General advantages of droplet-based microfluidics are the small liquid volumes of the droplets reducing reagent and sample consumption and thus paving the way for HTS applications. Additionally, the batch-mode operation scheme used in the nanoliter- to microliter-sized droplets represents a consistent further development of the classic assay protocols in, for example, well plates.

p1020 The pressure-driven approach combines these advantages with the high-throughput capabilities in a quasi-continuous operational scheme. The completely enclosed liquid droplets furthermore allow the incubation and storage of liquid assay

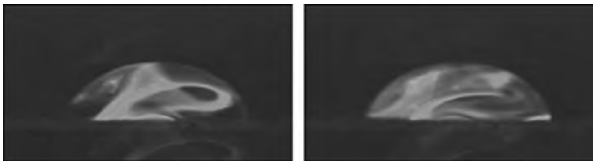

f0200 **Figure 40** Internal streaming is induced within an approximately 50-nl droplet, hit by SAW. The internal mixing process is visualized by a fluorescent dye placed on the surface of the chip, which is dissolved by the SAW agitation. (Source: Wixforth A, Strobl C, Gauer C, Toegl A, Scriba J, von Guttenberg Z 2004 Acoustic manipulation of small droplets. *Anal. Bioanal. Chem.* **379**, 982–91. With kind permission of Springer Science and Business Media.)

results over a long period of time without evaporation. However, the microfluidic functionality is engraved by the channel design and cannot be adopted during an assay, for example.

p1025 In contrast, the surface-based actuation schemes (EWOD and SAW) come up with a high flexibility since liquid processing paths can be freely programmed. In addition, the simple setup without any moving parts can be fabricated very cost-efficiently using standard lithographic processes.

p1030 When comparing the EWOD and SAW principle for droplet actuation on the planar surface, the electrical change of the contact angle depends on the liquid properties and can cause electrolysis while the SAW principle allows easier adoption of the liquid properties. Evaporation of liquid and the long-term stability of the hydrophobic and hydrophilic surface coatings are the major drawbacks of the surface-based techniques. Last but not least, all planar droplet-based platforms do not really work properly in nonplanar positions and therefore, for example, a handheld operation is not recommendable.

s0445 2.13.7 Free Scalable Noncontact Dispensing

s0450 2.13.7.1 Introduction and Motivation

p1035 The free scalable noncontact dispensing platform allows to deliver liquids as free-flying droplets onto planar substrates (e.g., microarrays), conventional containers such as well plates, or any other target. This approach is closest to the traditional lab routine, which is based on conducting assays via successive pipetting steps, manually or by automated lab equipment like robots. In these fields, the dispensing of droplets of different volumes (picoliter to milliliter range), from a single channel or up to thousands of channels in parallel, with different pitch sizes and individual controllability is required. An overview of the different fields of operation regarding the droplet volume on the one hand and the number of different liquids to be dispensed at once on the other hand is depicted in **Figure 41**. Here we focus on the simultaneous dispensing of a large number of different reagents in parallel and will not focus on noncontact printing technology in general (for an overview of ink-jet printing technologies, see Le[b0435] (1998)). All the three highlighted operating principles are based on one microfluidic platform as described in Section 2.13.7.2.

2.13.7.2 Unit Operations s0455

2.13.7.2.1 Metered dispensing s0460

p1040 One functional unit of the free scalable noncontact liquid dispensing platform is based on the combination of a reservoir for holding the liquid, a nozzle chamber with a nozzle from which the liquid is dispensed, and a capillary channel connecting reservoir and nozzle chamber. Depending on the arrangement of these components as well as the actuation principle, liquid volumes from several tens of picoliters to several microliters can be dispensed. Arranging several units on a so-called dosage chip enables the handling of up to thousands of different liquids in

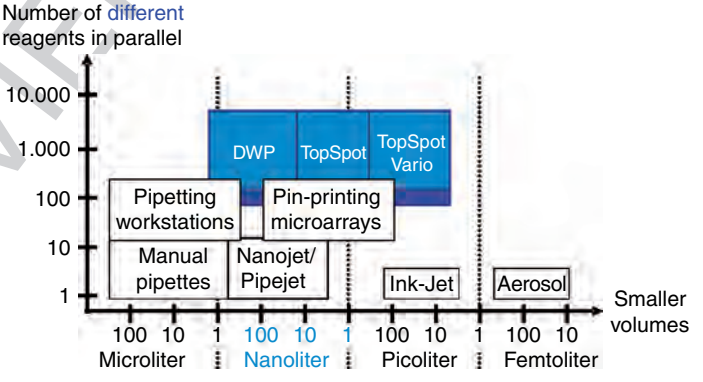

f0205 **Figure 41** Overview of low volume dispensing. The presented platform for noncontact dispensing depends on three different techniques to dispense well-defined liquid volumes. These techniques are named according to the pilot application they are used for (dispensing well plate (DWP), TopSpot®, TopSpot® Vario). The platform covers the volume range from several tens of picoliters (pl) to several microliters (μl). Several thousands of dispensing units can principally be arranged in parallel to handle the same number of different liquids, e.g., different biological reagents in parallel.

parallel and has been demonstrated at a pitch ranging from several hundreds of micrometers to several millimeters. Three different actuation schemes based on the same geometrical arrangement, namely the dispensing well plate (DWP) (Koltay *et al.* 2004a, b), the TopSpot® (de Heij *et al.* 2003, 2004), and the TopSpot® Vario (Steinert *et al.* 2004) technology are depicted in **Figure 42**.

p1045 The noncontact dispensing process, strictly speaking, represents two unit operations, liquid metering on the one hand and liquid transfer on the other hand. The metered liquid volume is delivered as a free-flying droplet or a jet in a noncontact manner to any substrate, receiving vessel, or the reservoir of another dispensing unit. The volume of that liquid portion is determined by the nozzle geometry and the external actuation mechanism.

p1050 The DWP principle is based on the complete drainage of the liquid volume within the nozzle chamber. The micromachined nozzle chamber can be considered as a metering structure, which is filled with liquid from the reservoir by capillary forces via the capillary channel between two dispensing events. The total liquid present in the nozzle chamber is dispensed by applying a pneumatic pressure of 30–80 kPa for 3–10 ms. Since this pressure pulse is applied on the liquid–air interface of the nozzle chamber and the reservoir, no pressure gradient evolves along the capillary channel and thus no backflow of liquid from the nozzle chamber to the reservoir is observed. The dosed volume is hardly affected by the liquid properties like viscosity, density, and surface tension, but is affected only by the geometry of the nozzle chamber, making this dispensing method very robust.

p1055 The TopSpot principle also depends on a pneumatic pressure pulse, which in this case is on the submillisecond timescale. Such a short pneumatic pressure pulse can be generated only by compression of an enclosed gas volume. Therefore an assembly of a piezo stack actuator driving a piston into a closed actuation cavity above the nozzle chambers is used. The pressure pulse acts equally on all nozzle chambers within the pressurized actuation cavity and causes the simultaneous ejection of single droplets out of each nozzle. The droplet volume is typically on the order of 1 nl for a 50-µm nozzle, which is in contrast to the DWP principle just a small fraction of the nozzle chamber volume. The exact droplet volume depends on the liquid properties, the actuation parameters, and the nozzle dimensions (Gutmann *et al.* 2004b).

p1060 In contrast to the pneumatic technologies described so far, the TopSpot Vario principle uses the direct displacement of an incompressible but easily deformable elastomer for actuation. The elastomer inlay replaces the air volume in the set-up (see **Figure 42**, *right*) and is displaced into the nozzle chambers by the piston movement if the piezo stack is actuated. A well-defined volume of liquid in the nozzle chamber is displaced by the elastomer and a droplet of the corresponding volume is ejected out of the nozzle. This direct displacement principle allows the independent control over the droplet volume and the droplet speed by adjusting the stroke and the speed of the piezo actuator. The tunable volume range of the droplets is from 100 pl up to 1400 pl (1.4 nl) for a 50-µm nozzle and can easily be adopted by varying the control voltage of the piezo actuator.

p1065 The basic structures like reservoirs, capillary channel, nozzle chamber, and nozzles can be fabricated by different technologies using different materials. Dry etching of silicon (deep reactive ion etching, DRIE) (Steinert *et al.* 2004), lithographic fabrication in SU-8 (Bohl *et al.* 2005), and

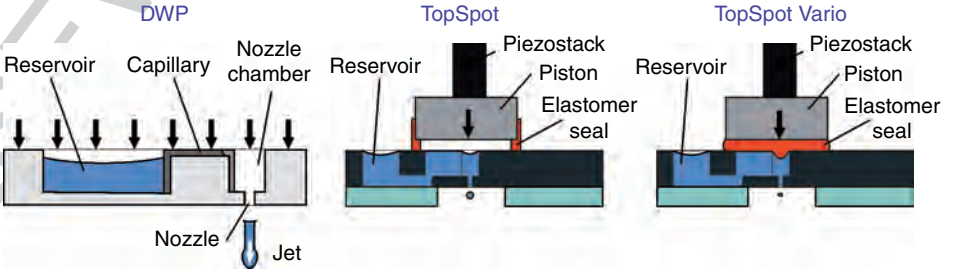

f0210 **Figure 42** Dispensing well plate (DWP): Pressure-based actuation for dispensing from 10 nl up to several microliters; TopSpot®: pressure-based actuation for dispensing volumes in the lower nanoliter range; TopSpot® Vario: direct displacement principle via an elastomer for dispensing volumes from 50 to 1.000 pl.

micromilling of plastics (Steger[b0710] *et al.* 2004) have been demonstrated. A high precision in the geometry of the dispensing units is needed for a high precision of the dispensed liquid volumes, and this results in the need for a high precision of the fabrication processes.

p1070 One unique feature of all the three dispensing principles described is the possibility to arrange many of them in parallel with a free scalable pitch of the nozzle chambers and the reservoirs. The capillary channel that connects these two substructures accomplishes the format conversion from a reservoir pitch of a few millimeters (enabling the filling of the dispensing chip using standard pipetting robots) to the pitch of the nozzle of a few hundred micrometers. This is important for the fabrication of microarrays, which is one application example for the platform, described in more detail in Section 2.13.7.3.1.

s0465 ***2.13.7.2.2 Incubation***

p1075 Besides the noncontact dispensing of a metered liquid volume, incubation steps at defined temperatures are also important for conducting biological assays. This can be realized on the free scalable noncontact dispensing platform by a reversible sealing of the structure openings, namely the nozzle, nozzle chamber, and the reservoirs preventing any liquid flow through the capillaries. The reservoirs and the nozzle chambers act as standard reaction cavities, then enabling incubation steps as long as the sealing is not removed (**Figure 43**, *left*).

s0470 ***2.13.7.2.3 Amplification***

p1080 Similar to the incubation described in Section 2.13.7.2.2, also temperature-initiated amplification using the polymerase chain reaction (PCR) method can be conducted within the cavities of the platform (**Figure 43**). Therefore, the sealed dispensing chip is mounted between an upper and a lower heating plate, which perform a certain temperature cycle between three temperatures (94°C, 53°C, and 72°C). This process is similar to the common PCR cycling within standard well plates. However, for the microcavities within the PCR slides the upper heating plate also has to change the temperature according to the cycling sequence in order to avoid temperature gradients within the PCR solution. Within the microwell plate, the upper heat plate can be fixed at a high temperature (to prevent condensation) since the air volume between the liquid and the heat plate acts as a thermal insulator. When the cycling is finished the PCR product (amplified DNA) can be dispensed in nanoliter portions into a microliter plate for further processing, onto a microarray for detection, or into another dispensing chip.

2.13.7.3 Application Examples

s0475

2.13.7.3.1 TopSpot for microarray spotting

s0480

A DNA microarray is an ensemble of microscopic DNA spots attached to a flat solid surface forming an array of different well-known capture molecules (probes) at well-defined positions. It can therefore be considered as a highly parallel biosensor, based on the lock and key principle. The probes on the surface react with a complex mixture of molecules (sample) during the hybridization phase of a microarray experiment. The sample molecules are equipped with fluorescent markers for later detection in a fluorescent readout device. The position of a positive fluorescent signal provides information about the identity of the sample (**Figure 44**).

p1085

p1090 The engineering challenge in the microarray fabrication is to immobilize up to 1000 different analytes as spots of approximately 1 nl volume, with a pitch of typically 500 µm and below, at high quality, high throughput, and low costs onto a substrate. One of the technical solutions to this problem is based on the TopSpot technology, a first application of the free scalable noncontact dispensing platform (Gutmann[b0250]

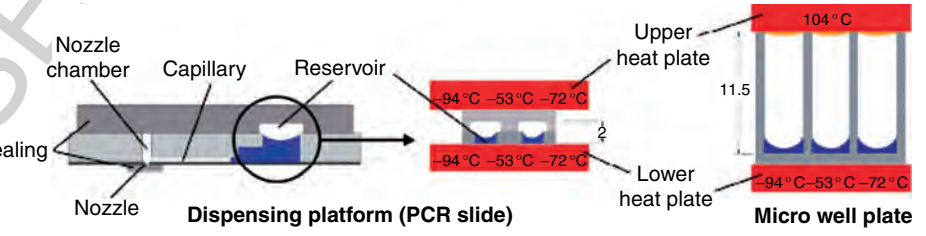

f0215 **Figure 43** The nozzle and the reservoir opening are sealed for incubation and amplification. Thermal cycling within the thin substrate (polymerase chain reaction (PCR) slide) requires an equal temperature for the upper and the lower plate at any time. Otherwise, inhomogeneous liquid temperatures can influence the assay performance.

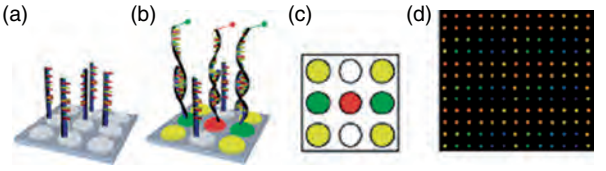

f0220 **Figure 44** Illustration of the working principle of a DNA microarray. (a) Probe molecules are immobilized as different spots with a certain pitch on the solid surface; (b) a binding reaction takes place between the probe and the sample molecule if the chemical structures are complementary; (c) the fluorescent readout after the microarray experiment indicates positive binding events; and (d) fluorescent image from a real microarray experiment.

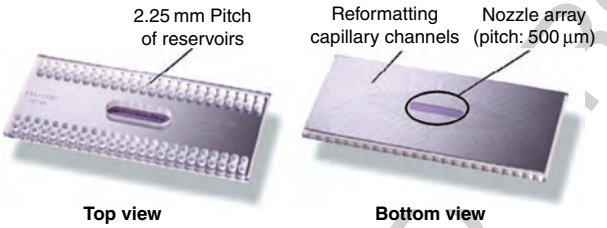

f0225 **Figure 45** Picture of a 96 TopSpot® printhead. The top view shows the reservoirs that are filled via manual pipetting or lab robots. The capillary channels that connect each reservoir with a certain nozzle chamber ending up in an array of nozzles of pitch 500 μm, a feature called reformatting, can be seen on the underside of the printhead (*right*).

et al. 2004a, b0260 c). A dispensing chip or so-called printhead featuring 96 parallel dispensing channels is depicted in **Figure 45**.

p1095 The key advantage of the noncontact dispensing platform for microarray fabrication is the ease to perform passive format conversion in the system. The reservoirs on top of the printhead are arranged at a pitch of 2.25 mm corresponding to the pitch of 384 well plates enabling the filling with standard lab equipment, e.g., pipetting robots. Several microliters of liquids can be loaded into each of the 96 reservoirs, which is enough for several thousand dispensing events without the need for refilling. Each reservoir is connected to a certain nozzle chamber in the middle of the printhead via a capillary channel. The liquids are simply transported to the nozzle chamber by capillary forces and stop at the nozzle until a pressure pulse is applied. The nozzles are arranged in an array of 500-μm pitch on the underside of the printhead defining the later spot positions on the microarray.

p1100 The typical CV of spot diameters on the microarray is found to be <1% for a single dispensing unit and <1.5% between all nozzles of a printhead for all relevant printing buffers used (b0250 Gutmann *et al.* 2004a). Using the TopSpot technology, protein microarrays as well as living cell microarrays have also been fabricated (b0265 Gutmann *et al.* 2005).

2.13.7.3.2 *Dispensing well plate* s0485

Well plates are the standard assay format in the life science industry, especially in HTS instrumentations for drug discovery. The assays are conducted by transferring different reagents between different containments called wells using pipetting robots. Different well plate standards such as the 96, 384, and 1536 format exist, differing in the pitch of the reservoirs (9.0, 4.5, and 2.25 mm, respectively) but all having the same outer dimensions (8 cm × 12 cm) according to the SBS standard. The trend toward smaller wells and consequently assay volumes also provokes the need for liquid handling systems being able to transfer small liquid volumes in the submicroliter range. p1105

p1110 A method for the simultaneous and contact-free dispensing of typically 50-nl liquid jets into microwell plates or onto flat substrates has been realized on the dispensing platform. The so-called DWP principle (**Figure 42**) uses a set of dispensing units, arranged according to the well plate format, each featuring a liquid reservoir, a capillary channel, and a nozzle chamber (**Figure 46**).

p1115 The nozzle chamber is filled with the liquid from the reservoir by capillary forces only. Afterward, all dispensing units are actuated in parallel by applying a pressure pulse on top of the dispensing chip initiating the simultaneous and complete drainage of all nozzle chambers through the nozzle. As a result, an array of

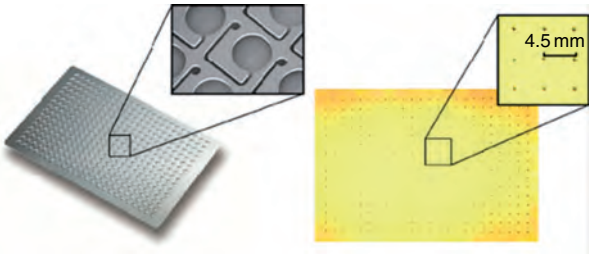

f0230 **Figure 46** Picture of a 384 dispensing well plate (DWP) dispensing a chip micromachined in silicon. The 384 reservoirs are connected to 384 nozzle chambers next to the reservoirs via capillary channels. No format transformation (reformatting) but the metering and allocation of a defined liquid volume is accomplished within each of the 384 units. All these liquid portions are then transferred to another platform within the pneumatically driven noncontact dispensing process (**Figure 42**) or to a flat surface as depicted on the right.

individual spots is delivered on another well plate or a plane substrate (**Figure 46**, *right*). After switching off the driving pressure, the nozzle chambers refill again from the reservoirs via the capillary channels. Since the reservoir contains a multiple of the nozzle chamber volume, many dispensing events can be performed before the chip has to be refilled. This, for example, enables the fast replication of a certain well plate loading into other plates (compound reformatting) or the addition of nanoliter volumes to plate-based assays. The reproducibility (CV) of the mean dosage volume has been reported to be better than 3% (Steger *et al.* 2004). b0710

s0490 **2.13.7.4 Strengths and Challenges of the Platform**

p1120 The wide range of dispensing volumes from 0.05 nl up to 1000 nl of the TopSpot Vario and the DWP, respectively, using the same basic geometric building blocks is certainly the main advantage of the free scalable noncontact dispensing platform. The three dispensing principles can easily be combined on one flat substrate with or without the reformatting by capillary channels and can be actuated in a highly parallel mode of operation.

p1125 However, the fabrication costs of the dispensing chips have to be reduced in the future making disposable printheads possible to avoid laborious washing procedures. Since cost reduction is not possible in silicon micromachining (no potential in downscaling of the footprint of the dispensing chips or printheads) microfabrication technologies for polymers like injection molding or hot embossing are likely the most promising alternatives. Today, this technology is pushed forward by the company Biofluidix GmbH (2006) in Germany.

2.13.8 Conclusion s0495

p1130 The collection of examples of microfluidic platforms given in the previous sections shows that the platform idea has already been taken up by many groups within the microfluidics community. They not only work on individual components fabricated using diverse technologies, and above all focus on the combination of validated fluidic elements by simple proved technologies. This approach allows to design and fabricate application-specific systems easily and will lead to a paradigm shift from a component and technology-based research to a system-oriented approach. The platforms will allow the microfluidics community to leave today's device-oriented research in order to face the next challenge: the flexible and cost-efficient design of thousands of different applications that might be accessible by using the full potential of microfluidic platforms without starting always from scratch.

p1135 A good indicator for the growing interest in microfluidic platform technologies can be also seen in the remarkable number of spin-off companies that arose during the last years trying to commercialize lab-on-a-chip products based on microfluidic platform concepts. Some of them have been mentioned in the previous sections, but there are many more in business already or to emerge in the near future.

References

b0005 Abaxis Inc. 2006 Union City, CA, USA, www.abaxis.com, accessed 2006

b0010 Abbott P-2006 East Windsor, NJ, USA, www.abbottpointofcare.com, accessed 2006

b0015 Advalytix AG 2006 Brunnthal, Germany, www.advalytix.de

b0020 Anderson N G 1969 Computer interfaced fast analyzers. *Science* **166**, 317–24

b0025 Andersson H, van den Berg A 2004 *Lab-on-Chips for Cellomics, Micro and Nanotechnologies for Life Science.* Kluwer Academic Publishers, Dordrecht, The Netherlands

b0030 Anna S L, Bontoux N, Stone H A 2003 Formation of dispersions using ''flow focusing'' in microchannels. *Appl. Phys. Lett.* **82**, 364–6

b0035 Auroux P A, Iossifidis D, Reyes D R, Manz A 2002 Micro total analysis systems. 2. Analytical standard operations and applications. *Anal. Chem.* **74**, 2637–52

b0040 Berthier J, Clementz P, Raccurt O, Jary D, Claustre P, Peponnet C, Fouillet Y 2006 Computer aided design of an EWOD microdevice. *Sens. Actuators A Phys.* **127**, 283–94

b0045 Bioluidix GmbH 2006 Freiburg, Germany, www.biofluidix.com

b0050 Bohl B, Steger R, Zengerle R, Koltay P 2005 Multi-layer SU-8 lift-off technology for microfluidic devices. *J. Micromech. Microeng.* **15**, 1125–30

b0055 Brenner T, Glatzel T, Zengerle R, Ducrée J 2005 Frequency-dependent transversal flow control in centrifugal microfluidics. *Lab Chip* **5**, 146–50

b0060 Bringer M R, Gerdts C J, Song H, Tice J D, Ismagilov R F 2004 Microfluidic systems for chemical kinetics that rely on chaotic mixing in droplets. *Philos. Trans. R. Soc. Lond. A Math. Phys. Eng. Sci.* **362**, 1087–104

b0065 Burns M A, Johnson B N, Brahmasandra S N, Handique K, Webster J R, Krishnan M, Sammarco T S, Man P M, Jones D, Heldsinger D, Mastrangelo C H, Burke D T 1998 An integrated nanoliter DNA analysis device. *Science* **282**, 484–7

b0070 Burtis C A, Anderson N G, Mailen J C, Scott C D, Tiffany T O, Johnson W F 1972 Development of a miniature fast analyzer. *Clin. Chem.* **18**, 753–61

b0075 Chatterjee D, Hetayothin B, Wheeler A R, King D J, Garrell R L 2006 Droplet-based microfluidics with nonaqueous solvents and solutions. *Lab Chip* **6**, 199–206

b0080 Chen D L, Gerdts C J, Ismagilov R F 2005 Using microfluidics to observe the effect of mixing on nucleation of protein crystals. *J. Am. Chem. Soc.* **127**, 9672–3

b0085 Chen D L L, Ismagilov R F 2006 Microfluidic cartridges preloaded with nanoliter plugs of reagents: An alternative to 96-well plates for screening. *Curr. Opin. Chem. Biol.* **10**, 226–31

b0090 Chen H, Meiners J C 2004 Topologic mixing on a microfluidic chip. *Appl. Phys. Lett.* **84**, 2193–5

b0095 Cheng Y T, Lin L W, Najafi K 2001 A hermetic glass-silicon package formed using localized aluminum/silicon-glass bonding. *J. Microelectromech. Syst.* **10**, 392–9

b0100 Cho S K, Moon H J, Kim C J 2003 Creating, transporting, cutting, and merging liquid droplets by electrowetting-based actuation for digital microfluidic circuits. *J. Microelectromech. Syst.* **12**, 70–80

b0105 Chou H P, Unger M A, Quake S R 2001 A microfabricated rotary pump. *Biomed. Microdevices* **3**, 323–30

b0110 Clark T J, McPherson P H, Buechler K F 2002 The triage cardiac panel. *Point Care* **1**, 42–6

b0115 Delamarche E, Bernard A, Schmid H, Michel B, Biebuyck H 1997 Patterned delivery of immunoglobulins to surfaces using microfluidic networks. *Science* **276**, 779–81

b0120 deMello A J 2003 Microfluidics – DNA amplification moves on. *Nature* **422**, 28–9

b0125 Dendukuri D, Tsoi K, Hatton T A, Doyle P S 2005 Controlled synthesis of nonspherical microparticles using microfluidics. *Langmuir* **21**, 2113–16

b0130 Ducrée J, Zengerle R 2004 *FlowMap – Microfluidics Roadmap for the Life Sciences.* Books on Demand GmbH, Norderstedt, Germany

b0135 Ducrée J, Haeberle S, Brenner T, Glatzel T, Zengerle R 2005 Patterning of flow and mixing in rotating radial microchannels. *Microfluidics Nanofluidics* **2**, 97–105

b0140 Ducrée J, Brenner T, Haeberle S, Glatzel T, Zengerle R 2006 Multilamination of flows in planar networks of rotating microchannels. *Microfluidics Nanofluidics* **2**, 78–84

b0145 Duffy D C, McDonald J C, Schueller O J A, Whitesides G M 1998 Rapid prototyping of microfluidic systems in poly(dimethylsiloxane). *Anal. Chem.* **70**, 4974–84

b0150 Duffy D C, Gillis H L, Lin J, Sheppard N F Jr., Kellogg G J 1999 Microfabricated centrifugal microfluidic systems: Characterization and multiple enzymatic assays. *Anal. Chem.* **71**, 4669–78

b0155 Effenhauser C S, Manz A, Widmer H M 1993 Glass chips for high-speed capillary electrophoresis separations with submicrometer plate heights. *Anal. Chem.* **65**, 2637–42

b0160 Effenhauser C S, Bruin G J M, Paulus A, Ehrat M 1997 Integrated capillary electrophoresis on flexible silicone microdevices: Analysis of DNA restriction fragments and detection of single DNA molecules on microchips. *Anal. Chem.* **69**, 3451–7

b0165 Ehrfeld W, Golbig K, Hessel V, Lowe H, Richter T 1999 Characterization of mixing in micromixers by a test reaction: Single mixing units and mixer arrays. *Ind. Eng. Chem. Res.* **38**, 1075–82

b0170 Ekstrand G, Thorsen T 2005 Liquid router. US 2005/0141344 A1

b0175 Ekstrand G, Holmquist C, Örlefors A E, Hellman B, Larsson A, Andersson P 2000 Microfluidics in a rotating CD. In: Van den Berg A, Olthius W, and Bergveld P (eds.) *Proc. Micro Total Analysis Systems 2000,* Enschede, The Netherlands, pp. 311–14

b0180 Erickson D 2005 Towards numerical prototyping of labs-on-chip: Modeling for integrated microfluidic devices. *Microfluidics Nanofluidics* **1**, 301–18

b0185 Fluidigm Corporation 2006 San Francisco, USA, www.fluidigm.com, accessed 2006

b0190 Fredrickson C K, Fan Z H 2004 Macro-to-micro interfaces for microfluidic devices. *Lab Chip* **4**, 526–33

b0195 Fu A Y, Spence C, Scherer A, Arnold F H, Quake S R 1999 A microfabricated fluorescence-activated cell sorter. *Nat. Biotechnol.* **17**, 1109–11

b0200 Garstecki P, Gitlin I, DiLuzio W, Whitesides G M, Kumacheva E, Stone H A 2004 Formation of monodisperse bubbles in a microfluidic flow-focusing device. *Appl. Phys. Lett.* **85**, 2649–51

b0205 Garstecki P, Fischbach M A, Whitesides G M 2005a Design for mixing using bubbles in branched microfluidic channels. *Appl. Phys. Lett.* **86**, 244108

b0210 Garstecki P, Stone H A, Whitesides G M 2005b Mechanism for flow-rate controlled breakup in confined geometries: A route to monodisperse emulsions. *Phys. Rev. Lett.* **94**, 164501

b0215 Gascoyne P R C, Vykoukal J V, Schwartz J A, Anderson T J, Vykoukal D M, Current K W, McConaghy C, Becker F F, Andrews C 2004 Dielectrophoresis-based programmable fluidic processors. *Lab Chip* **4**, 299–309

b0220 Geschke O, Klank H, Telleman P 2004 *Microsystem Engineering of Lab-on-a-Chip Devices.* Wiley-VCH, Weinheim

b0225 Goettsche T, Wolff A 2006 IntelliDrug – An integrated intelligent oral drug delivery system. *mst-news* **06**, 36–7

b0230 Gravesen P, Braneberg J, Jensen O S 1993 Microfluidics – A review. *J. Micromech. Microeng.* **3**, 168–82

b0235 Grumann M, Geipel A, Riegger L, Zengerle R, Ducrée J 2005 Batch-mode mixing on centrifugal microfluidic platforms. *Lab Chip* **5**, 560–5

b0240 Gunther A, Khan S A, Thalmann M, Trachsel F, Jensen K F 2004 Transport and reaction in microscale segmented gas–liquid flow. *Lab Chip* **4**, 278–86

b0245 Gunther A, Jhunjhunwala M, Thalmann M, Schmidt M A, Jensen K F 2005 Micromixing of miscible liquids in segmented gas–liquid flow. *Langmuir* **21**, 1547–55

b0250 Gutmann O, Kuehlewein R, Reinbold S, Niekrawietz R, Steinert C P, De H B, Zengerle R, Daub M 2004a A highly parallel nanoliter dispenser for microarray fabrication. *Biomed. Microdevices* **6**, 131–7

b0255 Gutmann O, Niekrawietz R, Kuehlewein R, Steinert C P, de Heij B, Zengerle R, Daub M 2004b Impact of medium properties on droplet release in a highly parallel nanoliter dispenser. *Sens. Actuators A Phys.* **116**, 187–94

b0260 Gutmann O, Niekrawietz R, Kuehlewein R, Steinert C P, Reinbold S, De H B, Daub M, Zengerle R 2004c Non-contact production of oligonucleotide microarrays using the highly integrated TopSpot nanoliter dispenser. *Analyst* **129**, 835–40

b0265 Gutmann O, Kuehlewein R, Reinbold S, Niekrawietz R, Steinert C P, de Heij B, Zengerle R, Daub M 2005 Fast and reliable protein microarray production by a new drop-in-drop technique. *Lab Chip* **5**, 675–81

b0270 Guttenberg Z, Muller H, Habermuller H, Geisbauer A, Pipper J, Felbel J, Kielpinski M, Scriba J, Wixforth A 2005 Planar chip device for PCR and hybridization with surface acoustic wave pump. *Lab Chip* **5**, 308–17

b0275 GYROS AB 2006 Uppsala, Sweden, www.gyros.com accessed 2006

b0280 Haeberle S, Brenner T, Schlosser H P, Zengerle R, Ducrée J 2005 Centrifugal micromixer. *Chem. Eng. Tech.* **28**, 613–16

b0285 Haeberle S, Brenner T, Zengerle R, Ducree J 2006a Centrifugal extraction of plasma from whole blood on a rotating disk. *Lab Chip* **6**, 776–81

b0290 Haeberle S, Naegele L, Zengerle R, Ducrée J 2006b A Digital Centrifugal Droplet Switch For Routing of Liquids. In: Kitamori T, Fujita H, Hasebe S (eds), *Proceedings of* μ*TAS 2006,* November 5–9, Tokyo, Japan, pp. 570–2.

b0295 Haeberle S, Zengerle R, Ducrée J 2007 Centrifugal generation and manipulation of droplet emulsions. *Microfluidics Nanofluidics* **3**, 65–75

b0300 Hansen C, Quake S R 2003 Microfluidics in structural biology: Smaller, faster··· better. *Curr. Opin. Struct. Biol.* **13**, 538–44

b0305 Hansen C L, Skordalakes E, Berger J M, Quake S R 2002 A robust and scalable microfluidic metering method that allows protein crystal growth by free interface diffusion. *Proc. Natl. Acad. Sci. USA* **99**, 16531–6

b0310 Harrison D J, Manz A, Fan Z H, Ludi H, Widmer H M 1992 Capillary electrophoresis and sample injection systems integrated on a planar glass chip. *Anal. Chem.* **64**, 1926–32

b0315 Harrison D J, Fluri K, Seiler K, Fan Z H, Effenhauser C S, Manz A 1993 Micromachining – A miniaturized capillary electrophoresis-based chemical-analysis system on a chip. *Science* **261**, 895–7

b0320 He M Y, Edgar J S, Jeffries G D M, Lorenz R M, Shelby J P, Chiu D T 2005 Selective encapsulation of single cells and subcellular organelles into picoliter- and femtoliter-volume droplets. *Anal. Chem.* **77**, 1539–44

b0325 de Heij B, Steinert C, Sandmaier H, Zengerle R 2003 A tunable and highly-parallel picolitre-dispenser based on direct liquid displacement. *Sens. Actuators A Phys.* **103**, 88–92

b0330 de Heij B, Daub M, Gutmann O, Niekrawietz R, Sandmaier H, Zengerle R 2004 Highly parallel dispensing of chemical and biological reagents. *Anal. Bioanal. Chem.* **378**, 119–22

b0335 Hessel V, Hardt S, Lowe H, Schonfeld F 2003 Laminar mixing in different interdigital micromixers: I. Experimental characterization. *AIChE J.* **49**, 566–77

b0340 Hessel V, Lowe H, Schonfeld F 2005 Micromixers – A review on passive and active mixing principles. *Chem. Eng. Sci.* **60**, 2479–501

b0345 Honda N, Lindberg U, Andersson P, Hoffman S, Takei H 2005 Simultaneous multiple immunoassays in a compact disc-shaped microfluidic device based on centrifugal force. *Clin. Chem.* **51**, 1955–61

b0350 Hong J W, Quake S R 2003 Integrated nanoliter systems. *Nat. Biotechnol.* **21**, 1179–83

b0355 Hong J W, Studer V, Hang G, Anderson W F, Quake S R 2004 A nanoliter-scale nucleic acid processor with parallel architecture. *Nat. Biotechnol.* **22**, 435–9

b0360 Hosokawa K, Fujii T, Endo I 1999 Handling of picoliter liquid samples in a poly(dimethylsiloxane)-based microfluidic device. *Anal. Chem.* **71**, 4781–5

b0365 Huang L R, Cox E C, Austin R H, Sturm J C 2004 Continuous particle separation through deterministic lateral displacement. *Science* **304**, 987–90

b0370 Jandik P, Weigl B H, Kessler N, Cheng J, Morris C J, Schulte T, Avdalovic N 2002 Initial study of using a laminar fluid diffusion interface for sample preparation in high-performance liquid chromatography. *J. Chromatogr. A* **954**, 33–40

b0375 Jiang F, Drese K S, Hardt S, Kupper M, Schonfeld F 2004 Helical flows and chaotic mixing in curved micro channels. *AIChE J.* **50**, 2297–305

b0380 Joanicot M, Ajdari A 2005 Applied physics – Droplet control for microfluidics. *Science* **309**, 887–8

b0385 Johnson T J, Ross D, Locascio L E 2002 Rapid microfluidic mixing. *Anal. Chem.* **74**, 45–51

b0390 Kamholz A E 2004 Proliferation of microfluidics in literature and intellectual property. *Lab Chip* **4**, 16N–20N

b0395 Khan S A, Gunther A, Schmidt M A, Jensen K F 2004 Microfluidic synthesis of colloidal silica. *Langmuir* **20**, 8604–11

b0400 Knight J B, Vishwanath A, Brody J P, Austin R H 1998 Hydrodynamic focusing on a silicon chip: Mixing nanoliters in microseconds. *Phys. Rev. Lett.* **80**, 3863–6

b0405 Kobayashi I, Mukataka S, Nakajima M 2005 Effects of type and physical properties of oil phase on oil-in-water emulsion droplet formation in straight-through microchannel emulsification, experimental and CFD studies. *Langmuir* **21**, 5722–30

b0410 Koltay P, Kalix J, Zengerle R 2004a Theoretical evaluation of the dispensing well plate method (DWP part II). *Sens. Actuators A Phys.* **116**, 472–82

b0415 Koltay P, Steger R, Bohl B, Zengerle R 2004b The dispensing well plate: A novel nanodispenser for the multiparallel delivery of liquids (DWP Part I). *Sens. Actuators A Phys.* **116**, 483–91

b0420 Kopp M U, de Mello A J, Manz A 1998 Chemical amplification: Continuous-flow PCR on a chip. *Science* **280**, 1046–8

b0425 Lai S, Wang S, Luo J, Lee L J, Yang S T, Madou M J 2004 Design of a compact disk-like microfluidic platform for enzyme-linked immunosorbent assay. *Anal. Chem.* **76**, 1832–7

b0430 Laser D J, Santiago J G 2004 A review of micropumps. *J. Micromech. Microeng.* **14**, R35–64

b0435 Le H P 1998 Progress and trends in ink-jet printing technology. *J. Imaging Sci. Technol.* **42**, 49–62

b0440 Lee G B, Hung C I, Ke B J, Huang G R, Hwei B H 2001a Micromachined pre-focused $1\times N$ flow switches for continuous sample injection. *J. Micromech. Microeng.* **11**, 567–73

b0445 Lee G B, Hwei B H, Huang G R 2001b Micromachined pre-focused $M\times N$ flow switches for continuous multi-sample injection. *J. Micromech. Microeng.* **11**, 654–61

b0450 Lee J, Kim C J 2000 Surface-tension-driven microactuation based on continuous electrowetting. *J. Microelectromech. Syst.* **9**, 171–80

b0455 Lee J, Moon H, Fowler J, Schoellhammer T, Kim C J 2002 Electrowetting and electrowetting-on-dielectric for microscale liquid handling. *Sens. Actuators A Phys.* **95**, 259–68

b0460 Li P C H 2006 *Microfluidic Lab-on-a-Chip for Chemical and Biological Analysis and Discovery.* Taylor & Francis Group, Boca Raton, FL

b0465 Link D R, Anna S L, Weitz D A, Stone H A 2004 Geometrically mediated breakup of drops in microfluidic devices. *Phys. Rev. Lett.* **92**, 054503

b0470 Lion N, Rohner T C, Dayon L, Arnaud I L, Damoc E, Youhnovski N, Wu Z Y, Roussel C, Josserand J, Jensen H, Rossier J S, Przbylski M, Girault H H 2003 Microfluidic systems in proteomics. *Electrophoresis* **24**, 3533–62

b0475 Liu J, Hansen C, Quake S R 2003 Solving the ''world-to-chip'' interface problem with a microfluidic matrix. *Anal. Chem.* **75**, 4718–23

b0480 Lotters J C, Olthuis W, Veltink P H, Bergveld P 1997 The mechanical properties of the rubber elastic polymer polydimethylsiloxane for sensor applications. *J. Micromech. Microeng.* **7**, 145–7

b0485 Madou M, Kellogg G J 1998 The LabCD: A centrifuge-based microfluidic platform for diagnostics. *Proc. SPIE* **3259**, 80–93, Systems and technologies for clinical diagnostics and drug discovery

b0490 Madou M, Lee J, Daunert S, Lai S, Shih C-H 2001 Design and fabrication of CD-like microfluidic platforms for diagnostics: Microfluidic functions. *Biomed. Microdevices* **3**, 245–54

b0495 Manz A, Graber N, Widmer H M 1990a Miniaturized total chemical-analysis system – A novel concept for chemical sensing. *Sens. Actuators B Chem.* **1**, 244–8

b0500 Manz A, Miyahara Y, Miura J, Watanabe Y, Miyagi H, Sato K 1990b Design of an open-tubular column liquid chromatograph using silicon chip technology. *Sens. Actuators B Chem.* **1**, 249–55

b0505 Manz A, Harrison D J, Verpoorte E M J, Fettinger J C, Paulus A, Ludi H, Widmer H M 1992 Planar chips technology for miniaturization and integration of separation techniques into monitoring systems – Capillary electrophoresis on a chip. *J. Chromatogr.* **593**, 253–8

b0510 Marcus J S, Anderson W F, Quake S R 2006a Microfluidic single-cell mRNA isolation and analysis. *Anal. Chem.* **78**, 3084–9

b0515 Marcus J S, Anderson W F, Quake S R 2006b Parallel picoliter RT-PCR assays using microfluidics. *Anal. Chem.* **78**, 956–8

b0520 Marko-Varga G, Nilsson J, Laurell T 2003 New directions of miniaturization within the proteomics research area. *Electrophoresis* **24**, 3521–32

b0525 Martin K, Henkel T, Baier V, Grodrian A, Schon T, Roth M, Kohler J M, Metze J 2003 Generation of larger numbers of separated microbial populations by cultivation in segmented-flow microdevices. *Lab Chip* **3**, 202–7

b0530 de Mello A J, Beard N 2003 Dealing with 'real' samples: Sample pre-treatment in microfluidic systems. *Lab Chip* **3**, 11N–19N

b0535 Micronics Inc. 2006 Redmond, WA, USA, www.micronics.net, accessed 2006

b0540 Mugele F, Baret J C 2005 Electrowetting: From basics to applications. *J. Phys. Condens. Matter* **17**, R705–74

b0545 Mugele F, Klingner A, Buehrle J, Steinhauser D, Herminghaus S 2005 Electrowetting: A convenient way to switchable wettability patterns. *J. Phys. Condens. Matter* **17**, S559–76

b0550 Nguyen N T, Wereley S T 2002 *Fundamentals and Applications of Microfluidics.* Artech House Books, Boston, MA

b0555 Nguyen N T, Wu Z G 2005 Micromixers – A review. *J. Micromech. Microeng.* **15**, R1–16

b0560 Nisisako T, Torii T, Higuchi T 2002 Droplet formation in a microchannel network. *Lab Chip* **2**, 24–6

b0565 Oh K W, Ahn C H 2006 A review of microvalves. *J. Micromech. Microeng.* **16**, R13–39

b0570 Okushima S, Nisisako T, Torii T, Higuchi T 2004 Controlled production of monodisperse double emulsions by two-step droplet breakup in microfluidic devices. *Langmuir* **20**, 9905–8

b0575 Oosterbroek R E, van den Berg A 2003 *Lab-on-a-Chip: Miniaturized Systems for (Bio)Chemical Analysis and Synthesis.* Elsevier Science, Amsterdam

b0580 Paik P, Pamula V K, Fair R B 2003a Rapid droplet mixers for digital microfluidic systems. *Lab Chip* **3**, 253–9

b0585 Paik P, Pamula V K, Pollack M G, Fair R B 2003b Electrowetting-based droplet mixers for microfluidic systems. *Lab Chip* **3**, 28–33

b0590 Pollack M G, Fair R B, Shenderov A D 2000 Electrowetting-based actuation of liquid droplets for microfluidic applications. *Appl. Phys. Lett.* **77**, 1725–6

b0595 Pollack M G, Shenderov A D, Fair R B 2002 Electrowetting-based actuation of droplets for integrated microfluidics. *Lab Chip* **2**, 96–101

b0600 Quake S R, Scherer A 2000 From micro- to nanofabrication with soft materials. *Science* **290**, 1536–40

b0605 Raschke G 2005 Molekulare Erkennung mit einzelnen Gold-Nanopartikeln. PhD-thesis, TU Muenchen

b0610 Ren H, Fair R B, Pollack M G 2004 Automated on-chip droplet dispensing with volume control by electro-wetting actuation and capacitance metering. *Sens. Actuators B Chem.* **98**, 319–27

b0615 Reyes D R, Iossifidis D, Auroux P A, Manz A 2002 Micro total analysis systems. 1. Introduction, theory, and technology. *Anal. Chem.* **74**, 2623–36

b0620 Roach L S, Song H, Ismagilov R F 2005 Controlling nonspecific protein adsorption in a plug-based microfluidic system by controlling interfacial chemistry using fluorous-phase surfactants. *Anal. Chem.* **77**, 785–96

b0625 Roche 2006 Basel, CH, www.roche.com, accessed 2006

b0630 Salemme F R 1972 Free interface diffusion technique for crystallization of proteins for X-ray crystallography. *Arch. Biochem. Biophys.* **151**, 533–9

b0635 Schembri C T, Ostoich V, Lingane P J, Burd T L, Buhl S N 1992 Portable simultaneous multiple analyte whole-blood analyzer for point-of-care testing. *Clin. Chem.* **38**, 1665–70

b0640 Schembri C T, Burd T L, Kopfsill A R, Shea L R, Braynin B 1995 Centrifugation and capillarity integrated into a multiple analyte whole-blood analyzer. *J. Automatic Chem.* **17**, 99–104

b0645 Schonfeld F, Hessel V, Hofmann C 2004 An optimised split-and-recombine micro-mixer with uniform 'chaotic' mixing. *Lab Chip* **4**, 65–9

b0650 Schwartz J A, Vykoukal J V, Gascoyne P R C 2004 Droplet-based chemistry on a programmable micro-chip. *Lab Chip* **4**, 11–17

b0655 Shestopalov I, Tice J D, Ismagilov R F 2004 Multi-step synthesis of nanoparticles performed on millisecond time scale in a microfluidic droplet-based system. *Lab Chip* **4**, 316–21

b0660 Shoji S, Esashi M 1994 Microflow devices and systems. *J. Micromech. Microeng.* **4**, 157–71

b0665 Shoji S, Esashi M, Matsuo T 1988 Prototype miniature blood-gas analyzer fabricated on a silicon-wafer. *Sens. Actuators* **14**, 101–7

b0670 Sia S K, Whitesides G M 2003 Microfluidic devices fabricated in poly(dimethylsiloxane) for biological studies. *Electrophoresis* **24**, 3563–76

b0675 Song H, Ismagilov R F 2003 Millisecond kinetics on a microfluidic chip using nanoliters of reagents. *J. Am. Chem. Soc.* **125**, 14613–19

b0680 Song H, Bringer M R, Tice J D, Gerdts C J, Ismagilov R F 2003a Experimental test of scaling of mixing by chaotic advection in droplets moving through microfluidic channels. *Appl. Phys. Lett.* **83**, 4664–6

b0685 Song H, Tice J D, Ismagilov R F 2003b A microfluidic system for controlling reaction networks in time. *Angew. Chem. Int. Ed.* **42**, 768–72

b0690 Song Y J, Zhao T S 2001 Modelling and test of a thermally-driven phase-change nonmechanical micropump. *J. Micromech. Microeng.* **11**, 713–19

b0695 SpinX Technologies 2006 Geneva, Switzerland, www.spinx-technologies.com accessed 2006

b0700 Squires T M, Quake S R 2005 Microfluidics: Fluid physics at the nanoliter scale. *Rev. Mod. Phys.* **77**, 977–1026

b0705 Srinivasan V, Pamula V K, Fair R B 2004 An integrated digital microfluidic lab-on-a-chip for clinical diagnostics on human physiological fluids. *Lab Chip* **4**, 310–15

b0710 Steger R, Bohl B, Zengerle R, Koltay P 2004 The dispensing well plate: A novel device for nanoliter liquid handling in ultra high-throughput screening. *J. Assoc. Lab. Autom.* **9**, 291–9

b0715 Steigert J, Grumann M, Brenner T, Mittenbühler K, Nann T, Rühe J, Moser I, Haeberle S, Riegger L, Riegler J, Bessler W, Zengerle R, Ducrée J 2005 Integrated sample preparation, reaction, and detection on a high-frequency centrifugal microfluidic platform. *J. Assoc. Lab. Autom.* **10**, 331–41

b0720 Steigert J, Grumann M, Brenner T, Riegger L, Harter J, Zengerle R, Ducrée J 2006 Fully integrated whole blood testing by real-time absorption measurement on a centrifugal platform. *Lab Chip* **6**, 1040–4

b0725 Steinert C P, Goutier I, Gutmann O, Sandmaier H, Daub M, de Heij B, Zengerle R 2004 A highly parallel picoliter dispenser with an integrated, novel capillary channel structure. *Sens. Actuators A Phys.* **116**, 171–7

b0730 Steinert C P, Mueller-Dieckmann J, Weiss M, Roessle M, Zengerle R, Koltay P 2007 Miniaturized and highly parallel protein crystallization on a microfluidic disc. Proceedings of the IEEE MEMS 2007, January 21–25, Kobe, Japan, pp. 561–4

b0735 Stone H A, Stroock A D, Ajdari A 2004 Engineering flows in small devices: Microfluidics toward a lab-on-a-chip. *Annu. Rev. Fluid Mech.* **36**, 381–411

b0740 Stroock A D, Dertinger S K W, Ajdari A, Mezic I, Stone H A, Whitesides G M 2002 Chaotic mixer for microchannels. *Science* **295**, 647–51

b0745 Sudarsan A P, Ugaz V M 2006 Fluid mixing in planar spiral microchannels. *Lab Chip* **6**, 74–82

b0750 Sugiura S, Nakajima M, Iwamoto S, Seki M 2001 Interfacial tension driven monodispersed droplet formation from microfabricated channel array. *Langmuir* **17**, 5562–6

b0755 Takagi J, Yamada M, Yasuda M, Seki M 2005 Continuous particle separation in a microchannel having asymmetrically arranged multiple branches. *Lab Chip* **5**, 778–84

b0760 Tay F E H 2002 *Microfluidics and BioMEMS Applications.* Kluwer Academic Publishers, Boston, MA

b0765 Terry S C, Jerman J H, Angell J B 1979 Gas-chromatographic air analyzer fabricated on a silicon-wafer. *IEEE Trans. Electron Devices* **26**, 1880–6

b0770 Thorsen T, Maerkl S J, Quake S R 2002 Microfluidic large-scale integration. *Science* **298**, 580–4

b0775 Tice J D, Song H, Lyon A D, Ismagilov R F 2003 Formation of droplets and mixing in multiphase microfluidics at low values of the Reynolds and the capillary numbers. *Langmuir* **19**, 9127–33

b0780 Tice J D, Lyon A D, Ismagilov R F 2004 Effects of viscosity on droplet formation and mixing in microfluidic channels. *Anal. Chim. Acta* **507**, 73–7

b0785 Unger M A, Chou H P, Thorsen T, Scherer A, Quake S R 2000 Monolithic microfabricated valves and pumps by multilayer soft lithography. *Science* **288**, 113–16

b0790 Urban G A 2006 *BioMEMS.* Springer, Berlin

b0795 Utada A S, Lorenceau E, Link D R, Kaplan P D, Stone H A, Weitz D A 2005 Monodisperse double emulsions generated from a microcapillary device. *Science* **308**, 537–41

b0800 Van Lintel H T G, Vandepol F C M, Bouwstra S 1988 A piezoelectric micropump based on micromachining of silicon. *Sens. Actuators* **15**, 153–67

b0805 Vilkner T, Janasek D, Manz A 2004 Micro total analysis systems. Recent developments. *Anal. Chem.* **76**, 3373–85

b0810 Waibel G, Kohnle J, Cernosa R, Storz M, Schmitt M, Ernst H, Sandmaier H, Zengerle R, Strobelt T 2003 Highly integrated autonomous microdosage system. *Sens. Actuators A Phys.* **103**, 225–30

b0815 Weigl B H, Bardell R L, Cabrera C R 2003 Lab-on-a-chip for drug development. *Adv. Drug Deliv. Rev.* **55**, 349–77

b0820 Wheeler A R, Moon H, Kim C J, Loo J A, Garrell R L 2004 Electrowetting-based microfluidics for analysis of peptides and proteins by matrix-assisted laser desorption/ionization mass spectrometry. *Anal. Chem.* **76**, 4833–8

b0825 Wixforth A 2003 Acoustically driven planar microfluidics. *Superlattices Microstruct.* **33**, 389–96

b0830 Wixforth A, Strobl C, Gauer C, Toegl A, Scriba J, von Guttenberg Z 2004 Acoustic manipulation of small droplets. *Anal. Bioanal. Chem.* **379**, 982–91

b0835 Woias P 2005 Micropumps – Past, progress and future prospects. *Sens. Actuators B Chem.* **105**, 28–38

b0840 Xia Y N, Whitesides G M 1998a Soft lithography. *Annu. Rev. Mater. Sci.* **28**, 153–84

b0845 Xia Y N, Whitesides G M 1998b Soft lithography. *Angew. Chem. Int. Ed.* **37**, 551–75

b0850 Xia Y N, Kim E, Zhao X M, Rogers J A, Prentiss M, Whitesides G M 1996 Complex optical surfaces formed by replica molding against elastomeric masters. *Science* **273**, 347–9

b0855 Yadav M K, Gerdts C J, Sanishvili R, Smith W W, Roach L S, Ismagilov R F, Kuhn P, Stevens R C 2005 In situ data collection and structure refinement from microcapillary protein crystallization. *J. Appl. Crystallogr.* **38**, 900–5

b0860 Yamada M, Seki M 2004 Nanoliter-sized liquid dispenser array for multiple biochemical analysis in microfluidic devices. *Anal. Chem.* **76**, 895–9

b0865 Yamada M, Seki M 2005 Hydrodynamic filtration for on-chip particle concentration and classification utilizing microfluidics. *Lab Chip* **5**, 1233–9

b0870 Yamada M, Seki M 2006 Microfluidic particle sorter employing flow splitting and recombining. *Anal. Chem.* **78**, 1357–62

b0875 Yamada M, Nakashima M, Seki M 2004 Pinched flow fractionation: Continuous size separation of particles utilizing a laminar flow profile in a pinched microchannel. *Anal. Chem.* **76**, 5465–71

b0880 Yokoyama Y, Takeda M, Umemoto T, Ogushi T 2004 Thermal micro pumps for a loop-type micro channel. *Sens. Actuators A Phys.* **111**, 123–8

b0885 Zheng B, Ismagilov R F 2005 A microfluidic approach for screening submicroliter volumes against multiple reagents by using preformed arrays of nanoliter plugs in a three-phase liquid/liquid/gas flow. *Angew. Chem. Int. Ed.* **44**, 2520–3

b0890 Zheng B, Roach L S, Ismagilov R F 2003 Screening of protein crystallization conditions on a microfluidic chip using nanoliter-size droplets. *J. Am. Chem. Soc.* **125**, 11170–1

b0895 Zheng B, Tice J D, Ismagilov R F 2004a Formation of arrayed droplets of soft lithography and two-phase fluid flow, and application in protein crystallization. *Adv. Mater.* **16**, 1365–8

b0900 Zheng B, Tice J D, Ismagilov R F 2004b Formation of droplets of in microfluidic channels alternating composition and applications to indexing of concentrations in droplet-based assays. *Anal. Chem.* **76**, 4977–82

b0905 Zheng B, Tice J D, Roach L S, Ismagilov R F 2004c A droplet-based, composite PDMS/glass capillary microfluidic system for evaluating protein crystallization conditions by microbatch and vapor-diffusion methods with on-chip X-ray diffraction. *Angew. Chem. Int. Ed.* **43**, 2508–11

b0910 Zheng B, Gerdts C J, Ismagilov R F 2005 Using nanoliter plugs in microfluidics to facilitate and understand protein crystallization. *Curr. Opin. Struct. Biol.* **15**, 548–55

b0915 Zimmermann M, Bentley S, Schmid H, Hunziker P, Delamarche E 2005 Continuous flow in open microfluidics using controlled evaporation. *Lab Chip* **5**, 1355–9

b0920 Zoval J V, Madou M J 2004 Centrifuge-based fluidic platforms. *Proc. IEEE* **92**, 140–53

Biographies

Stefan Haeberle is a Ph.D. student in the laboratory for MEMS applications at the Department of Microsystems Engineering (IMTEK) at the University of Freiburg, Germany. He received his diploma degree in Microsystem Engineering in 2004 from the University of Freiburg. His research concentrates on the development of lab-on-a-chip systems based on the centrifugal microfluidics platform. Freiburg, 02.11.2006 Stefan Haeberle.

Prof. Dr. Roland Zengerle is the head of the laboratory for MEMS applications at the Department of Microsystems Engineering (IMTEK) at the University of Freiburg, Germany. In addition, he is a director at the Institute for Micro- and Information Technology of the Hahn-Schickard-Gesellschaft (HSG-IMIT). HSG-IMIT is a nonprofit organization supporting industries in the development of new products based on MEMS technologies.

The research of Dr. Zengerle and his team of 50 engineers is focused on microfluidics and covers topics like miniaturized and autonomous dosage systems, implantable drug delivery systems, nanoliter and picoliter dispensing, lab-on-a-chip systems, thermal sensors, miniaturized fuel cells as well as micro- and nanofluidics simulation. Dr. Zengerle coauthored more than 200 technical publications and 25 patents. He is the European editor of the *Springer Journal of Microfluidics and Nanofluidics*. Dr. Zengerle serves on the international steering committee of the IEEE-MEMS conference as well as on the technical program committees of several other international conferences.